

REPUBLIC OF TURKEY  
YILDIZ TECHNICAL UNIVERSITY  
GRADUATE SCHOOL OF SCIENCE AND ENGINEERING

FREQUENCY SELECTIVE SURFACES FOR AEROSPACE  
APPLICATIONS

Hacı Mehmet IŞIK

MASTER OF SCIENCE THESIS  
Department of Electronic and Communication Engineering  
Program of Electronic Engineering

Supervisor  
Prof. Dr. Tülay YILDIRIM

January, 2022

**REPUBLIC OF TURKEY**  
**YILDIZ TECHNICAL UNIVERSITY**  
**GRADUATE SCHOOL OF SCIENCE AND ENGINEERING**

**FREQUENCY SELECTIVE SURFACES FOR AEROSPACE  
APPLICATIONS**

A thesis submitted by Hacı Mehmet IŞIK in partial fulfillment of the requirements for the degree of **MASTER OF SCIENCE** is approved by the committee on 11.01.2022 in Department of Electronic and Communication Engineering, Program of Electronic Engineering.

Prof. Dr. Tülay YILDIRIM  
Yıldız Technical University  
Supervisor

**Approved By the Examining Committee**

Prof. Dr. Tülay YILDIRIM, Supervisor  
Yıldız Technical University

\_\_\_\_\_

Assist. Prof. Dr. Zehra Gülru ÇAM TAŞKIRAN, Member  
Yıldız Technical University

\_\_\_\_\_

Assist. Prof. Dr. Sibel ÜNALDI, Member  
Bilecik Şeyh Edebali University

\_\_\_\_\_

I hereby declare that I have obtained the required legal permissions during data collection and exploitation procedures, that I have made the in-text citations and cited the references properly, that I haven't falsified and/or fabricated research data and results of the study and that I have abided by the principles of the scientific research and ethics during my Thesis Study under the title of Frequency Selective Surfaces For Aerospace Applications supervised by my supervisor, Prof. Dr. Tlay YILDIRIM. In the case of a discovery of false statement, I am to acknowledge any legal consequence.

Hacı Mehmet IŐIK

Signature

*Dedicated to my lovely wife  
and my parents*



## ACKNOWLEDGEMENTS

---

I would like to thank everyone who made this thesis possible and supported me endlessly.

First of all, I would like to thank my dear advisor, Prof. Dr. Tlay Yıldırım , for giving me a direction throughout my undergraduate and graduate life.

I would like to thank my school friend Bşra Nur Darendeli Kiraz, who was always with me during my undergraduate and graduate education and especially sacrificed her own thesis during my thesis process.

I would like to thank Zeynep Ergnen Yavař for her inspiring support and encouraging support to the studies.

I would also like to express my endless thanks to all my family members who have contributed to my success. I would like to express my endless gratitude to my mother Glay and my father Bayram, and then to my brothers Ali, Ferhat and my sister Gizem Naz. I'm a family with you

Last but not least, special thank my very precious wife, dear Gizem. I cannot express the importance of the countless sacrifices you have made to focus on my thesis during this painful process. Thank you so much for always providing me with a peaceful, safe and inspiring working environment.

Hacı Mehmet IŐIK

# TABLE OF CONTENTS

---

<b>LIST OF ABBREVIATIONS</b>	<b>vii</b>
<b>LIST OF FIGURES</b>	<b>viii</b>
<b>ABSTRACT</b>	<b>xiv</b>
<b>ÖZET</b>	<b>xvi</b>
<b>1 INTRODUCTION</b>	<b>1</b>
1.1 Literature Review . . . . .	1
1.2 Objective of the Thesis . . . . .	2
1.3 Hypothesis . . . . .	2
<b>2 FREQUENCY SELECTIVE SURFACES</b>	<b>3</b>
2.1 Definition . . . . .	3
2.2 Equivalent Circuit . . . . .	4
2.2.1 Equivalent Circuit Modeling of Rectangular FSS . . . . .	4
2.3 Using in Aerospace Applications . . . . .	8
2.3.1 Electromagnetic Wave Absorber Frequency Selective Surfaces . . . . .	8
2.4 Affecting Factors . . . . .	13
2.4.1 Influence of Physical Design . . . . .	13
2.4.2 Size Effect . . . . .	15
2.4.3 The Effect of the Dielectric Material Used as A Substrate . . . . .	16
2.4.4 Material Type Influence . . . . .	17
2.5 Frequency Selective Surface Types and Filtering Features . . . . .	17
2.5.1 Band Stop Filters . . . . .	19
2.5.2 Band Pass Filters . . . . .	21
2.5.3 Low Pass Filters . . . . .	22
2.5.4 High Pass Filters . . . . .	23
<b>3 DESIGN OF FREQUENCY SELECTIVE SURFACE</b>	<b>24</b>
3.1 Simulation of The Desired FSS Design . . . . .	25
3.1.1 Development of the Unit Cell of FSS Design . . . . .	26

3.1.2	FSS Tuning Based on Influence of FSS Design Parameters . . . .	30
<b>4</b>	<b>FSS IMPLEMENTATION TO 3D GEOMETRIC MODELS</b>	<b>38</b>
4.1	FSS Implementation in Airfoil Format for Aircraft Wings . . . . .	40
4.2	FSS Implementation for Aircraft Body Part in the Form of Cylindrical Surfaces . . . . .	49
4.3	FSS Implementation for Aircraft Nose Area in The Form of Conical Surfaces . . . . .	55
<b>5</b>	<b>RESULTS AND DISCUSSION</b>	<b>74</b>
5.1	Conclusions . . . . .	74
5.2	Future Perspectives . . . . .	75
	<b>REFERENCES</b>	<b>76</b>
<b>A</b>	<b>APPENDIX</b>	<b>82</b>
	<b>PUBLICATIONS FROM THESIS</b>	<b>89</b>

## LIST OF ABBREVIATIONS

---

AFSS	Active Frequency Selective Surface
BW	Bandwidth
CST	Computer Simulation Technology
dB	Decibel
EM	Electromagnetic
EMI	Electromagnetic Interference
FDTD	Finite Difference Time Domain
FIT	Finite Integration Technique
FSS	Frequency Selective Surface
GHz	Giga Hertz
HFSS	High Frequency Structural Simulator
MHz	Mega Hertz
MUT	Material Under Test
RADAR	Radio Detecting and Ranging
RAM	Radar Absorber Material
RCS	Radar Cross Section
TE	Transverse Electric
Thz	Tera Hertz
TM	Transverse Magnetic

## LIST OF FIGURES

---

<b>Figure 2.3</b>	Modeling the effect of capacitance on FSS . . . . .	5
<b>Figure 2.4</b>	Manufactured tunable FSS prototype. a) front side. (b) back side and inserted dielectric. (c) demonstration of different retraction depths $d$ from 0 to 10 mm.[21] . . . . .	5
<b>Figure 2.5</b>	Grid-shaped FSS equivalent circuit model . . . . .	6
<b>Figure 2.6</b>	Rectangular patch-shaped FSS equivalent circuit model . . . . .	7
<b>Figure 2.7</b>	Fundamental Shapes of FSS [36] . . . . .	13
<b>Figure 2.8</b>	Examples of fractal FSS developed in different studies [23] . . . . .	14
<b>Figure 2.9</b>	Creating iterative fractal FSS using Koch Curve [39] . . . . .	15
<b>Figure 2.10</b>	Basic FSS equivalent circuit representations [42] . . . . .	16
<b>Figure 2.11</b>	General filter characteristic acquired with FSSs a) low pass Filter b) High Pass Filter . . . . .	17
<b>Figure 2.12</b>	Filter characteristics obtained by the combination of patch and cavity FSSs c) Band Stop Filter d) Band Pass Filter . . . . .	18
<b>Figure 2.13</b>	Angular effect of shielding effectiveness. (a) TE wave mode (b) TM wave mode [50] . . . . .	19
<b>Figure 2.14</b>	The effect of parameter changes on the reflection coefficient in a band stop FSS design. (a) front and perspective view of the FSS, (b) equivalent circuits of FSS structures, (c) the effect of changing the long side of the FSS structure, (d) the effect of the dielectric change of the substrate on which the FSS structure is placed, (e) effect of variation of vertical distance between two FSS structures, (f) effect of variation of horizontal distance between two FSS structures, (g) the effect of changing the short side of the FSS structure, (h) the effect of the substrate thickness on which the FSS structure is placed [8] . . . . .	20
<b>Figure 2.15</b>	Produced THz FSS (a) , optical microscope image of (b) the top metal layer, (c) the middle metal layer, (d) the bottom metal layer, scale bar= $30\mu\text{m}$ [57] . . . . .	21
<b>Figure 2.16</b>	Effect of filter order on low-pass filter characteristics [58] . . . . .	22

<b>Figure 2.17</b>	Comparison of Chebyshev Type-I Filter, Chebyshev Type-II Filter, Elliptical Filter vs. Butterworth Low Pass Filter [61] . . . . .	22
<b>Figure 2.18</b>	Effect of filter order on high-pass filter characteristics [58] . . . . .	23
<b>Figure 3.1</b>	Representation of S parameters in a 2-port system . . . . .	24
<b>Figure 3.2</b>	Unit cell representation of the FSS . . . . .	26
<b>Figure 3.3</b>	Unit cell representation of the FSS in CST Studio . . . . .	27
<b>Figure 3.4</b>	Boundary conditions and periodic representation of an unit FSS cell	28
<b>Figure 3.5</b>	Unit representation of FSS from cross view . . . . .	28
<b>Figure 3.6</b>	Result of draft FSS in CST Studio . . . . .	29
<b>Figure 3.7</b>	Slightly oversized unit cell of FSS design in CST Studio . . . . .	30
<b>Figure 3.8</b>	Result of slightly oversized unit cell of FSS design in CST Studio .	31
<b>Figure 3.9</b>	Unit cell of FSS dimensions optimized for 10 GHz in CST Studio .	31
<b>Figure 3.10</b>	View of unit cell of FSS optimized for 10 GHz from different angles in CST Studio a) Perspective view of FSS b) Horizontal section view of FSS . . . . .	32
<b>Figure 3.11</b>	Result of unit cell of FSS optimized for 10 GHz in CST Studio . . .	32
<b>Figure 3.12</b>	Result of optimized unit cell of FSS of different sizes in CST Studio	33
<b>Figure 3.13</b>	The result of unit cell of FSS optimized for 10 GHz using quartz substrate . . . . .	34
<b>Figure 3.14</b>	Changing of metal thickness of unit cell of FSS a)FSS thickness=0.15mm b)0.45mm . . . . .	35
<b>Figure 3.15</b>	The result of FSS metal thickness change . . . . .	35
<b>Figure 3.16</b>	S11 result of unit cell of FSS due to incident wave phi angle changing	36
<b>Figure 3.17</b>	S21 result of unit cell of FSS due to incident wave phi angle changing	36
<b>Figure 3.18</b>	S11 result of unit cell of FSS due to incident wave theta angle changing . . . . .	37
<b>Figure 3.19</b>	S21 result of unit cell of FSS due to incident wave theta angle changing . . . . .	37
<b>Figure 4.1</b>	Illustration of Boeing B-727 commercial jet aircraft geometric components [71] . . . . .	38
<b>Figure 4.2</b>	Most commonly used airfoil examples [72] . . . . .	40
<b>Figure 4.3</b>	Front view of the airfoil made of aluminium . . . . .	41
<b>Figure 4.4</b>	View of material under test setup . . . . .	41
<b>Figure 4.5</b>	Front view of the substrate coated airfoil . . . . .	42
<b>Figure 4.6</b>	Rear view of the substrate coated airfoil . . . . .	42
<b>Figure 4.7</b>	Front view of the FSS coated airfoil . . . . .	43
<b>Figure 4.8</b>	Rear view of the FSS coated airfoil . . . . .	43
<b>Figure 4.9</b>	Cross view of the FSS coated airfoil at material under test setup . .	44
<b>Figure 4.10</b>	Side view of the FSS coated airfoil at material under test setup . .	44

<b>Figure 4.11</b> Result of airfoil S11 made of pure aluminum . . . . .	45
<b>Figure 4.12</b> Result of airfoil S12 made of pure aluminum . . . . .	45
<b>Figure 4.13</b> Result of airfoil S21 made of pure aluminum . . . . .	45
<b>Figure 4.14</b> Result of airfoil S22 made of pure aluminum . . . . .	45
<b>Figure 4.15</b> S11 result of FSS coated airfoil . . . . .	46
<b>Figure 4.16</b> S12 result of FSS coated airfoil . . . . .	46
<b>Figure 4.17</b> S21 result of FSS coated airfoil . . . . .	46
<b>Figure 4.18</b> S22 result of FSS coated airfoil . . . . .	46
<b>Figure 4.19</b> Comparison of S11 parameters of FSS coated airfoil analysis and aluminum airfoil analysis . . . . .	47
<b>Figure 4.20</b> Comparison of S12 parameters of FSS coated airfoil analysis and aluminum airfoil analysis . . . . .	47
<b>Figure 4.21</b> Comparison of S21 parameters of FSS coated airfoil analysis and aluminum airfoil analysis . . . . .	47
<b>Figure 4.22</b> Comparison of S22 parameters of FSS coated airfoil analysis and aluminum airfoil analysis . . . . .	48
<b>Figure 4.23</b> Left cross view of the test setup . . . . .	49
<b>Figure 4.24</b> Right cross view of the test setup . . . . .	50
<b>Figure 4.25</b> Left cross view of the FSS coated cylinder . . . . .	51
<b>Figure 4.26</b> Perpendicular view of the FSS coated cylinder . . . . .	51
<b>Figure 4.27</b> Left cross view of the FSS coated cylinder analysis setup . . . . .	52
<b>Figure 4.28</b> Perpendicular view of the FSS coated cylinder analysis setup . . . . .	52
<b>Figure 4.29</b> Comparison of S11 parameters of FSS coated cylinder analysis and aluminum cylinder analysis . . . . .	52
<b>Figure 4.30</b> Comparison of S12 parameters of FSS coated cylinder analysis and aluminum cylinder analysis . . . . .	53
<b>Figure 4.31</b> Comparison of S21 parameters of FSS coated cylinder analysis and aluminum cylinder analysis . . . . .	53
<b>Figure 4.32</b> Comparison of S22 parameters of FSS coated cylinder analysis and aluminum cylinder analysis . . . . .	53
<b>Figure 4.33</b> Side view of aluminum cone . . . . .	55
<b>Figure 4.34</b> Right cross view of aluminum cone . . . . .	55
<b>Figure 4.35</b> Left cross view of aluminum cone . . . . .	56
<b>Figure 4.36</b> Right cross view of aluminum cone . . . . .	56
<b>Figure 4.37</b> Side view of aluminum cone . . . . .	56
<b>Figure 4.38</b> Result of cone S11 made of pure aluminum . . . . .	57
<b>Figure 4.39</b> Result of cone S12 made of pure aluminum . . . . .	57
<b>Figure 4.40</b> Result of cone S21 made of pure aluminum . . . . .	57
<b>Figure 4.41</b> Result of cone S22 made of pure aluminum . . . . .	57

<b>Figure 4.42</b> Side view of FSS coated cone with 3 circular loops consisting of 7 FSS . . . . .	58
<b>Figure 4.43</b> Top view of FSS coated cone with 3 circular loops consisting of 7 FSS	58
<b>Figure 4.44</b> Left cross view of FSS coated cone with 3 circular loops consisting of 7 FSS . . . . .	59
<b>Figure 4.45</b> Left cross view of FSS coated cone with 3 circular loops consisting of 7 FSS under test setup . . . . .	59
<b>Figure 4.46</b> Right cross view of FSS coated cone with 3 circular loops consisting of 7 FSS under test setup . . . . .	60
<b>Figure 4.47</b> Side view of FSS coated cone with 3 circular loops consisting of 7 FSS under test setup . . . . .	60
<b>Figure 4.48</b> Comparison of S11 parameters of 3x7 FSS coated cone analysis and aluminum cone analysis . . . . .	60
<b>Figure 4.49</b> Comparison of S22 parameters of 3x7 FSS coated cone analysis and aluminum cone analysis . . . . .	61
<b>Figure 4.50</b> Side view of FSS coated cone with 5 circular loops consisting of 7 FSS . . . . .	61
<b>Figure 4.51</b> Top view of FSS coated cone with 5 circular loops consisting of 7 FSS	62
<b>Figure 4.52</b> Left cross view of FSS coated cone with 5 circular loops consisting of 7 FSS under test setup . . . . .	62
<b>Figure 4.53</b> Side view of FSS coated cone with 5 circular loops consisting of 7 FSS under test setup . . . . .	62
<b>Figure 4.54</b> Comparison of S11 parameters of 5x7 FSS coated cone analysis and aluminum cone analysis . . . . .	63
<b>Figure 4.55</b> Comparison of S22 parameters of 5x7 FSS coated cone analysis and aluminum cone analysis . . . . .	63
<b>Figure 4.56</b> Left cross view 1 of 10% enlarged FSS coated cone . . . . .	64
<b>Figure 4.57</b> Side view of 10% enlarged FSS coated cone . . . . .	64
<b>Figure 4.58</b> Opposite view of 10% enlarged FSS coated cone . . . . .	64
<b>Figure 4.59</b> Left cross view 2 of 10% enlarged FSS coated cone . . . . .	64
<b>Figure 4.60</b> Left cross view of 10% enlarged FSS coated cone and 5x7 constant FSS coated . . . . .	65
<b>Figure 4.61</b> Right cross view of 10% enlarged FSS coated cone and 5x7 constant FSS coated . . . . .	65
<b>Figure 4.62</b> Top view of 10% enlarged FSS coated cone and 5x7 constant FSS coated . . . . .	65
<b>Figure 4.63</b> Left cross view 2 of 10% enlarged FSS coated cone and 5x7 constant FSS coated under test . . . . .	66

<b>Figure 4.64</b>	Comparison of S11 parameters of 5x7 constant FSS coated cone analysis and 10% enlarged FSS coated cone analysis . . . . .	66
<b>Figure 4.65</b>	Comparison of S12 parameters of 5x7 constant FSS coated cone analysis and 10% enlarged FSS coated cone analysis . . . . .	67
<b>Figure 4.66</b>	Comparison of S21 parameters of 5x7 constant FSS coated cone analysis and 10% enlarged FSS coated cone analysis . . . . .	67
<b>Figure 4.67</b>	Comparison of S22 parameters of 5x7 constant FSS coated cone analysis and 10% enlarged FSS coated cone analysis . . . . .	67
<b>Figure 4.68</b>	Side view of added FSS coated cone . . . . .	68
<b>Figure 4.69</b>	Right cross view of added FSS coated cone . . . . .	68
<b>Figure 4.70</b>	Top view of added FSS coated cone . . . . .	69
<b>Figure 4.71</b>	Comparison of S11 parameters of 5x7 constant FSS coated cone analysis and added FSS coated cone analysis . . . . .	69
<b>Figure 4.72</b>	Comparison of S12 parameters of 5x7 constant FSS coated cone analysis and added FSS coated cone analysis . . . . .	70
<b>Figure 4.73</b>	Comparison of S21 parameters of 5x7 constant FSS coated cone analysis and added FSS coated cone analysis . . . . .	70
<b>Figure 4.74</b>	Comparison of S22 parameters of 5x7 constant FSS coated cone analysis and added FSS coated cone analysis . . . . .	70
<b>Figure 4.75</b>	Comparison of All S11 Parameter Results . . . . .	71
<b>Figure 4.76</b>	Comparison of All S12 Parameter Results . . . . .	71
<b>Figure 4.77</b>	Comparison of All S21 Parameter Results . . . . .	72
<b>Figure 4.78</b>	Comparison of All S22 Parameter Results . . . . .	72
<b>Figure A.1</b>	Right cross detailed view of FSS coated cone with 5 circular loops consisting of 7 FSS . . . . .	82
<b>Figure A.2</b>	Comparison of S12 parameters of 3x7 FSS coated cone analysis and aluminum cone analysis . . . . .	82
<b>Figure A.3</b>	Comparison of S21 parameters of 3x7 FSS coated cone analysis and aluminum cone analysis . . . . .	83
<b>Figure A.4</b>	Comparison of S22 parameters of 3x7 FSS coated cone analysis and aluminum cone analysis . . . . .	83
<b>Figure A.5</b>	Result of S11 parameters of 5x7 FSS coated cone analysis . . . . .	83
<b>Figure A.6</b>	Result of S21 parameters of 5x7 FSS coated cone analysis . . . . .	84
<b>Figure A.7</b>	Result of S12 parameters of 5x7 FSS coated cone analysis . . . . .	84
<b>Figure A.8</b>	Result of S22 parameters of 5x7 FSS coated cone analysis . . . . .	84
<b>Figure A.9</b>	Comparison of S12 parameters of 5x7 FSS coated cone analysis and aluminum cone analysis . . . . .	85
<b>Figure A.10</b>	Comparison of S21 parameters of 5x7 FSS coated cone analysis and aluminum cone analysis . . . . .	85

<b>Figure A.11</b>	Result of S11 parameters of 10% enlarged FSS coated cone analysis	85
<b>Figure A.12</b>	Result of S12 parameters of 10% enlarged FSS coated cone analysis	86
<b>Figure A.13</b>	Result of S21 parameters of 10% enlarged FSS coated cone analysis	86
<b>Figure A.14</b>	Result of S22 parameters of 10% enlarged FSS coated cone analysis	86
<b>Figure A.15</b>	Result of S11 parameters of added FSS coated cone analysis . . . .	87
<b>Figure A.16</b>	Result of S21 parameters of added FSS coated cone analysis . . . .	87
<b>Figure A.17</b>	Result of S12 parameters of added FSS coated cone analysis . . . .	87
<b>Figure A.18</b>	Result of S22 parameters of added FSS coated cone analysis . . . .	88



# Frequency Selective Surfaces For Aerospace Applications

Hacı Mehmet IŞIK

Department of Electronic and Communication Engineering

Master of Science Thesis

Supervisor: Prof. Dr. Tülay YILDIRIM

Frequency selective surfaces (FSS) consist of periodic arrays of elements whose absorption, reflection or transmission properties can be adjusted with different design solutions. FSSs should not be thought of as different from filter circuits that consist of normal passive elements such as resistors, coils or capacitors. With the created FSS design, it is used as filter circuits that filter electromagnetic waves according to the desired band. When filtering in FSSs, features such as bandwidth or absorption value are due to the physical design of the FSS. As the dimensions of the FSS change, the capacitance, coil and resistance values in the electrical equivalent circuit also change, and accordingly the values such as the bandwidth of the filter created change.

In this study, the FSS was designed as a radar absorber. Absorbers can be used to reduce the radar cross section (RCS) area of aircraft. An FSS design whose frequency characteristic is suitable for the absorption characteristic is adjusted to absorb in the 10GHz band. While making these adjustments; The effects of these changes on the resonance frequency were observed by making analyzes with features such as FSS thickness, electromagnetic wave incidence angle, FSS size. S parameters were used while interpreting the analysis results.

The effects of the FSS design, tuned to 10 GHz, have been observed as a result of applying it to different surfaces of the aircraft. These analyzes were made with two horn antennas. While making the surface application of the aircraft, based on the assumption that it consists of three main parts such as wing, fuselage and nose, applications were made on airfoil, cylindrical and conical shapes, respectively. In all

analyses made, it was confirmed with all geometries that FSS showed absorption in the 10GHz region. The analyses were made in the CST Studio program.

**Keywords:**

frequency selective surface, metamaterial, aerospace, absorber, stealth



# HAVACILIK UYGULAMALARI İÇİN FREKANS SEÇİCİ YÜZEYLER

Hacı Mehmet IŞIK

Elektronik Mühendisliği Anabilim Dalı  
Yüksek Lisans Tezi

Danışman: Prof. Dr. Tülay YILDIRIM

Frekans seçici yüzeyler (FSY), soğurma, yansıma veya iletim özellikleri farklı tasarım çözümleri ile ayarlanabilen periyodik eleman dizilerinden oluşur. FSY'ler, dirençler, bobinler veya kapasitörler gibi normal pasif elemanlardan oluşan filtre devrelerinden farklı olarak düşünülmemelidir. Oluşturulan FSS tasarımı ile elektromanyetik dalgaları istenilen banda göre filtreleyen filtre devreleri olarak kullanılmaktadır. FSY'lerde filtreleme yaparken, bant genişliği veya absorpsiyon değeri gibi özellikler FSY'nin fiziksel tasarımından kaynaklanmaktadır. FSY'nin boyutları değiştikçe elektriksel eşdeğer devredeki kapasitans, bobin ve direnç değerleri de değişir ve buna bağlı olarak oluşturulan filtrenin bant genişliği gibi değerler de değişir.

Bu çalışmada, FSS bir radar soğurucu olarak tasarlanmıştır. Soğurucular, uçağın radar kesit (RCS) alanını azaltmak için kullanılabilir. Frekans karakteristiği soğurma karakteristiğine uygun olan bir FSS tasarımı, 10GHz bandında soğurma yapacak şekilde ayarlanır. Bu ayarlamaları yaparken; FSS kalınlığı, elektromanyetik dalga geliş açısı, FSS boyutu gibi özelliklerle analizler yapılarak bu değişikliklerin rezonans frekansına etkileri gözlemlenmiştir. Analiz sonuçları yorumlanırken S parametreleri kullanılmıştır.

10 GHz'ye ayarlanmış FSS tasarımının etkileri, uçağın farklı yüzeylerine uygulanması sonucunda gözlemlendi. Bu analizler iki adet horn anten ile yapılmıştır. Uçağın yüzey uygulaması yapılırken kanat, gövde ve burun olmak üzere üç ana parçadan oluştuğu varsayımından hareketle sırasıyla kanat profili, silindirik ve konik şekillerde uygulamalar yapılmıştır. Yapılan tüm analizlerde FSS'nin 10GHz bölgesinde soğurma

gösterdiği tüm geometrilerle doğrulanmıştır. Analizler CST Studio programında yapılmıştır.

**Anahtar Kelimeler:** frekans seçici yüzey, metalmalzeme, havacılık ve uzay, soğurucu



### 1.1 Literature Review

Frequency selective surfaces (FSS) are two-dimensional structures that consist of different physical structures on a dielectric substrate and can filter by interacting with electromagnetic waves at certain frequencies[1]. In other words, the transmission and reflection characteristics of frequency-selective surfaces change according to the frequency of the incident electromagnetic wave [2]. According to another definition, FSSs are metasurfaces that demonstrate electrical response [3]. As seen in all these definitions, FSSs have been developed by utilizing electromagnetic (EM) theories and electrical circuit theory[4].

A lot of research has been done on FSSs as they are for unique properties and many applications. The first known study on the subject was carried out by Marconi and Franklin in February 1919. Research on this subject began to be used for military purposes from the mid-1960s, and the first articles began to appear only in the mid-1970s, since it was confidential[5]. The use of FSSs as antennas first appeared in an article published in 1973. In this article, the use of FSS as a hyperbolic subreflector for dual-band reflector antenna design is investigated [6]. Later, FSS was used in many different applications[7][8].

With the rapid increase in the importance of defense technologies, it has become inevitable to define technologies developed for friendly or enemy elements as "targets". A study aiming to detect or not detect the target requires the control of the reflections originating from the target surface, the radiation and scattering occurring on and around the target surface, and the absorptions originating from the material from which the target is produced, in the frequency band of interest.

The detectability of a target can be measured in terms of radar cross-section (RCS). The radar cross-section is determined by the size, shape and material of the electrical target, and it can be briefly defined as a kind of ratio of the electromagnetic wave sent

to the target and reflected from the target[9].

Radar absorber materials are used on aircraft to reduce the radar cross-sectional area. FSS structures can be thinner in thickness than radar absorber materials so they make the aircraft lighter. FSSs have been tried to be used as absorbers in many applications [10][11][12][13].

Active FSSs(AFSS) can be used when switching is required for the transmission and cutting of the radome used in aircraft [14]. FSS containing active circuit elements are called AFSS. Some of the more detailed recent studies on FSSs are described in 2.2 and 2.1 tables.

## **1.2 Objective of the Thesis**

In this thesis, it is aimed to design a radar absorber FSS that can be applied to all surfaces of the aircraft at the 10GHz frequency within the X-band. In other words, the FSS to be designed should be able to provide the absorption effect on different inclined surfaces. In order to see the absorption effect on these different surfaces, FSSs will be coated on sample sections from aircraft surfaces. The obtained FSS coated aircraft parts will be measured with the help of two horn antennas and the effects of FSSs on transmission and reflection coefficients will be examined. With this study it is expected to provide a large amount of absorption on the inclined surfaces of aircraft, especially at 10GHz. Thus, the aircraft will not be detected by radars broadcasting in the 10GHz band so in the 10GHz band, the aircraft will be stealth.

## **1.3 Hypothesis**

In this study, firstly, an FSS cell design will be made that will show absorption in the 10GHz band. An FSS design will be made in which the transmission and reflection coefficients are appropriate in the 10GHz band, taking into account the periodic effect and other physical change effects. It will be ensured that the designed FSS cell is properly covered on the aircraft surfaces. Later, when analyzes are made on this inclined aircraft surface in the form of transceiver by means of horn antennas, it will be seen that the analyzes covered with FSS provide absorption by utilizing the transmission and reflection coefficients. In other words, FSS will provide absorption especially in the 10GHz band.

# 2

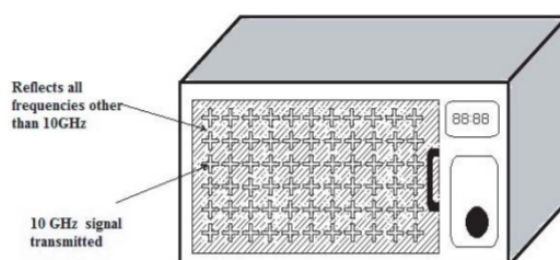
## FREQUENCY SELECTIVE SURFACES

---

Frequency selective surfaces (FSS) are electromagnetic filter circuits that can be adjusted by changes such as physical size and thickness[1]. Physical shapes designed for frequency selective surfaces consist of periodic structures [15]. Filtering can be done with frequency selective surface applications according to the electromagnetic wave that is desired to be filtered. Filtering can be adjusted according to the frequency of the incoming electromagnetic wave. It has a selective effect according to the desired frequency of the incoming electromagnetic wave. Frequency selection process is done thanks to these created surfaces, just like passive filtering in electronic circuits is implemented with capacitors, inductor and resistors. Thus, every FSS design can be considered as designing a circuit in the background [16].

### 2.1 Definition

FSSs have been the subject of research for over seventy years. FSSs were originally used mostly for military purposes. FSSs produced for military purposes are intended to reduce the radar cross section(RCS). In addition, it is used in various applications such as microwave oven applications [7], antenna designs[17], filter designs[8]. Physically, there are many frequency selective surface designs available. For example, thanks to the FSS application in the glass partition at the front of the microwave ovens, the electromagnetic wave in the oven is prevented from coming out Figure 2.1.



**Figure 2.1** Microwave oven with FSS Structures [7]

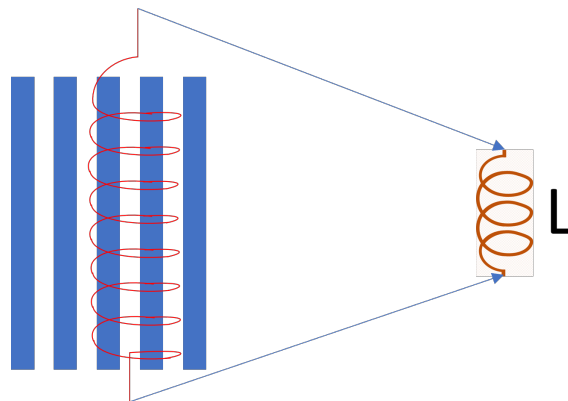
## 2.2 Equivalent Circuit

Frequency selective surfaces are obtained by shaping the surfaces of the materials from which they are made. FSSs mostly use rectangular structures. The reason for this is both the ease of their production and the ease of equivalent circuit modelling. Most FSS problems can be modeled using circuit theory and electromagnetic theory [1]. All FSSs exhibit properties such as capacitance and inductance used in basic electronic circuits [18]. FSS can be modeled as a mechanism constructed from capacitances and inductances [19].

### 2.2.1 Equivalent Circuit Modeling of Rectangular FSS

The simplest of the most used FSS designs is rectangular frequency-selective surfaces. Rectangular frequency selective surface can act as two different circuit elements, capacitance and inductance, according to the direction of the electric field. Inductance and capacitance values are affected by parameters such as the length and thickness of the frequency selective surface, the type of FSS material and the distance of the air gap between two FSS.

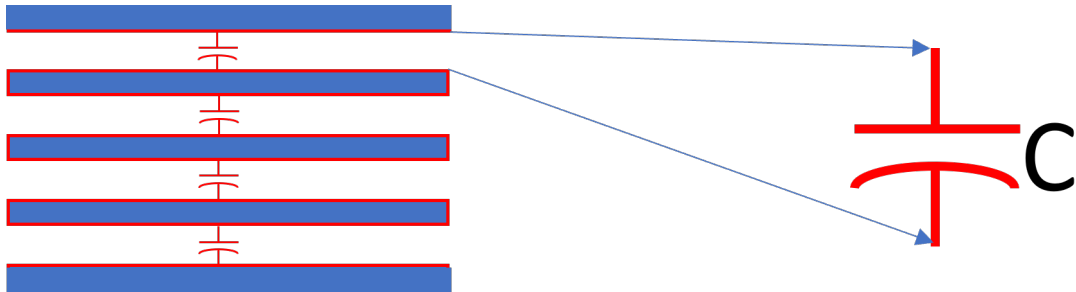
If there is an electric field parallel to the long side of rectangular frequency selective surfaces, an inductive effect occurs due to the coupling between the two rectangular structures [20]. We can model this inductive effect with a circuit element known as inductance. Figure 2.2 is a representative illustration of the FSS design modeled as an inductance.



**Figure 2.2** Modeling the effect of inductance on FSS

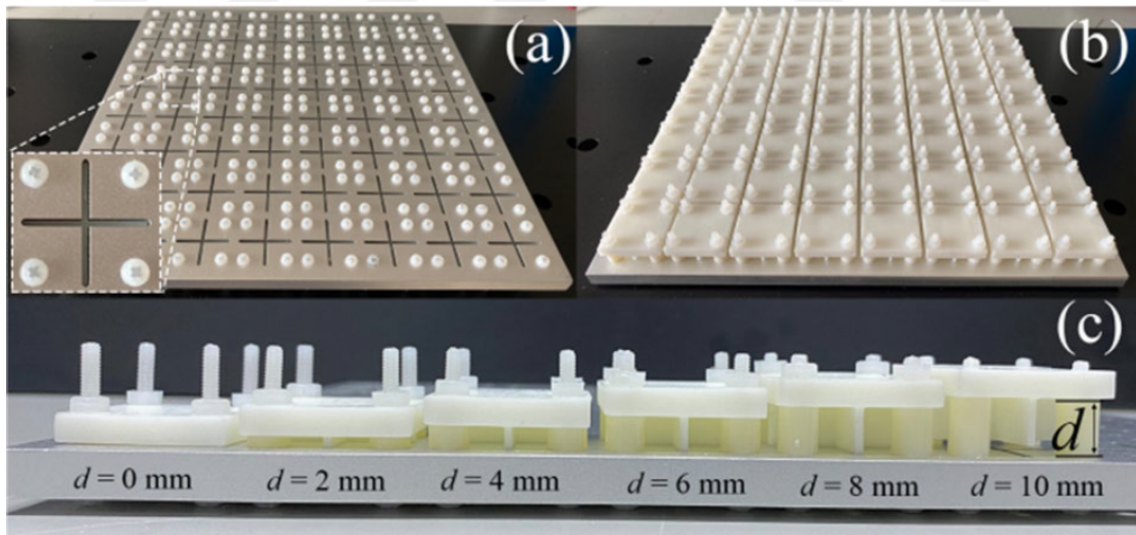
If there is an electric field perpendicular to the long side of rectangular frequency selective surfaces, a capacitive effect occurs due to the generation of opposite electric charges between the two rectangular structures. Since each rectangular FSS part is polarized with the previous FSS part and the next FSS part, a capacitive effect is observed between both neighboring rectangular FSS. We can model this capacitive

effect with a circuit element known as capacitance[19]. As it is known, an insulator is needed between two conductive plates for the formation of a capacitance. While the rectangular frequency selective surfaces act as conductors, the air gap between them acts as an insulator. Figure 2.3 is a representative illustration of the FSS design modeled as an capacitance.



**Figure 2.3** Modeling the effect of capacitance on FSS

For example, as a very special application, FSS design can be made in the desired frequency range with the effect of the change of material thickness on the capacitance, in other words, the resonance frequency can be adjusted by using a variable capacitance. In this way, a wide and variable absorption band can be obtained. Thanks to the variable capacity effect, more flexibility in bandwidth can be achieved compared to other variable capacities[21].



**Figure 2.4** Manufactured tunable FSS prototype. a) front side. (b) back side and inserted dielectric. (c) demonstration of different retraction depths  $d$  from 0 to 10 mm.[21]

FSS design produced with 3D printing technique, in which the frequency band can be adjusted with variable capacitance, is shown in Figure 2.4.

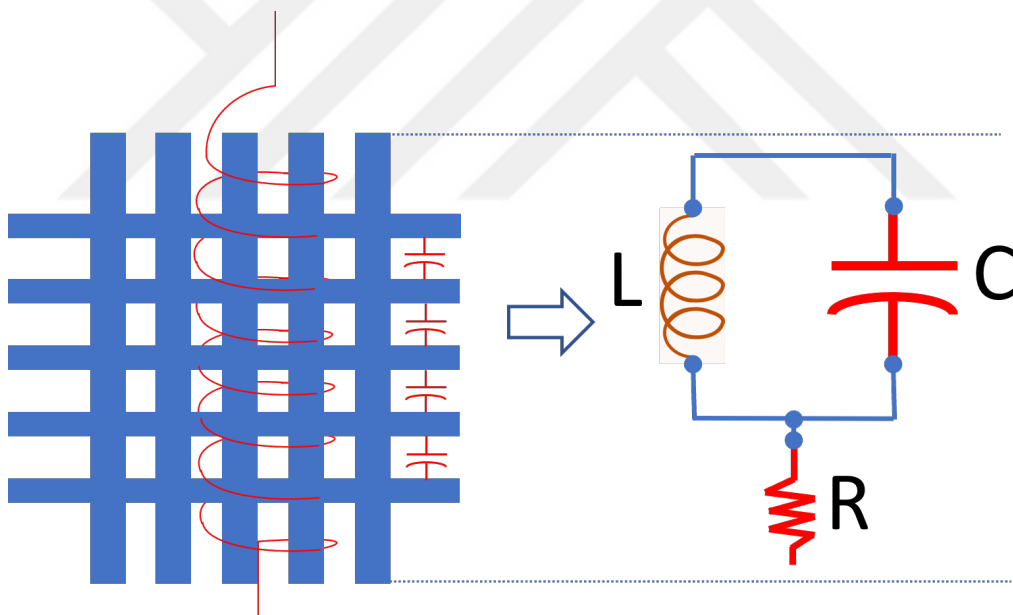
Finally, it is possible to model the resistance of frequency selective surfaces against the

conductivity of electromagnetic wave with the circuit element known as resistor.

If not only the capacitance value but also the L values or R values were changed as in Figure 2.4, a more flexible FSS design could be made.

Thanks to these equivalent circuits, all passive circuit elements are obtained by the simplest frequency selective surface. Just like in analog circuits, while designing filters with frequency selective surfaces, the desired filter response is tried to be obtained by changing the parameters of these passive circuit elements. While these parameters are obtained by connecting the necessary circuit element to the circuit in conventional circuits, they are obtained by changing the physical designs created in structures consisting of frequency selective surfaces.

The representation of the frequency selective surface in the form of a grid, which will be formed by combining 2 different frequency selective surfaces formed horizontally and vertically on the same plane perpendicular to each other, is given in Figure 2.5. Filters such as band-pass filters can also be designed thanks to grid-shaped FSSs [22].



**Figure 2.5** Grid-shaped FSS equivalent circuit model

The resistor element indicated by R is used to model the conduction loss in the circuit. C and L values can be changed for the required filter characteristics by using the equivalent circuit model. For example, if a larger capacitive effect is desired in the filter circuit to be created, the distance between the 2 rectangles perpendicular to the electric field should be reduced, as can be understood from the capacitance equation shown in equation 2.1.

$$C = \epsilon_0 \epsilon_r \frac{A}{d} \quad (2.1)$$

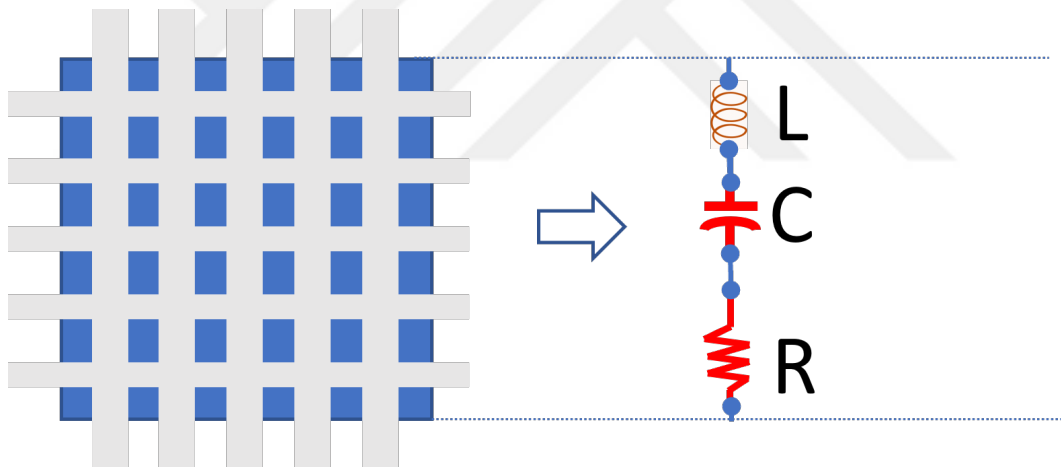
C is the capacitance, A is the area where the two plates overlap,

$\epsilon_0$  is the dielectric constant of vacuum,

$\epsilon_r$  is the relative dielectric coefficient and d is the distance between the plates.

If FSS is to be used in the form of equal sides like a square, it can be used independently of the direction. Because, provided that the electric field acting on the frequency selective surface is perpendicular, the capacitive and inductive effects of the frequency selective surface will be the same regardless of which side it comes from.

The equivalent circuit modelling of the FSS design consisting of small rectangular patches is shown in Figure 2.6. In other words, it can be said that the FSS design shown in Figure 2.6 is also designed by carving the grid-shaped frequency selector surface shown in Figure 2.5 from a whole plate.



**Figure 2.6** Rectangular patch-shaped FSS equivalent circuit model

The side lengths of the FSS design may not be equal in length according to the electric field direction. The square patch FSS is not named because of the possibility of these side sizes being inequality. For this reason, this equivalent circuit model is named rectangular patch FSS. Both adjacent rectangular patches show different inductive and capacitive effects horizontally and vertically. However, when the effect of these different inductive and capacitive effects on the FSS is reduced to unit cells, it can be modeled as a unit cell consisting of one capacitor, one inductor and a resistor.

## 2.3 Using in Aerospace Applications

In the defense sector, studies have been carried out to reduce the Radar Cross Section in general. Radar absorber materials (RAM) are used for this process. However, one of the most difficult areas was reducing the number of antennas. Research has proven that using arrays of conductive elements can at least narrow the frequency range to act on the surface. In other words, it has led to the emergence of new research topics such as filtering at certain frequencies (stopping certain frequencies or transmitting certain frequencies). Because a lot of antennas are used in airplanes. While these antennas continue their communication in a certain frequency range, functions such as absorption or reflection of EM waves coming by radars are needed. To meet this need, frequency selective surfaces can be used quite effectively. For example, since the part where the aircraft radomes are located contains an antenna, it is expected that the antenna will transmit maximum in the broadcast range, while at the same time, the reflection is expected to be minimum.

Frequency selective surfaces actually provide filters by changing the capacitance (C) and inductance (L) with physical changes, as explained in the equivalent circuit section. However, any change in the FSS dimensional parameters leads to an equivalent variation in the L and C values. Physically, when a unit cell of an FSS is illuminated by the EM wave, it can be converted to an equivalent resonance circuit. The resonance frequency can be found by equation 2.2, in which L and C represent the equivalent inductance and the capacitance of an FSS unit cell, respectively [23].

$$f_r = \frac{1}{2\pi\sqrt{LC}} \quad (2.2)$$

Frequency-selective surfaces have a wide usage area just like microwave circuits. It is possible to use frequency selectors for different purposes.

### 2.3.1 Electromagnetic Wave Absorber Frequency Selective Surfaces

FSSs produce beautiful reflection properties with band-stop filtering. Absorbing can calculate as  $\Gamma$  is reflection coefficient, T is transmission coefficient by equation 2.3

$$Absorption = 1 - |\Gamma|^2 - |T|^2 \quad (2.3)$$

In this type of absorber FSS, parameters such as the width of the absorption band and the reflection coefficient are important. FSSs, which are used as absorbers,

are developed to provide stealth in applications for the defense industry. These applications require high bandwidth, light weight and high absorption amplitude. Because these applications should not be caught by the radar and should not make the platform heavier in order not to reduce performances such as maneuvering. Since it will not be possible to achieve all these capabilities with a single FSS design, FSS design specific to each application should be made. Nowadays, studies in this field are current issues and some studies are compiled in the Table 2.1 below.

**Table 2.1** Publications of FSS designs used as radar absorber material

Publication Name	Publication Content
Design of Wideband Frequency Selective Absorber Based on Multilayer Structures [12]	Combining 2 FSSs with different absorption values, they changed the dimensions of the FSS and obtained a 3-layer absorber with an air gap and a ground layer on the ground. At the same time, they produced this FSS and compared it with the simulation result.
Ultra-Broadband 3-D Absorptive Frequency-Selective Transmission Structure Using Commercial Absorber [24]	A 3D absorber was made with commercially available materials. They got very close results with the measurement results and simulation results.
Multi-band Absorptive Frequency Selective Reflection Structures [25]	Multi-band absorber design has been made. An absorber was placed at the bottom before commercial materials, and then a cavity FSS was placed vertically above it. An absorber design consisting of 3 reflective bands has been made. In this way, it offers a wide absorption band. Obtained using commercial materials.
A Simple Frequency Selective Absorber Surface Design [13]	After optimizing the cross-dipole FSS, which they designed with an equivalent circuit approach, on top of the equivalent circuit optimization they had done before in the simulation program, they achieved the absorption in the desired band range (2-7GHz).

Another challenge for the designed FSS is to try to achieve all the features needed with a single FSS design. To overcome some of these difficulties, pin diode, which is one of the active circuit elements, is used. Frequency selective surface behavior can be changed thanks to the switching feature of the pin diode. For example, the diode can act as an FSS absorber when conducting, and as a reflector when off [26]. Such frequency selective surfaces formed by active circuit elements are called Active Frequency Selective Surfaces (AFSS). There is no general rule that AFSSs can only be achieved with pin diodes. FSSs formed with all electrical circuit elements known as active circuit elements are called AFSS. For example, an FSS created with a variable resistor is also considered AFSS. AFSSs not only change the behavior of the filter as absorber and raserber, but also contribute to bandwidth adjustment [27]. In this study, FSS and variable resistor are used to absorb the incoming wave at the desired frequency and size. Amplitude and frequency can be adjusted thanks to the variable resistor. Some publications on AFSSs are summarized in the Table 2.2 below.

**Table 2.2** Publications of AFSS designs used as radar absorber/raserber

Publication Name	Publication Content
A Wideband Switchable Absorber-Reflector Based on Active Frequency Selective Surface [28]	This study provides a compact design in terms of being used as both absorber and reflector in the same FSS cell. The signal to be transmitted can be transmitted without the need for design of FSS change.
A broadband active FSS absorber [29]	In this study, they designed a hexagonal ring FSS and controlled it by placing a diode between it and carried out their simulations. They have achieved a bandwidth of 6 GHz. In this bandwidth, they have achieved an absorption of 20dB.
Circuit Model Analysis of Switchable Perfect Absorption/Reflection in an Active Frequency Selective Surface [30]	They aimed to use the FSS as both a reflector and an absorber by using a pin diode. Then they produced the equivalent circuit model and simulated it in the simulation program. It completes the reflector/absorber switching function with 99% success.

**Table 2.2** Publications of AFSS designs used as radar absorber/rasorber (continued)

<b>Publication Name</b>	<b>Publication Content</b>
Active Absorption-Transmission FSS using Diodes [31]	By adding a pin diode between periodic FSSs, it acts as a conductive surface when transmitting, that is, when PIN diode is on. When PIN Diode is off, it acts as an absorber. At 9GHz, it has an absorption value between 95% and 99.5% in absorption, while it has a value of 87% absorption in transmission.
Tunable and Broadband Radar Absorber Based on PIN Diodes Controllable FSS [32]	In this paper, they propose a fast tunable broadband microwave absorber based on active frequency selective surface (AFSS).
The research on the effects of an active FSS with circle element on the characteristics of Radar Absorbing Materials [33]	In the analyzes in this study, its effect on the absorption band was observed by changing the resistance value. In some applications, the effect of this situation on the absorption band was observed by adding 2 FSSs and changing the FSS dimensions instead of the resistance value.
An Ultra-Wideband Metamaterial Absorber With Active Frequency Selective Surface [34]	It is formed as a result of combining 2 pieces of material with a semi-circle on one side and a triangle on the other with a PIN diode. It was simulated in simulation program and then produced and the results were compared. A designed broadband metamaterial absorber with a total thickness of 4.15 mm is obtained, it can be adjusted continuously in the range of 2 GHz to 14 GHz as the bias voltage of PIN diodes ranges from 0.60 V to 1.00 V.

**Table 2.2** Publications of AFSS designs used as radar absorber/rasorber (continued)

<b>Publication Name</b>	<b>Publication Content</b>
Switchable Broadband Dual-Polarized Frequency-Selective Rasorber/Absorber [35]	Rasorber/absorber design is made with a double-sided FSS and a diode placed on the upper FSS. The produced FSS measurements were compared with the simulation results. By controlling the bias conditions of the PIN diodes, switchable functionality between rasorber and absorber modes can be realized. The measurement results and the simulations were compatible.
Design of a broadband and switchable absorber using an absorb/reflective FSS [10]	In this study, rasorber/absorber transition can be made with diode switching and analyzed up to 8 GHz band

## 2.4 Affecting Factors

Small size, low periodicity, duality of polarization, being unaffected by angle, high bandwidth, multiplicity of resonance frequency and easy reproducibility are the most important features of FSSs. While these features are important, it is very difficult to make designs suitable for these parameters [1]. In order to make the best frequency selection, it is necessary to evaluate all the parameters of the FSS well. The best way to use these parameters is sometimes to change the spaces and sometimes to use patches. Therefore, the frequency region in which FSSs resonate is affected by many parameters.

### 2.4.1 Influence of Physical Design

One of the most important factors determining the frequency properties of frequency selective surfaces is the geometrical structures of the elements forming the unit cells. There is no restriction on the geometric shapes of the elements forming the frequency selective surfaces. Any geometric shape can be used for an FSS design that provides suitable characteristics. The most used FSSs can be examined in 4 main groups according to their physical properties [1].

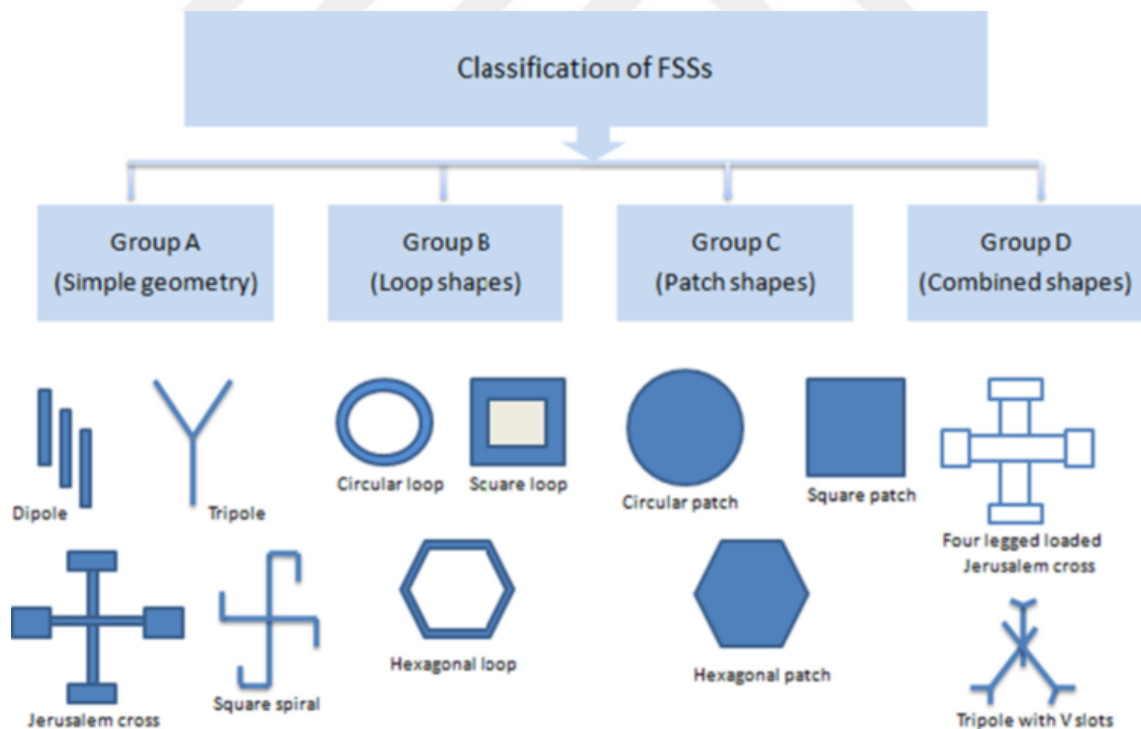
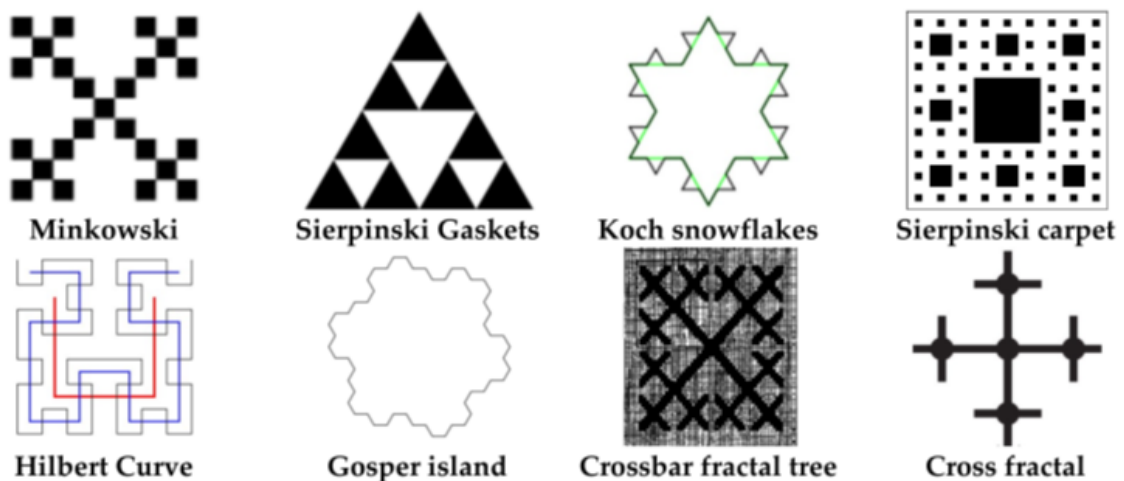


Figure 2.7 Fundamental Shapes of FSS [36]

These four basic groups, shown in Figure 2.7, can be expressed as:

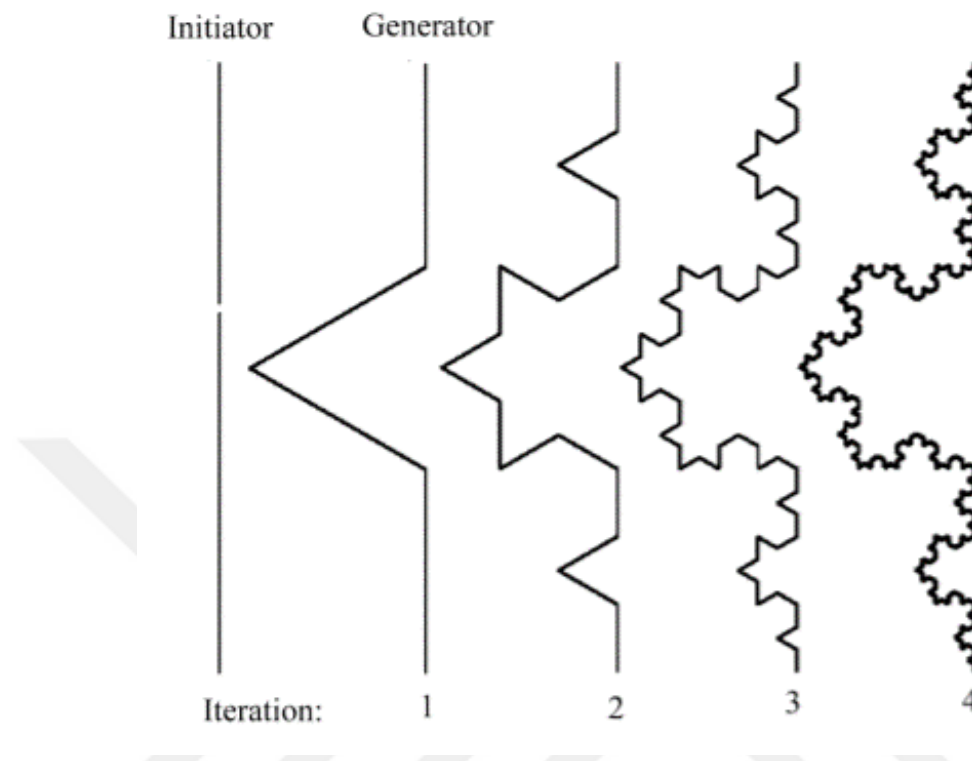
- **Group-A:** Centrally connected or N-poles, for example simple straight element, anchor elements, Jerusalem Cross etc.
- **Group-B:** Loop structures, such as three – or four legged elements, circular loops, square and hexagonal loops.
- **Group-C:** Solid interior or plate types of various shapes, Square patch, circular patch etc.
- **Group-D:** Hybrid structures or mixed of all combinations.

Today, FSS designs associated with fractal geometry theory are also developing rapidly due to their fascinating properties [37]. Fractals are produced by endlessly repetitive combinations of a created geometric shape in different combinations [38]. Below is an example of FSS with many fractal structures in Figure2.8.



**Figure 2.8** Examples of fractal FSS developed in different studies [23]

Iterative methods are used when designing fractal FSSs [39]. The Koch curve was used to reduce the dimensions of the metallic Koch fractal FSS [40]. Figure 2.9 shows how to construct a fractal FSS using the Koch curve step by step.



**Figure 2.9** Creating iterative fractal FSS using Koch Curve [39]

#### 2.4.2 Size Effect

In addition to the shapes of the geometries used in the FSS design, their size is one of the important factors that determine the frequency properties of frequency selective surfaces. Efficiency of electromagnetic waves can be controlled by the distance between two neighboring FSS cells at different incidence angles [41].

Size change in frequency selectors is a multidimensional parameter. In other words, as the size increases, the resonance frequency decreases because the frequency is related to the wavelength, but this is not a general truth. Because the effect of size change on each Frequency selective surface is different. This can be explained by the fact that their equivalent circuits are different. Therefore, the size change causes different changes in capacitive, resistive and inductive values in each FSS [42]. Equivalent circuit modeling of some of the most well-known frequency selector surfaces in the circuit is given in the Figure 2.10 below.

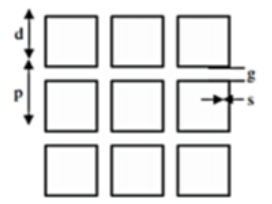
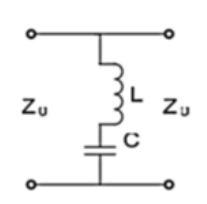
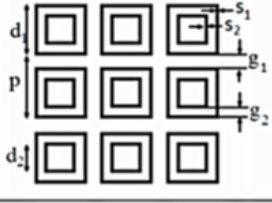
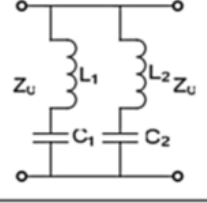

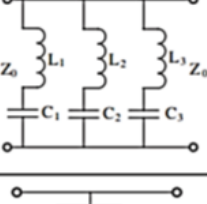
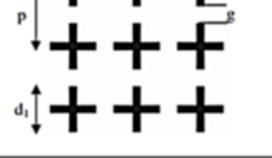
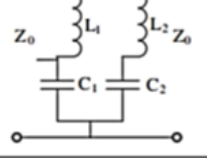
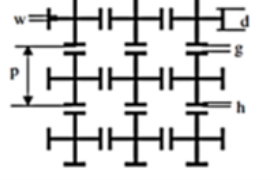
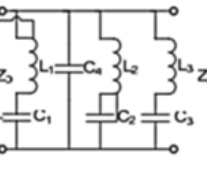
S. No	FSS	Circuit	Equivalent Circuit	Equivalent Inductance	Equivalent Capacitance
1	Single Square Loop			$\frac{X_L}{Z_0} = \frac{d}{p} F(p, 2s, \lambda)$	$\frac{B_C}{Z_0} = 4 \frac{d}{p} F(p, g, \lambda)$
2	Double Square Loop			$\left(\frac{X_L}{Z_0}\right)_1 = F(p, s_1, \lambda)$ $\left(\frac{X_L}{Z_0}\right)_2 = F(p, s_2, \lambda)$	$\left(\frac{B_C}{Z_0}\right)_1 = 4F(p, g_1, \lambda)$ $\left(\frac{B_C}{Z_0}\right)_2 = 4F(p, g_2, \lambda)$
3	Triple Square Loop			$\left(\frac{X_L}{Z_0}\right)_1 = F(p, s_1, \lambda)$ $\left(\frac{X_L}{Z_0}\right)_2 = F(p, s_2, \lambda)$ $\left(\frac{X_L}{Z_0}\right)_3 = F(p, s_3, \lambda)$	$\left(\frac{B_C}{Z_0}\right)_1 = 4F(p, g_1, \lambda)$ $\left(\frac{B_C}{Z_0}\right)_2 = 4F(p, g_2, \lambda)$ $\left(\frac{B_C}{Z_0}\right)_3 = 4F(p, g_3, \lambda)$
4	Cross Dipole			$\frac{X_L}{Z_0} = \frac{d}{p} F(p, w, \lambda, \epsilon)$	$B_x = 4 \frac{w}{p} F(p, g, \lambda)$ $B_d = 4 \frac{d}{p} F(p, p-w, \lambda)$
5	Jerusalem Cross Array			$\frac{X_L}{Z_0} = \left(\frac{d}{p}\right) F(p, w, \lambda)$	$B_d = 4 \frac{(2h+g)}{p} F(p, p-d, \lambda)$ $B_x = 4 \frac{d}{p} F(p, g, \lambda)$

Figure 2.10 Basic FSS equivalent circuit representations [42]

Therefore, setting the FSS size depends on the structure of the FSS itself.

### 2.4.3 The Effect of the Dielectric Material Used as A Substrate

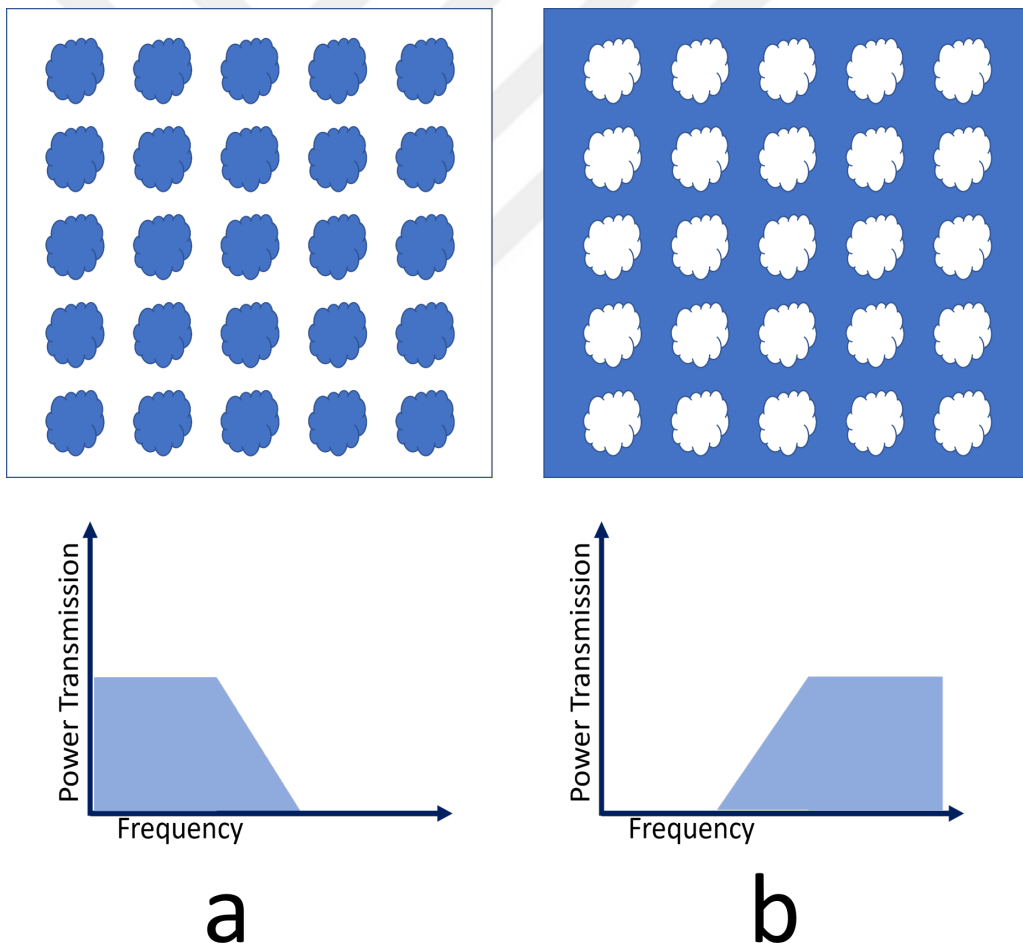
Dielectric substrates on which frequency selective surfaces are placed are also an important parameter in the design. This may cause the resonant frequency of the FSS to shift due to unsuitable substrates and as a result the FSS is not designed properly. The dielectric constant and thickness of the dielectric material show that they affect the resonance frequency of the FSS [43]. In order to adjust the resonance frequency correctly, appropriate dielectric material should be used and its thickness should be adjusted accordingly. The dielectric layer may consist of several layers as well as being the substrate. So substrates can also be used as inter layers [44].

#### 2.4.4 Material Type Influence

As described in the previous sections, frequency selective surfaces can be modeled with capacitance (C), inductance (L) and resistances (R) corresponding to conductor losses [45]. Generally, materials with high conductivity are chosen to reduce the loss in this resistor. In addition, when setting the FSS center frequency, it has little effect from the surface impedance [46].

### 2.5 Frequency Selective Surface Types and Filtering Features

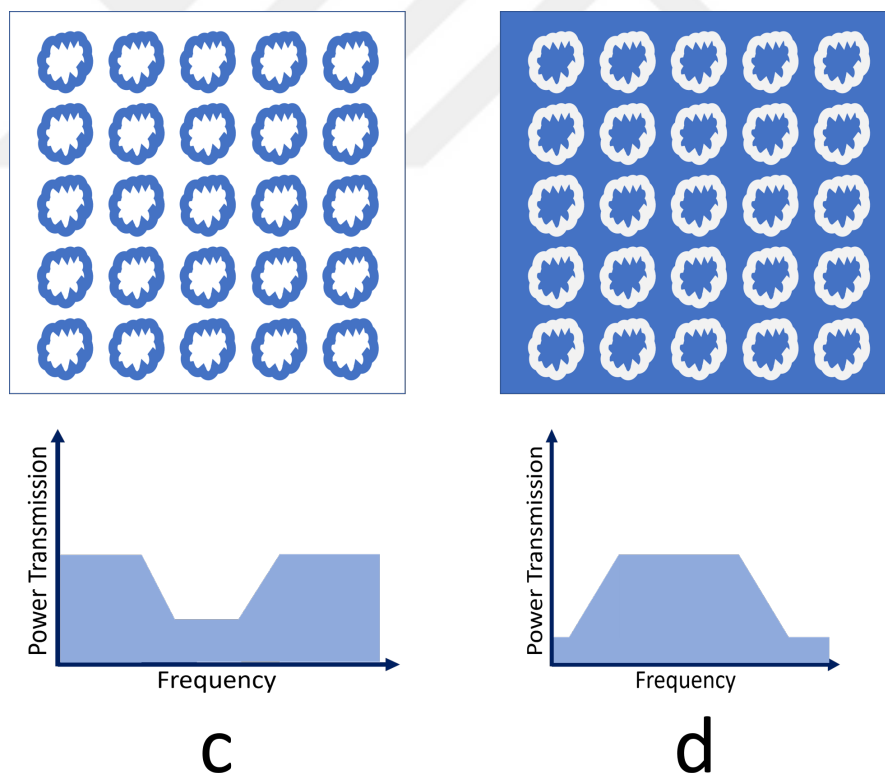
Generally, frequency selective surfaces are divided into two different designs in the form of cavities and patches. Thanks to the different designs of these cavities and patches, different filter characteristics can be obtained. In general, the filter characteristics realized with different frequency selective surfaces formed by the combinations of cavity and patch surfaces are as in Figure 2.11 below.



**Figure 2.11** General filter characteristic acquired with FSSs a) low pass Filter b) High Pass Filter

While it is possible to create low-pass filter structures with frequency selective surfaces designed as patch arrays, high pass filters are obtained with frequency selective surfaces designed as cavities. From the combination of these 2 fundamental Frequency-selective surfaces, which have different filter characteristics, the filters in the Figure 2.12 below, known as band-pass filters and band-stop filters, can be obtained.

Actually frequency selective surfaces are customized filters, as can be understood from their basic filter characteristics. The elements of these filters are the cavities and patches that make up the structure. All these filters are not easy to do with FSS. It has problems such as bandwidth, angular stability, low transmission coefficient and low reflection coefficient response. These FSS structures can be similar to capacitive and inductive circuit elements also used in electronic circuits. In other words, each hole and patch in the FSS corresponds to the capacitance, inductance and resistance, which are passive circuit elements that we use in analog circuits. Frequency selective surfaces are affected by many parameters and as a result of these parameter changes, filtering characteristics change [8].

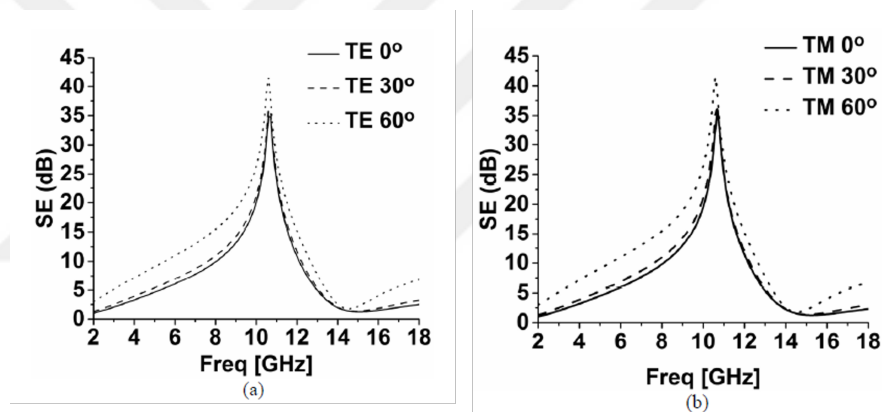


**Figure 2.12** Filter characteristics obtained by the combination of patch and cavity FSSs c) Band Stop Filter d) Band Pass Filter

### 2.5.1 Band Stop Filters

The FSS structure allows EM waves of certain frequencies to pass, and sometimes FSSs act as band-stop filters, blocking the waves in the specified frequency range [1]. This band-stop filter feature can be used to protect against unwanted EM waves. This situation is encountered in many applications as the prevention of electromagnetic interference (EMI). EMI, electronic/avionic equipment will cause false results or malfunction. EMI is mostly encountered as a problem to be overcome in aerospace applications (planes, satellites, antenna design) [47]. Shields are used to protect from EMI [48]. Band-stop filter applications made with FSS are mostly used for protection from electromagnetic interference [49]. The frequency characteristic of radar absorbers is usually band-stopping filter characteristic. Shielding efficiency is important in a narrowband band-stopping filter characteristic [50].

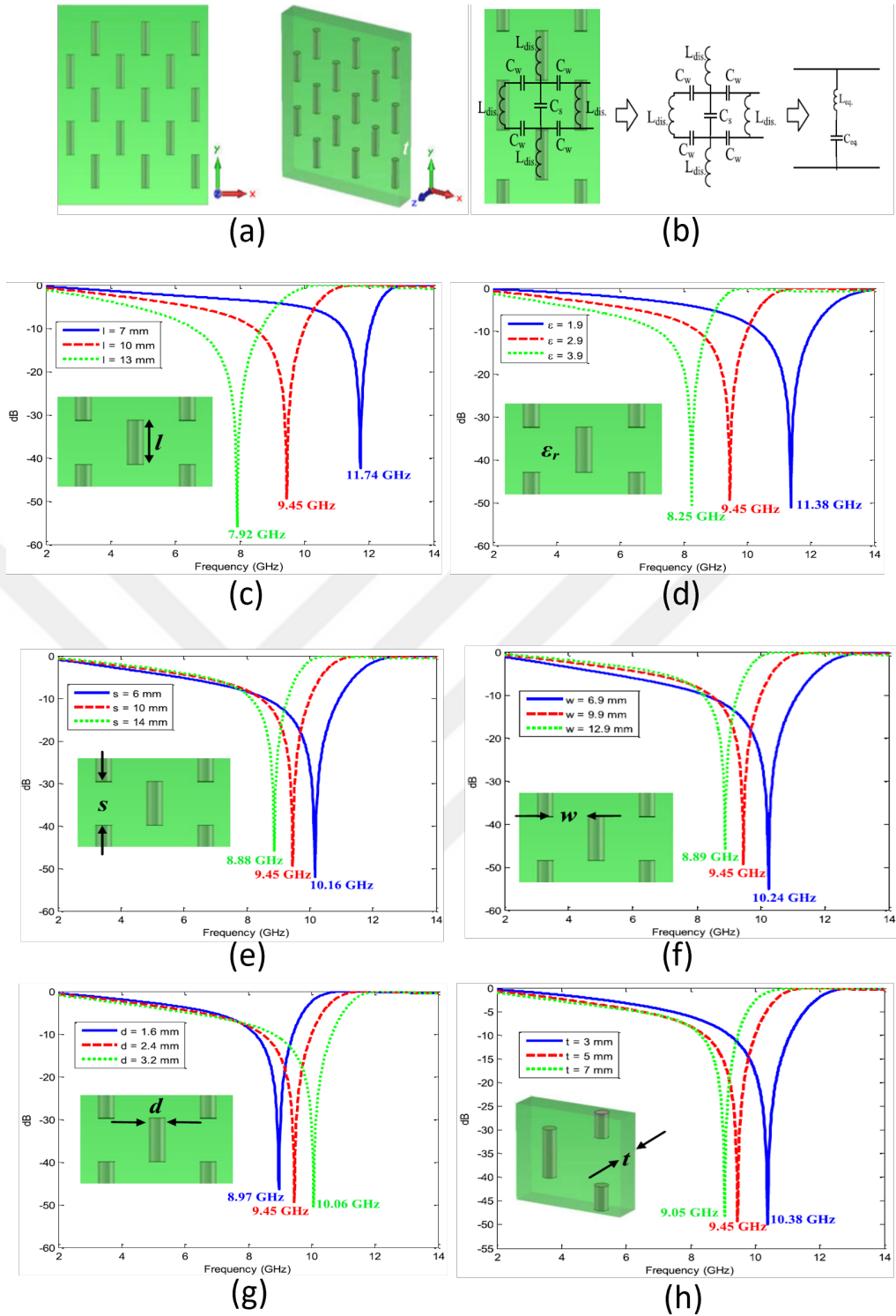
The angular effect of the FSS design with a well-optimized shield efficiency on transverse electric (TE) and transverse magnetic (TM) is as in Figure 2.13 below.



**Figure 2.13** Angular effect of shielding effectiveness. (a) TE wave mode (b) TM wave mode [50]

Frequency selective surfaces are mostly customized for a particular bandwidth. These FSSs are usually customized to bands known as X band, KU band and KA band covering 8 GHz to 40 GHz [51]. Not every FSS provides a broadband filter characteristic, some FSS implementations are specialized to a single band gap, such as X band [47]. Some FSS implementations can filter out multiple discontinuous bands (non-adjacent bands), [52]. Multi-band filters can be made thanks to multiple layers [11] [12].

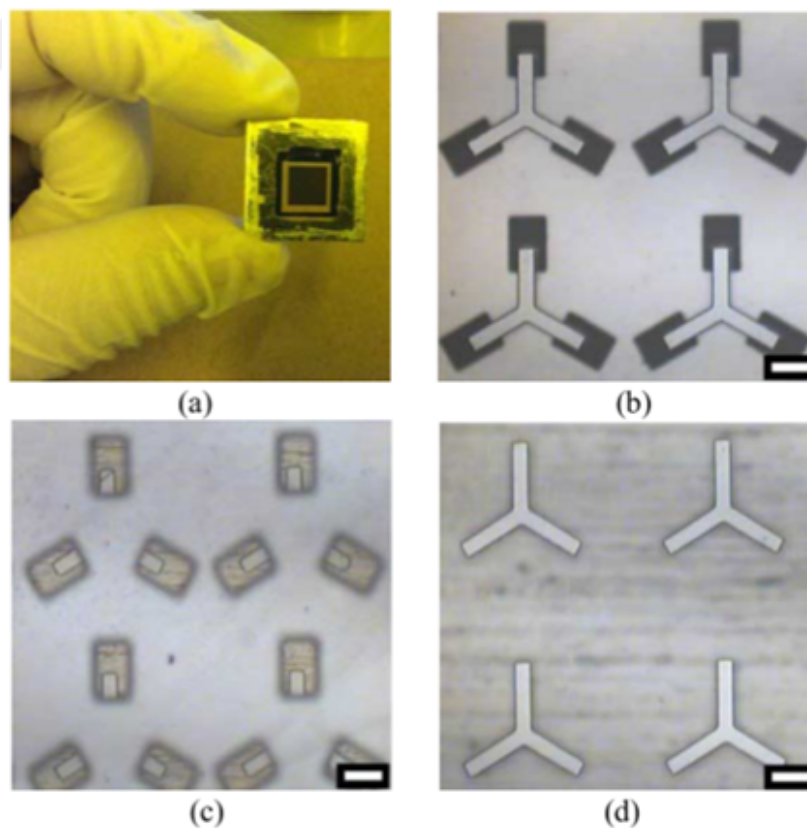
Band-stop filters should also be evaluated with all their parameters. Some of these parameters are the thickness of the FSS, the vertical and horizontal distance between adjacent FSS cells, the vertical and horizontal length of the FSS, the value of the dielectric constant of the substrate [8]. Figure 2.14 shows the effect of changes in all these parameters in the FSS design on the frequency characteristic of a bandstop filter.



**Figure 2.14** The effect of parameter changes on the reflection coefficient in a band stop FSS design. (a) front and perspective view of the FSS, (b) equivalent circuits of FSS structures, (c) the effect of changing the long side of the FSS structure, (d) the effect of the dielectric change of the substrate on which the FSS structure is placed, (e) effect of variation of vertical distance between two FSS structures, (f) effect of variation of horizontal distance between two FSS structures, (g) the effect of changing the short side of the FSS structure, (h) the effect of the substrate thickness on which the FSS structure is placed [8]

### 2.5.2 Band Pass Filters

Band-pass filters, as explained in the previous sections, are filters that allow EM waves in a certain frequency band to pass and prevent EM waves at other frequencies from passing. Unlike bandstop filters, this type of filter adjusts the amplitude and bandwidth of the frequency of the EM wave to be transmitted. Band-stop filters are mostly used as absorbers, while band-pass filters are used where EM wave transmission is very sensitive in certain frequency ranges, such as radome [53]. Since radomes are not flat surfaces, the designed frequency selectors must be customized according to the surface geometry and material type [54]. FSSs with bandpass filter capabilities can be tuned to customized bandwidth such as X band [55]. FSSs designed for extremely high frequencies are also available. As the frequency increases, the FSS dimensions decrease as the wavelength decreases. FSS designs required to filter frequencies in the terahertz range are also quite small [56]. The selectivity efficiency of FSS filters designed at such high frequencies should also be quite high [57]. FSS can be made multi-layered to provide sufficient frequency sensitivity and bandwidth. The bandpass FSS designed in the terahertz region is very difficult to produce and see because its dimensions are quite small. Figure 2.15 below has an example of a bandpass FSS customized to the terahertz region.



**Figure 2.15** Produced THz FSS (a) , optical microscope image of (b) the top metal layer, (c) the middle metal layer, (d) the bottom metal layer, scale bar= $30\mu\text{m}$  [57]

### 2.5.3 Low Pass Filters

Low-pass filters allow frequencies up to the set frequency to pass through, and they are filters that attenuate sufficiently by taking higher frequencies to the cutoff. According to the low-pass filter characteristic shown as a representative in Figure 2.11(a), the circuit allows frequencies up to the desired frequency to pass, and if it is above the determined frequency, it gradually cuts off. This damping decreases after a while and ends completely. In the ideal filter characteristic, it is desired that the damping frequency range be zero. The process of optimizing filters presents several challenges. the higher the degree of the filter circuit, the closer the filter characteristic to the ideal ratio is [58] . If the filter order could be infinite, ideal filter characteristics would be obtained [59]. The problem of reaching this ideal characteristic is called the approximation problem [60]. In Figure [2.16], the effect of the filter order on the low pass filter properties is seen.

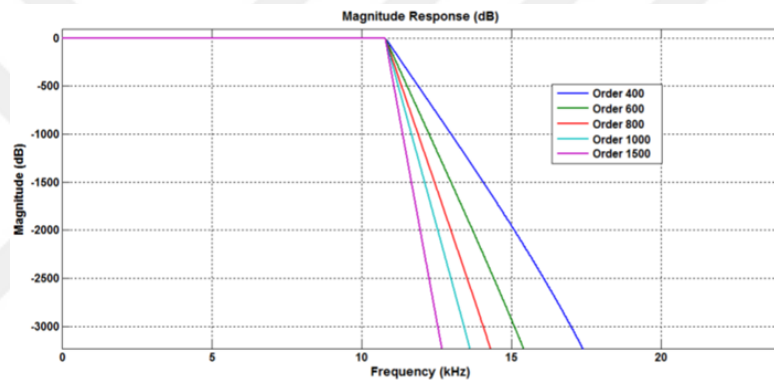


Figure 2.16 Effect of filter order on low-pass filter characteristics [58]

As the filter degree increases, the complexity of the circuits also increases. Various methods have been developed to reduce these complexities. Chebyshev and Butterworth methods are the most known and used methods. Figure 2.17 shows the effect of various methods on the filter characteristics[61].

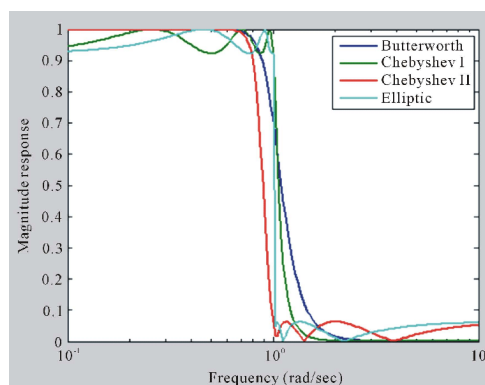
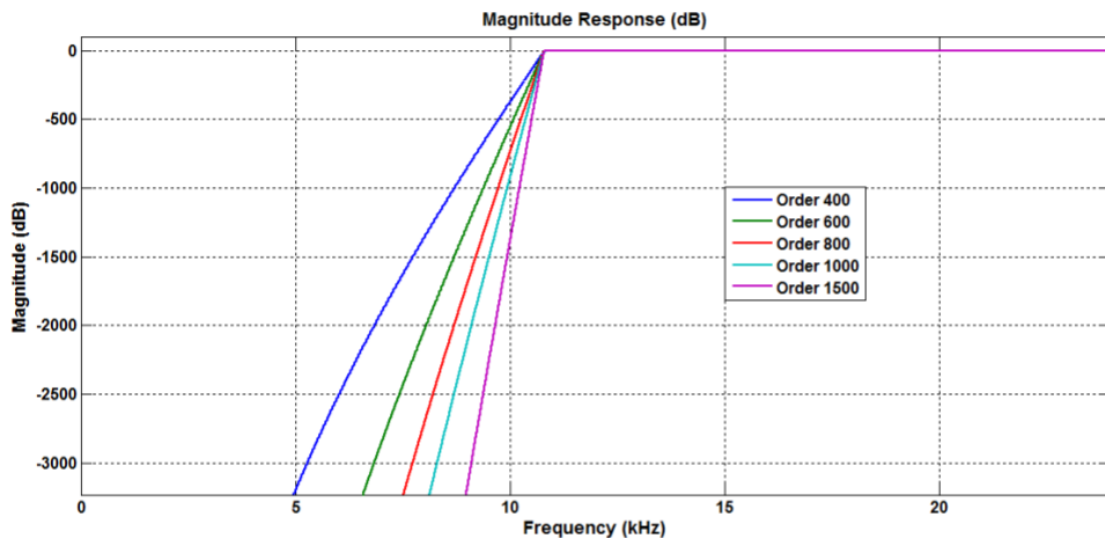


Figure 2.17 Comparison of Chebyshev Type-I Filter, Chebyshev Type-II Filter, Elliptical Filter vs. Butterworth Low Pass Filter [61]

Low-pass filter applications have been made with FSS for a long time [62]. Just like in electronic circuit theory, there are similar purposes when designing filtering circuits with FSSs. While filtering with frequency selector surfaces, higher order more ideal filters can be designed [63] [64] [65]

#### 2.5.4 High Pass Filters

High-pass filters prevent frequencies below the specified frequency from passing. Just as low-pass filters suppress high frequencies, high-pass filters suppress low frequencies. According to the high-pass filter characteristic shown in Figure 2.11(b), the circuit prevents frequencies up to the desired frequency from passing through and allows them to pass above the determined frequency. It can be said that high-pass filters are the duality of low-pass filters. Parameters such as filter order effect and approximation problem, which are valid for low-pass filters, are also valid for high-pass filters. The approximation problem also applies to high-pass filters. The order of the filter increases to provide the ideal high-pass filter characteristics. In Figure 2.18, the effect of the filter order on the low pass filter properties is seen.



**Figure 2.18** Effect of filter order on high-pass filter characteristics [58]

A band-pass or band-stop filter actually includes both low-pass and high-pass filters. In other words, the high-pass filter is inside the band-pass filter. High pass filter does not mean that it can only be used at high frequencies. It is generally used in terahertz applications, which are high frequency applications[66] [65].

# 3

## DESIGN OF FREQUENCY SELECTIVE SURFACE

---

FSSs have a very wide usage area that It was explained in the previous sections. In this thesis, an FSS that provides absorption in the 10GHz region and can be applied to different surfaces will be designed. Since it will be applied to an aircraft for stealth feature, maximum absorption is desired. The formula for absorption was mentioned in equation 2.3. The reflection and transmission coefficients directly affect the absorption. Therefore, evaluations will be made on the  $S_{11}$  parameter and  $S_{21}$  parameters throughout the thesis. Radio frequency networks are characterized using S (scattering) parameters, and this video provides an easy introduction to S parameters and how they are used to quantify impedance matching and power transfer in radio frequency networks [67]. The Figure 3.1 below shows a representative representation of the S parameter modeling of a 2-port system.



**Figure 3.1** Representation of S parameters in a 2-port system

$S_{11}$  is the input port voltage reflection coefficient,  $S_{12}$  is the reverse voltage gain,  $S_{21}$  is the forward voltage gain and  $S_{22}$  is the output port voltage reflection coefficient [67].

FSSs are theoretically infinite periodic arrays, but in reality it is not possible to realize an infinitely long array. FSSs containing a finite number of elements are particularly affected by the change in the angle of incidence of the wave. The two most important parameters to be considered in frequency selective surface design are angular stability and polarization independence. Being independent of polarization can be achieved if the designed unit cell is symmetrical horizontally and vertically. It is usually a good idea to make a unit cell smaller because it generally provides better resonance stability with the angle of incidence and possibly larger bandwidth. For angular stability, the unit cell must be very small. because the smaller the cell, the better the incidence angle of the wave on the cell and better resonance stability. For this reason, an infinitesimal cell is important for Angular stability. However, since FSS cell cannot be infinitely small, it would be good to design cells as small as possible. Then it is necessary to decide what filter modeling will best suit this purpose. Finally, it is necessary to model the most suitable physical design for the filter model that will achieve this object by supporting it with analysis. There are several commercial EM Analysis programs available to perform these designs and analyzes. Some of these programs are ANSYS HFSS, ALTAIR FEKO and CST Studio Suite. The studies carried out throughout this thesis were obtained in the CST Studio 2020 program. CST Studio Suite can be used to simulate and design FSS through the whole workflow, from the design of the resonator to the implementation in a full device.

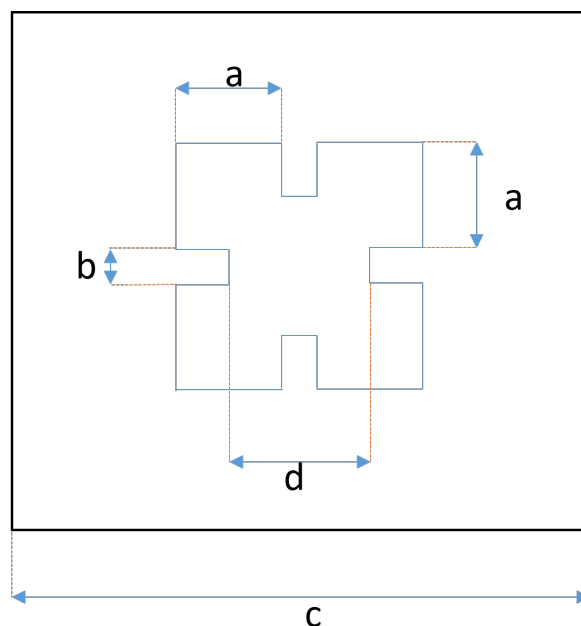
### **3.1 Simulation of The Desired FSS Design**

Electromagnetic simulation programs use numerical modeling such as Maxwell's equations Finite Integration Technique (FIT)[68] or Finite Difference Time Domain (FDTD)[69] technique to model EM propagation. The FIT and FDTD methods are similar. The difference between them is due to the form of Maxwell's equations. FIT uses the integral form as the name suggests, while FDTD uses the differential form of Maxwell's equations. FIT provides high flexibility in geometric modeling and boundary machining according to FDTD[70]. Due to these advantages and the user friendly interface, FSSs are modeled in the CST program. Periodic structures such as Frequency Selective Surfaces (FSS) or metamaterials (DNG, AMC, etc.) can be modelled by a single cell if infinite extent of the structure is assumed. Unit Cell boundary conditions with a full Floquet port mode formulation can be used to simulate arbitrary angles of wave incidence; if only normal incidence is of interest, Periodic boundaries can be used. CST has a special tool for periodic structures. In this way, unit cells can be modeled directly and periodic conditions can be assigned automatically.

### 3.1.1 Development of the Unit Cell of FSS Design

Each designed FSS must be chosen specific to the application. Because every FSS provides advantages and disadvantages to the application with its physical properties and filtering characteristics. As a physical feature, the smaller they can be designed and implemented, the less design problems they have. The most important factor is the adjustment of the filtering characteristics, as their physical properties often present very similar difficulties.

**Selection of Suitable Filter Characteristic:**When designing frequency-selective surfaces, first of all, it should be decided for what purpose it will be used. While some basic FSSs can provide the desired filtering directly, some FSSs need to be optimized according to the desired frequency. In this thesis, basic FSSs were mentioned in fig 2.8. Each FSS type has different filtering characteristics. The main types of FSS associated with these different filters are shown in figures 2.11 and 2.12. Radar absorber FSSs generally work on a band-specific basis. In this study, FSS design was made to select the 10GHz band. In other words, absorption will be provided around 10GHz. Different types of frequency selective surfaces have been tried to meet this requirement. While designing a frequency selective surface, it is physically easy to produce and its applicability to surfaces is as important as the importance of frequency selection. Because an FSS that cannot be produced will not be meaningful even if its performance is verified by simulations to be very good. Similarly, its applicability is also important. In the light of all this information, the design of the frequency selective surface designed below figure 3.2 will be realized in this thesis.



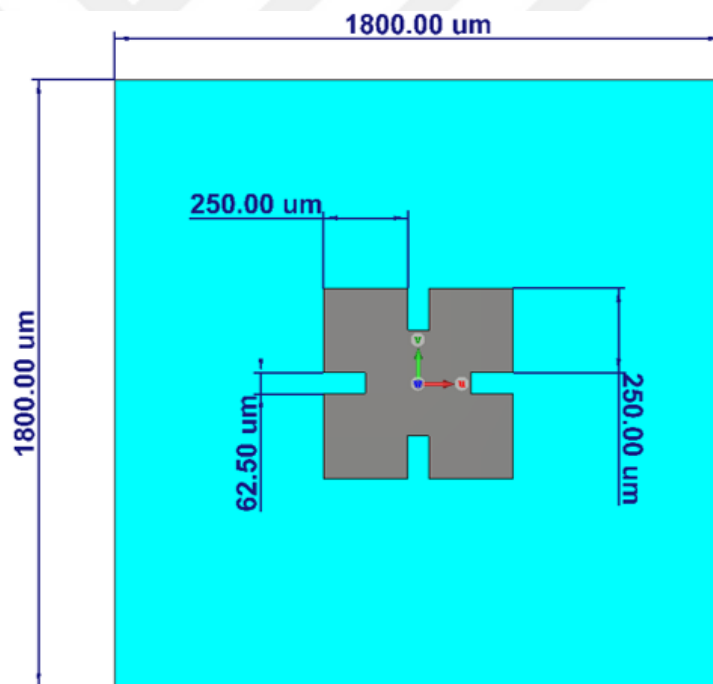
**Figure 3.2** Unit cell representation of the FSS

Here, the distances indicated by a, b, c and d are given as ratios.

- $a=250$  units,
- $b=62.5$  units,
- $c=1800$  units,
- $d=312.2$  units,

Here,  $c$  is the side length of a periodic cell, that is, the substrate length of the unit cell is 1800 units. The edge length of the FSS design produced with PEC is approximately 562.5 units.

The first version of when 1 unit is calculated as 1 micrometer, the resulting CST design is as follows figure 3.3.



**Figure 3.3** Unit cell representation of the FSS in CST Studio

The substrate thickness of the design created is 60 units.

The following image 3.5 is a representation of the image in Figure 3.3 from another angle.

Figure 3.4 shows the boundary conditions and periodicity of an FSS cell in the CST program. It analyzes an FSS cell as if it were an infinite periodic structure.

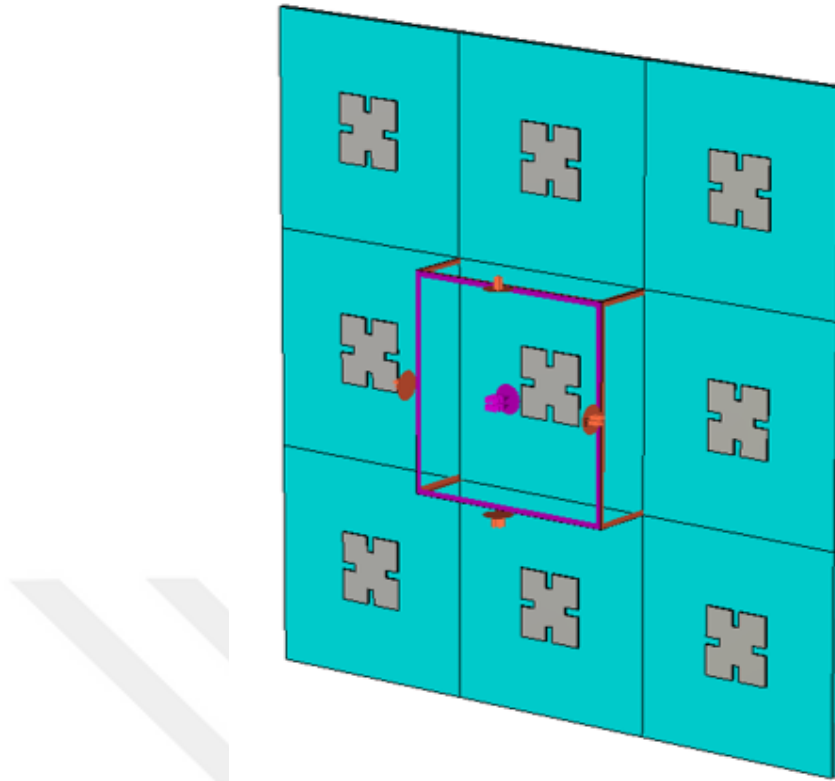


Figure 3.4 Boundary conditions and periodic representation of an unit FSS cell

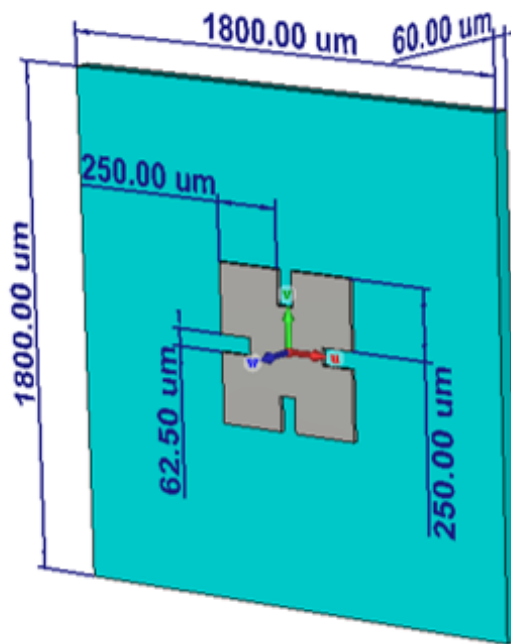
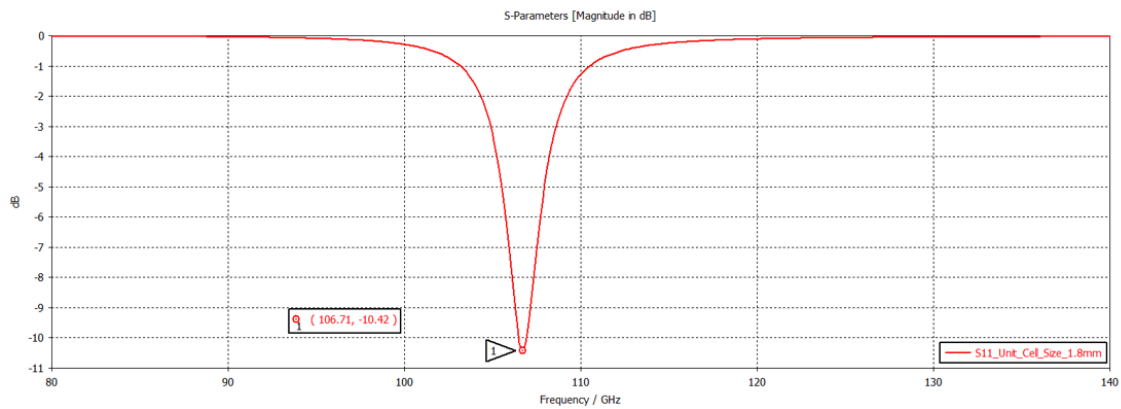


Figure 3.5 Unit representation of FSS from cross view

FR-4 Epoxy sheet is used as substrate. FSS is designed as a perfect conductor (PEC). When the designed FSS unit cell was analyzed, the following figure 3.6 result was obtained.



**Figure 3.6** Result of draft FSS in CST Studio

It was expected that the FSS design would absorb high frequencies due to its small dimensions. As expected, the FSS resonated in the very high frequencies 100-120 GHz region. The number 1 marker indicates the frequency of the central resonance and the magnitude of the reflection coefficient. The center frequency is 106.72MHz and the corresponding S11 value is -10.42dB. So more than 90% percent is absorbed by the FSS.

As a result, the frequency selective surface showed a good absorption characteristic as a draft. However, it is not at the expected values due to the fact that the size of the FSS is very small and the resonance frequency is very high. In addition, the production of FSS designed in those dimensions will be very difficult.

For this reason, the resonance frequency should be adjusted to the desired frequency value, 10 GHz, and at the same time, FSS dimensions should be increased to a reproducible level. Then, the best results will be obtained by performing various parametric analyzes in that region. To set the operating frequency of the frequency selective surface around 10 GHz, the following operations will be performed.

- **Scaling on the FSS**
- **Thickness changing of FSS**
- **Thickness changing and substrate**
- **Incident wave angle changing**

These items are very important design parameters for any FSS to be designed. Because a specific FSS design is made for each application. It may be possible to provide the same frequency band with different FSSs. The important thing is to use the design parameters correctly and to provide the desired resonance frequency and sufficient S parameters.

### 3.1.2 FSS Tuning Based on Influence of FSS Design Parameters

The resonance frequency can be adjusted with variables such as the physical size changes of the frequency selective surfaces, the angle of the incident wave and the effect of the substrate material.

#### 3.1.2.1 Effect of Scaling on the FSS

With the design made in the draft FSS design in the previous section, the resonant frequency was set to 106.71GHz. A larger FSS design is generally needed to reduce the resonant frequency to lower frequencies. The reason for this is that the FSS dimensions interact with the increase in wavelength as the frequency decreases. This size increase does not always keep the frequency characteristic the same, allowing for minor adjustment. Large size changes sometimes result in two resonant frequencies, sometimes resulting in features such as bandpass filters. For example, our new FSS design, which is formed by small changes in our FSS dimensions, is shown below with the result.

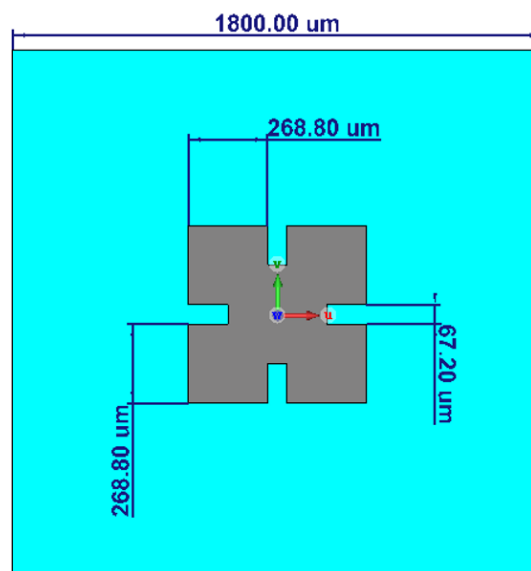
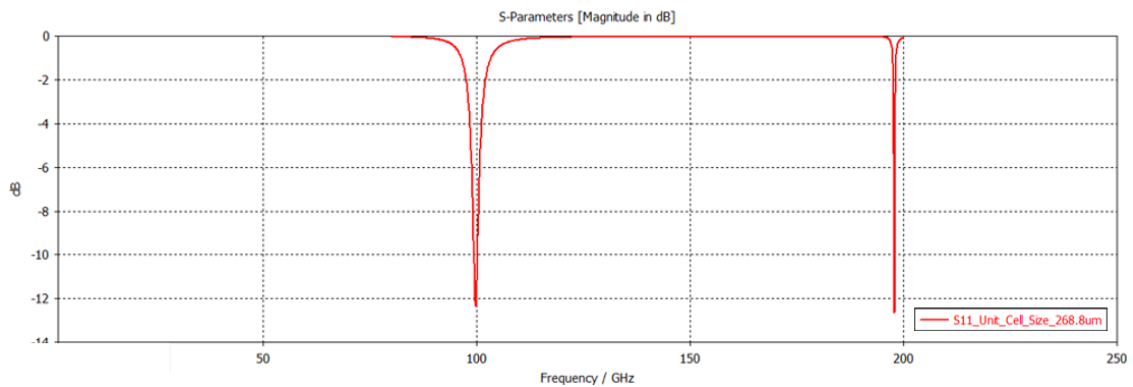


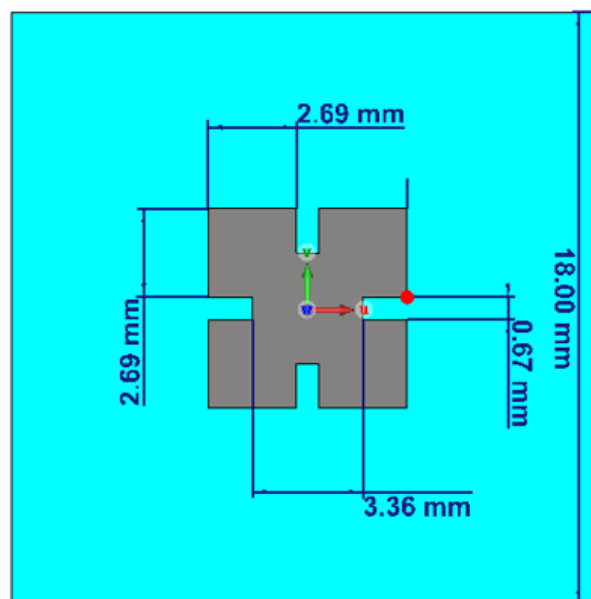
Figure 3.7 Slightly oversized unit cell of FSS design in CST Studio

As can be seen from the analysis in Figure 3.8, the resonance frequency has shifted a little towards 100GHz with little increase in frequency selective surface sizes. However, a second resonance frequency was observed. Because capacitive and inductive effects occur in the frequency selective surface equivalent circuit, dimensions matched with a second resonant frequency have been reached with the size change. Such an effect was seen for this FSS type. Third resonance frequency could be observed with another variation of dimensions.



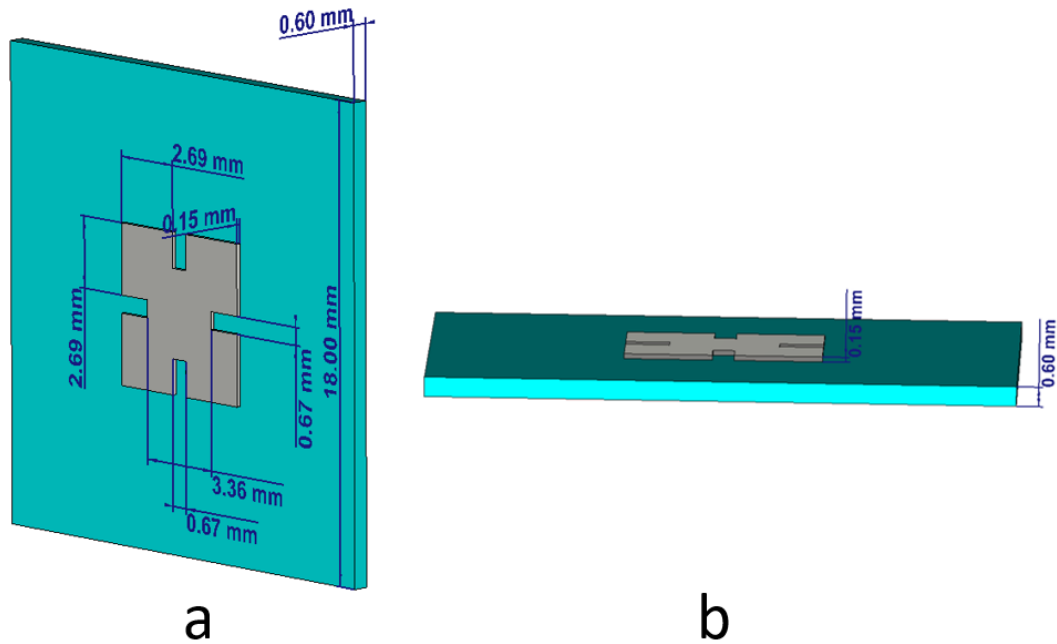
**Figure 3.8** Result of slightly oversized unit cell of FSS design in CST Studio

The resulting two resonance frequencies are at 100 GHz and 195 GHz, respectively, and have a value of approximately -12.3 dB. As can be seen from this result, the size of the frequency selective surface must increase much more in order to reach the 10GHz band. In order to decrease it from 100 GHz to 10GHz, when we increase the FSS size by about 10 times, a design like Figure 3.9 below is obtained. The representation of this design from different angles is as in Figure 3.10. FR-4 material is used as substrate.



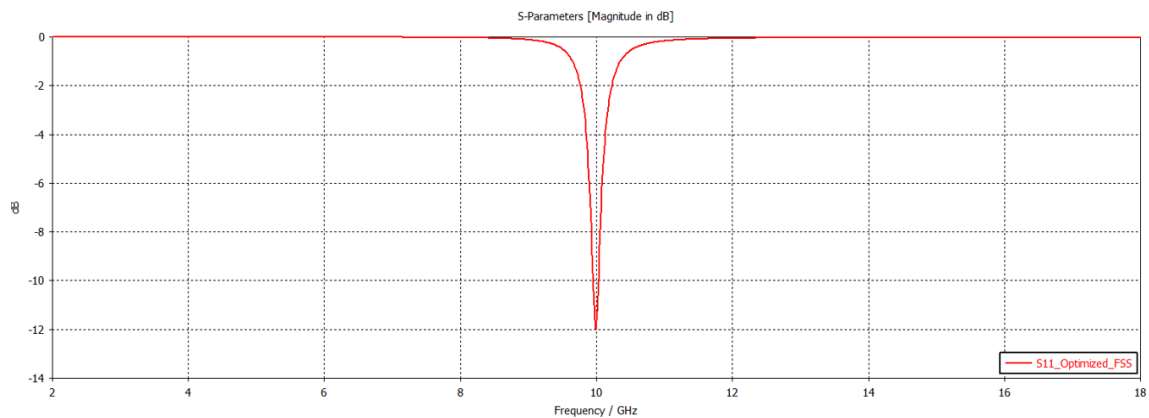
**Figure 3.9** Unit cell of FSS dimensions optimized for 10 GHz in CST Studio

As can be seen from Figure 3.10 below, the FSS PEC thickness is 0.15 mm and the substrate thickness is 0.6 mm and the total thickness is 0.75mm.



**Figure 3.10** View of unit cell of FSS optimized for 10 GHz from different angles in CST Studio a) Perspective view of FSS b) Horizontal section view of FSS

The result of FSS tuned according to 10GHz is in the figure below. FSS has a value of about -12dB at 10GHz. FSS provided an absorption of over 90% of the transmitted signal at 10GHz. FSS has a bandwidth of about 100MHz between 9.95Ghz and 10.05Ghz below -10dB.

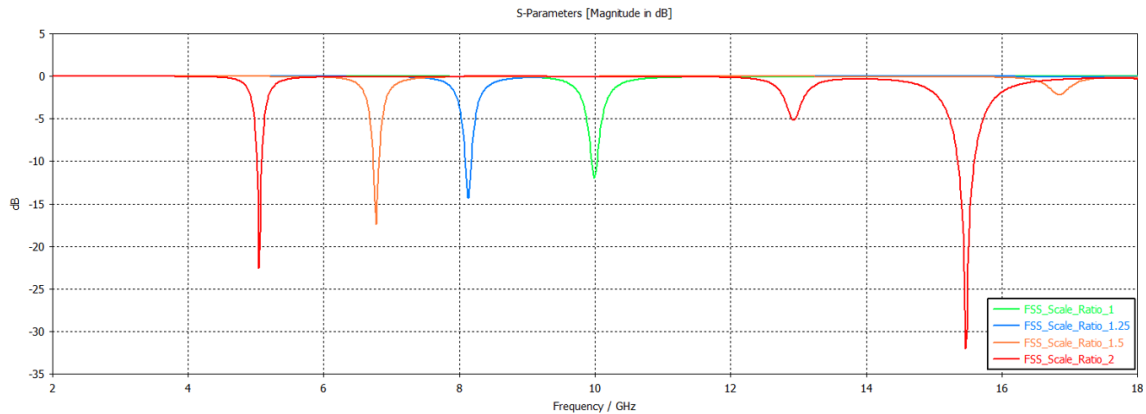


**Figure 3.11** Result of unit cell of FSS optimized for 10 GHz in CST Studio

FSS was obtained in the desired filter characteristic and size. It is necessary to make other analyzes in order to see the proportional effect of the horizontal dimension change on the frequency characteristic.

If the ratio of the horizontal dimensions of the FSS in Figure 3.9 above is accepted as

1 and the ratio is increased by 50% in each step up to 3, the result will be as in Figure 3.13 below.



**Figure 3.12** Result of optimized unit cell of FSS of different sizes in CST Studio

As can be seen from the legend shown in the graph, the green line shows the original FSS size set to 10Ghz.

The blue line shows the result of the original FSS multiplied by 1.25 times its dimensions. The resonant frequency is about 8.15 Ghz and the S11 value here is -14.5dB.

The orange line shows the result of the original FSS multiplied by 1.5 times its dimensions. The resonant frequency is about 6.85 Ghz and the S11 value here is -17.5 dB.

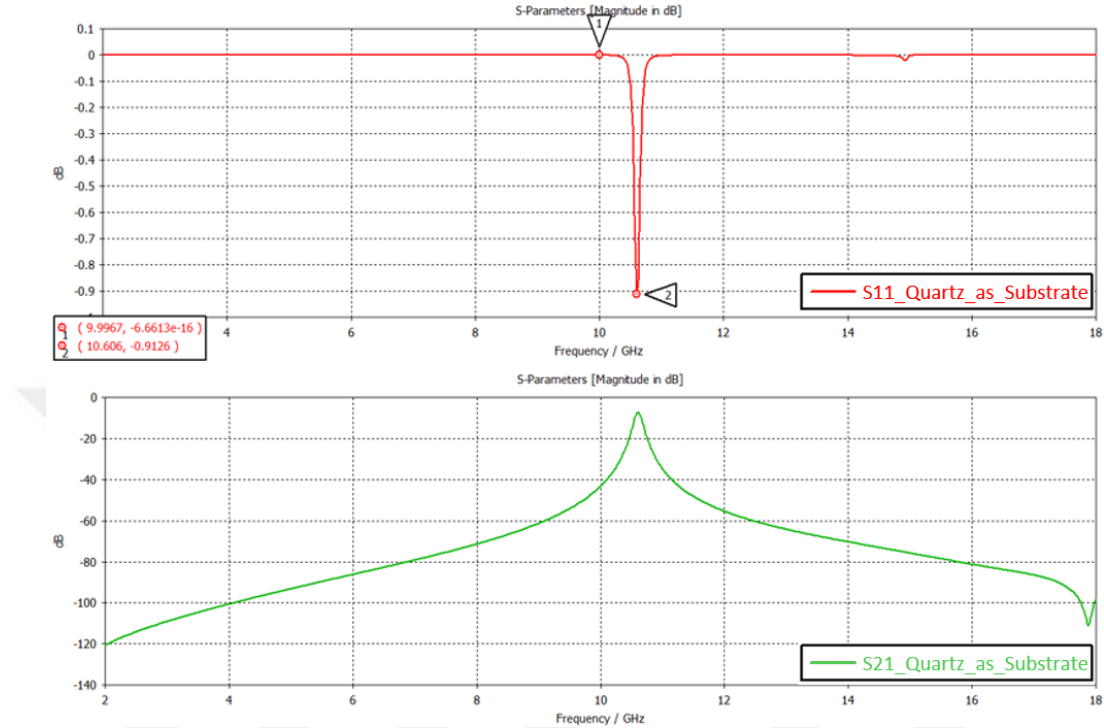
The red line shows the result of the original FSS multiplied by 1.5 times its dimensions. In this dimension, more than one resonance frequency is observed. In this graph shown in red, these 2nd and 3rd resonance frequencies, which are caused by wavelength and reflection, are actually present in the graph shown in orange when looked carefully. The reason why the analysis is not seen as clearly as indicated by the red line in the graph shown with the orange line is that the analysis is limited to 18GHz. If the analyzes were done up to 30Ghz, a new resonance frequency would be observed around 20Ghz. The resonant frequency of the FSS design shown with the red line is 5.1Ghz, 13 and 15.5 GHz, respectively. The S11 parameters corresponding to the frequency values are -22.5dB, -5dB and -32.5db, respectively.

Generally FSS horizontal dimensions are changed, thickness is not changed.

In the next articles, it will be explained how other factors affect this filter characteristic.

### 3.1.2.2 Effect of Substrate

For the result in Figure 3.11, FR-4 was used as the substrate material. When quartz material with a dielectric constant of 3.8 is used at the same thickness, the resonance frequency changes as in the result graph below 3.13.



**Figure 3.13** The result of unit cell of FSS optimized for 10 GHz using quartz substrate

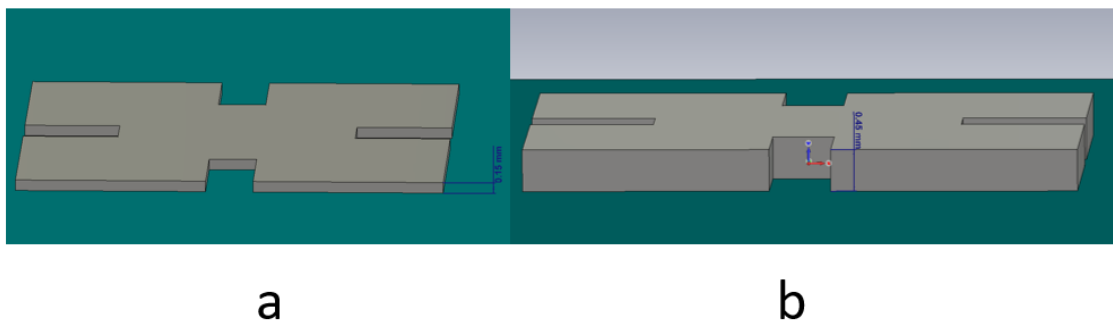
In figure 3.13 above, the graph shown with the red line shows the S11 parameter, while the graph with the green line shows the S21 parameter. Marker 1 shows that the S11 parameter is almost zero when at 10 GHz. The number 2 marker shows the 10.6 GHz resonance frequency. A shift occurred at the resonant frequency of about 600MHz and the S11 value was -0.9dB. As a result, the substrate change actually changed the FSSin S11 parameter graph considerably. Because the dielectric constant changes with the substrate change, the FSS design needs to be re-optimized. There are several ways to do this optimization.

The procedures that can be done to tune the resonant frequency using a quartz substrate are given below.

- **Re-scaling on the FSS**
- **Re-scaling substrate thickness**
- **Re-scaling substrate**

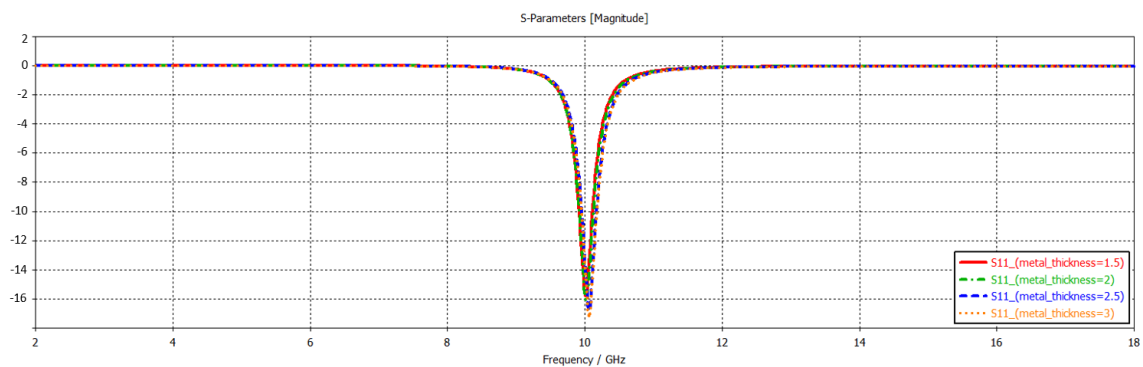
### 3.1.2.3 Effect of Metal Thickness on the FSS

So far, the effect of horizontal dimension change on the resonance frequency has been observed on frequency selective surfaces. Generally, thickness changes are not preferred in FSSs because they make the thicknesses with standard plates. Since the thickness of these plates cannot be changed, there is usually horizontal dimension change. However, if the thickness could be changed or if a new plate was to be produced according to the optimized design, the parametric sweep analysis in Figure 3.14 below was performed in order to show the effect of the thickness change on the resonance frequency. The FSS model shown as in Figure 3.14 a) belongs to the original FSS design, which is 0.15mm thick and adjusted to 10GHz, shown on the right in Figure 3.14 b) is the 0.45 mm thick FSS designed.



**Figure 3.14** Changing of metal thickness of unit cell of FSS a)FSS thickness=0.15mm b)0.45mm

The result in the Figure 3.15 below is the analysis result of the thickness change.



**Figure 3.15** The result of FSS metal thickness change

According to the results of this analysis, the change in FSS thickness does not affect the resonance frequency as much as the horizontal dimension change. FSS thickness changing analysis result shows that the 0.45mm thick design with the maximum thickness and the design shown in orange provide maximum absorption with approximately -18dB. As a result, S11 parameter size increased as the thickness increased.

### 3.1.2.4 Effect of Incident Wave Angle

In all analyzes up to now, the incident wave was acting at a right angle to the surface. To see the angle effect, it will be sufficient to see intermediate values such as 30 degrees and 60 degrees. In order to see the effect of the FSS signal interacting with this right angle and the effect of the signal coming from different angles, it is necessary to analyze the waves coming from different angles. The result of the analysis made to see the effect of the phi angle change is as in Figure 3.16 below. Figure 3.17 shows the effect of angle change on the result of S21.

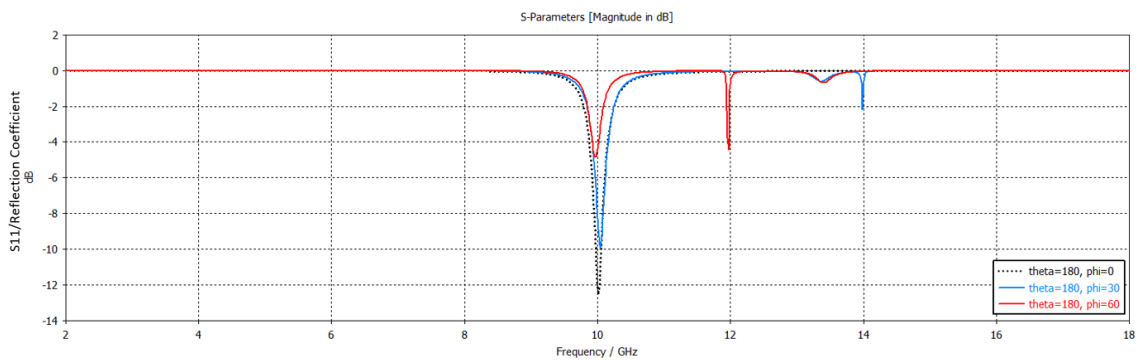


Figure 3.16 S11 result of unit cell of FSS due to incident wave phi angle changing

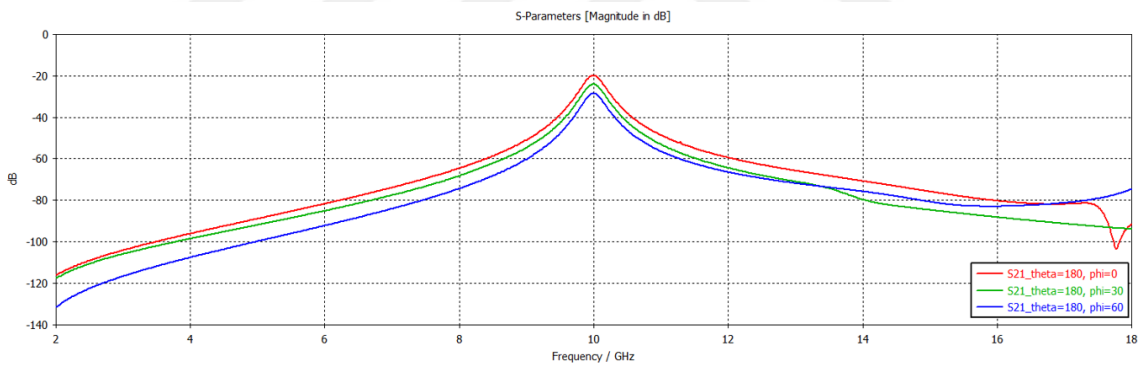
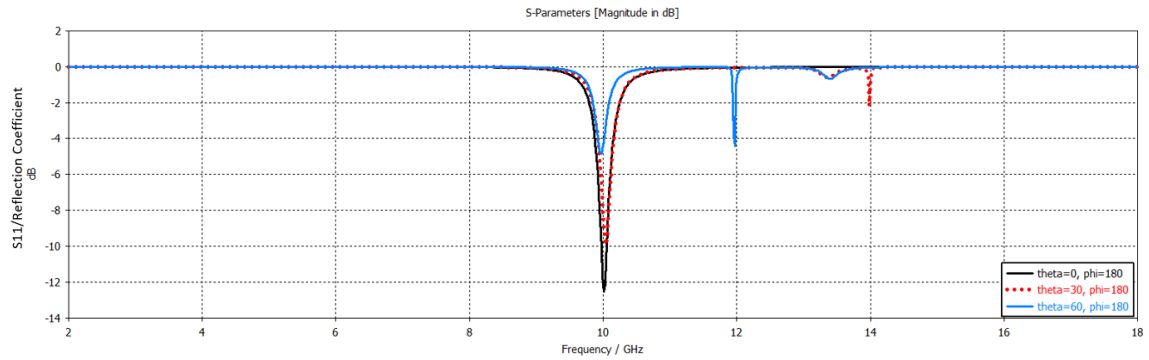


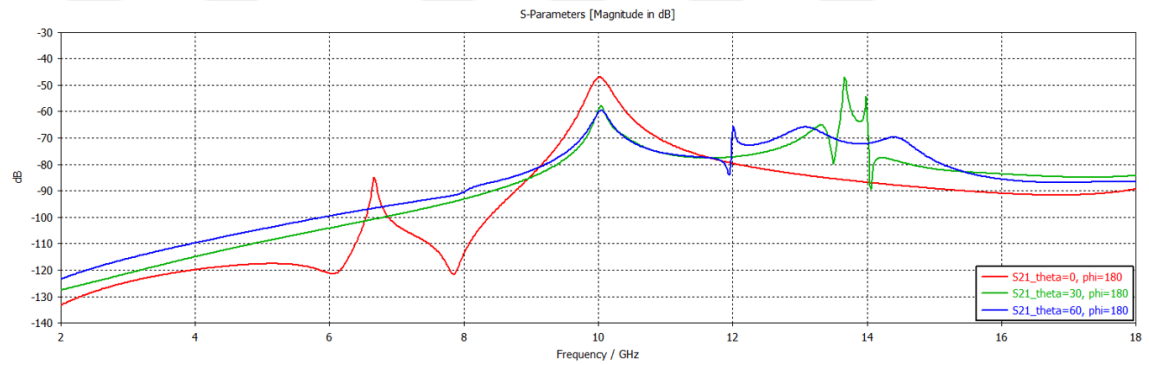
Figure 3.17 S21 result of unit cell of FSS due to incident wave phi angle changing

The result of the analysis made to see the effect of the theta angle change is as in Figure 3.18 below. Figure 3.19 shows the effect of angle change on the result of S21.



**Figure 3.18** S11 result of unit cell of FSS due to incident wave theta angle changing

Figure 3.19 shows the effect of angle change on the result of S21.



**Figure 3.19** S21 result of unit cell of FSS due to incident wave theta angle changing

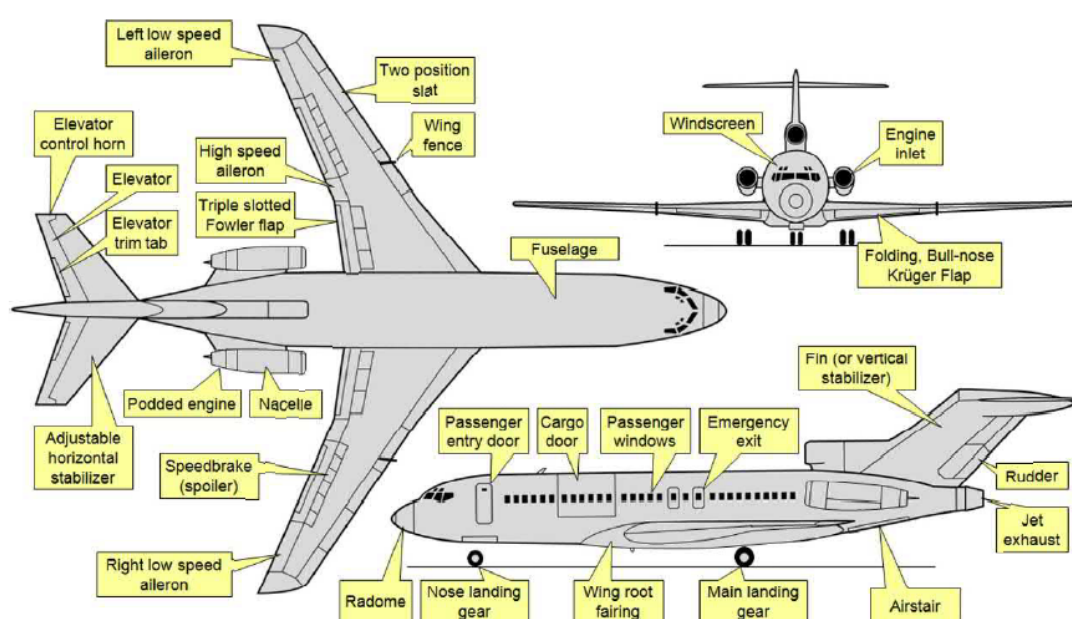
As seen in the analysis results, it cannot be said that the angle change changes the resonance frequency too much, but it can be said that it changes the S parameter values.

## FSS IMPLEMENTATION TO 3D GEOMETRIC MODELS

In the previous section, the development of the optimized FSS design for 10GHz was explained in detail. In this section, the absorption effect of FSS will be observed when the designed FSS is applied to different geometries that may be on the aircraft. Before observing the effect of FSS and FSS on the aircraft, brief information about the general surfaces of the aircraft is given below.

The outer surface geometries of airplanes are designed according to their purpose. Some of these purposes consist of commercial aircraft sometimes used to carry passengers, while others consist of warplanes. Although they have different external geometric structures, there are basic surfaces necessary for flight.

The Figure 4.1 below showing the aircraft outer core parts and control surfaces is of a commercial passenger aircraft.



**Figure 4.1** Illustration of Boeing B-727 commercial jet aircraft geometric components [71]

Although the dimensions of the planes change, their outer geometries consist of similar shapes in general terms. Because these designs have been optimized as the most aerodynamically optimal form for flight characteristics. Based on the general plane shapes, the planes basically consist of the nose (radome), fuselage and wings. Other parts make up the details, they will not be examined in this section.

In this section, the effect on absorption when FSS surfaces are coated on the surfaces of these basic geometries will be discussed based on the parameters S11 and S21. When FSS is coated on the exact geometry of the aircraft, a lot of hardware is needed for analysis, analysis times increase and detailed drawings are required. In order to overcome such problems, the aircraft surfaces were divided into a few simple geometric shapes, and then FSSs were coated on these simple geometries and analyzes were made. These simple surface simulations are modeled as follows:

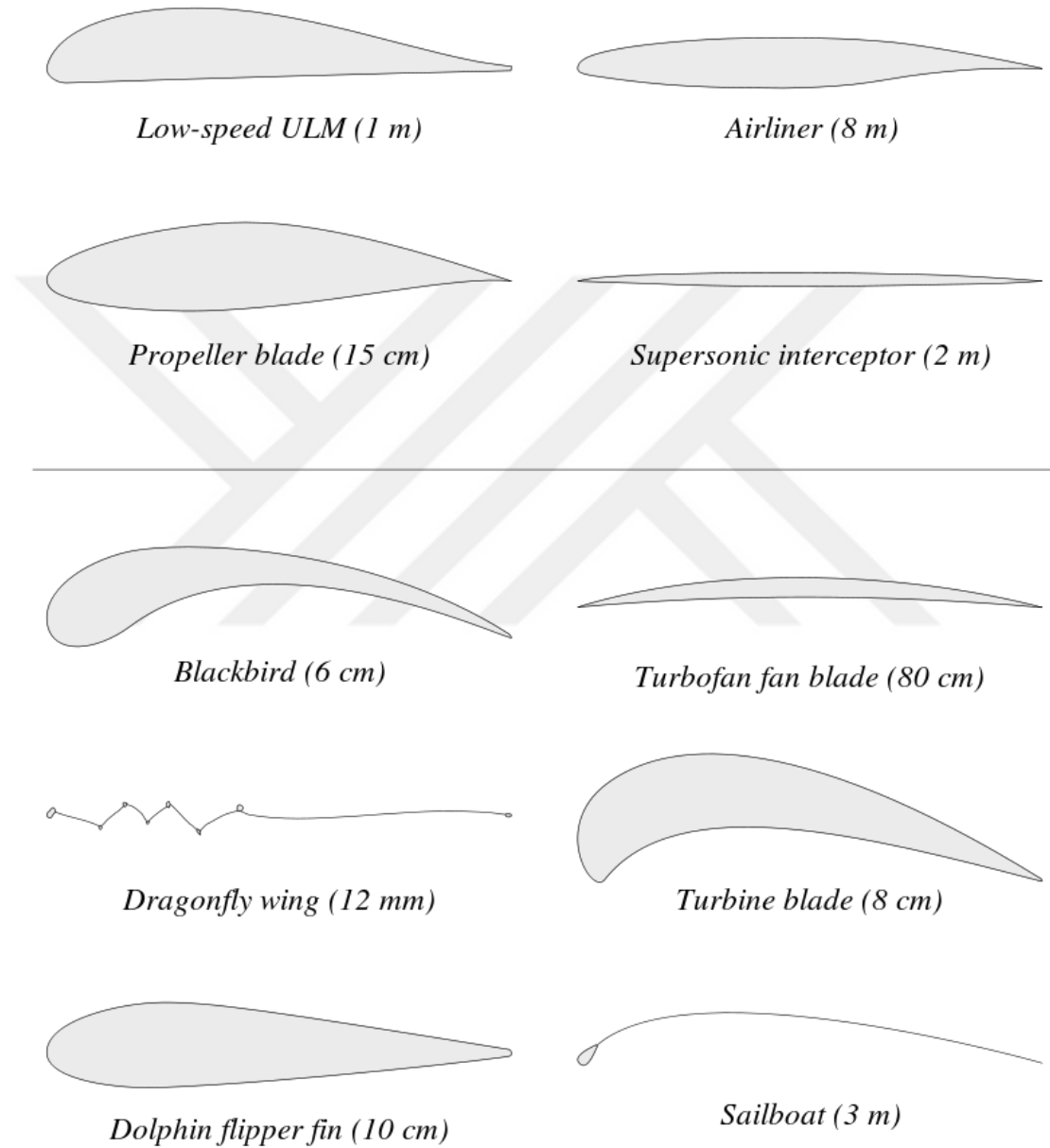
- **One airfoil for modeling wings**
- **One cylinder for modeling the body part**
- **Cone for nose and cockpit**

FSS designs applied to different surfaces and the absorption performance of FSS in different geometries will be evaluated. All surfaces are thought to be designed with aluminum material. Afterwards, all surfaces are coated with FR-4 substrate so that FSS can be applied. Finally, the FSS adjusted for 10GHz was applied to all surfaces periodically at equal intervals.

The tool for modeling periodic materials such as FSS etc. cannot be used to analyze the designed 3D geometric surfaces. To overcome this problem, a test setup consisting of two antennas was used. Generally, the antenna on the right constitutes port 1 and the antenna on the left constitutes port 2. The material to be measured is placed in the middle of both antennas. Analyzes were performed between 2-20GHz frequencies. Equation 2.3 will be used when interpreting the results. In other words, the change in absorption will be observed based on the changes in the S11 and S21 parameters around 10GHz. Generally, in some applications where the parameter S11 can be used as a reflection coefficient (by adding PEC to the back of the material being measured and thus resetting S21), it can also be interpreted as direct absorption. In this section, the results obtained by interpreting both result graphs will be included. In short, if both parameters decreased at 10GHz, it can be said that FSS absorbs.

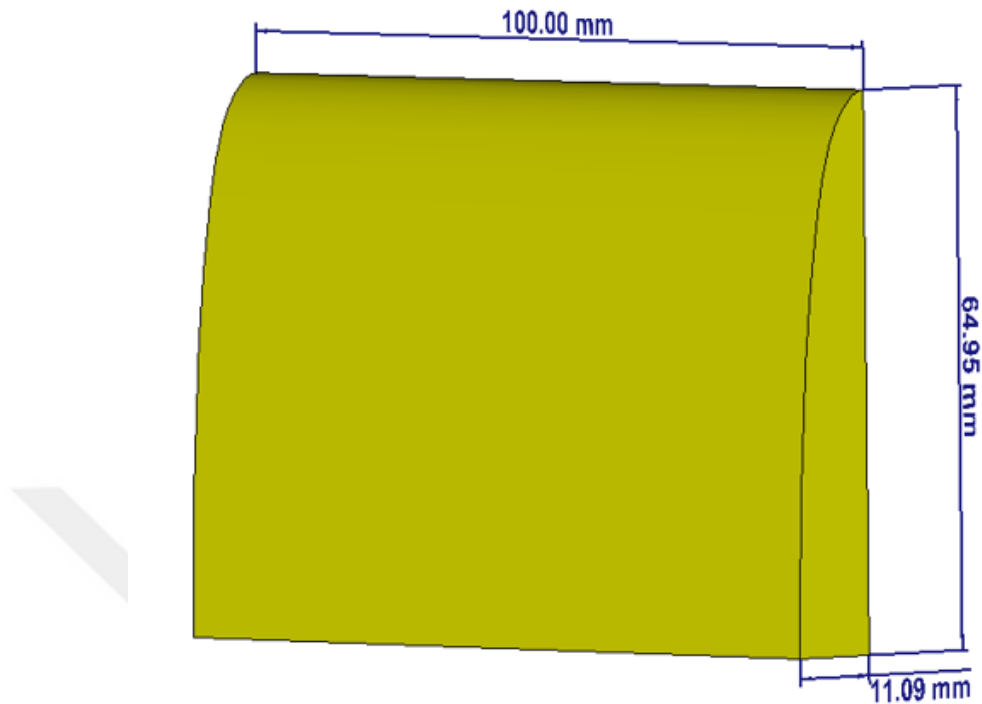
## 4.1 FSS Implementation in Airfoil Format for Aircraft Wings

Aircraft wings have different structures for each type of aircraft. The two-dimensional structure of this wing structure is called the airfoil. There are many types of airfoils and some of the common ones are standardized. Figure 4.2 below contains some of the most frequently used airfoil profiles.



**Figure 4.2** Most commonly used airfoil examples [72]

The following Figure 4.3 is the structure where the tests will be done on the created airfoil section. Airfoil is assumed to be made of aluminum

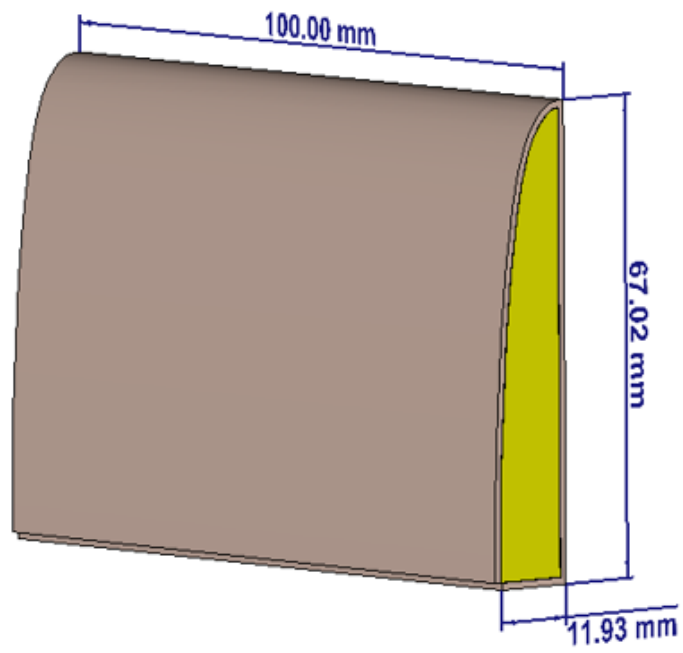


**Figure 4.3** Front view of the airfoil made of aluminium

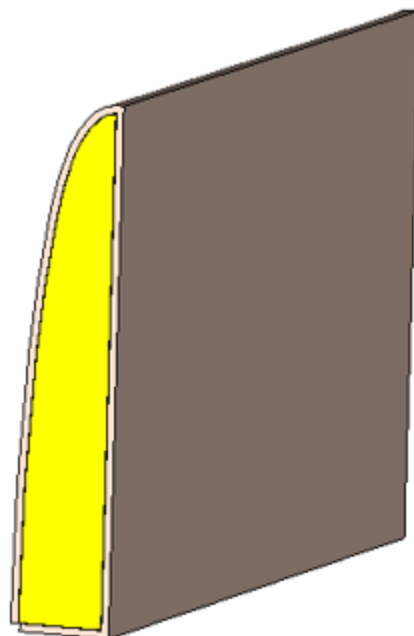
Illustrations of an example airfoil section created from the front and rear are shown in figures 4.5 and 4.6 below, respectively. The place shown in yellow represents the airplane wing. The portion represented in brown on the outside represents the substrate made of FR-4. The test setup we made through antennas is as in Figure 4.4 below. Analyzes were carried out with materials placed between 2 antennas. The figure shown with star represents a material under test (MUT).



**Figure 4.4** View of material under test setup



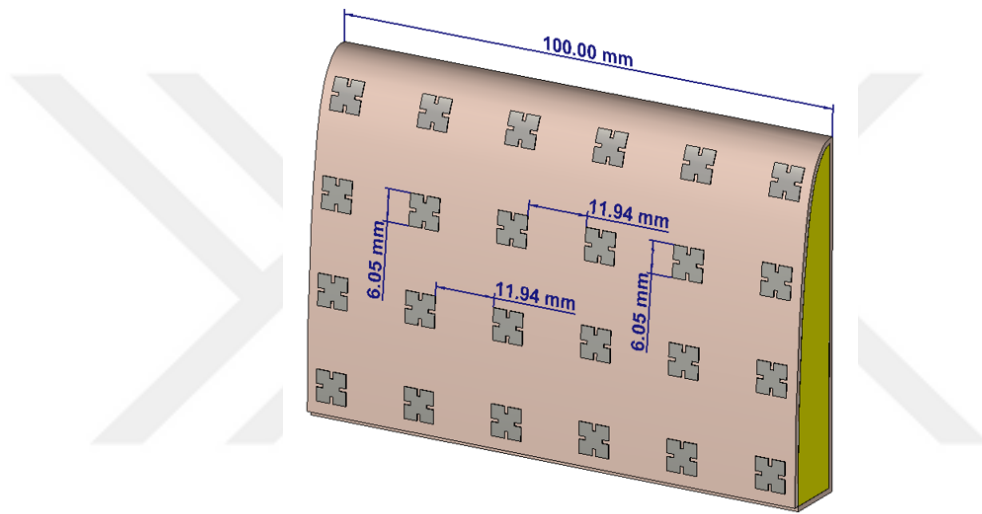
**Figure 4.5** Front view of the substrate coated airfoil



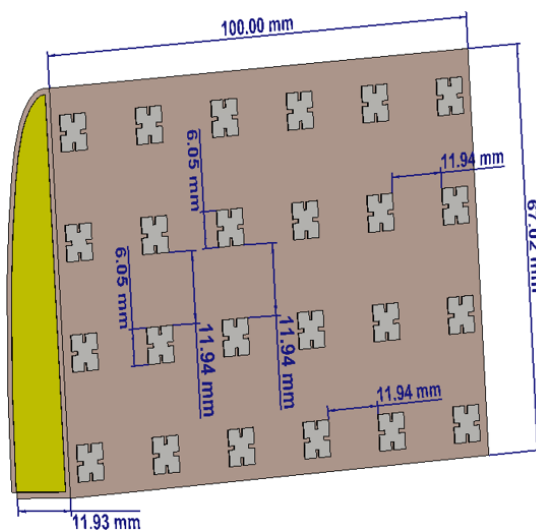
**Figure 4.6** Rear view of the substrate coated airfoil

First of all, only the section consisting of the wing profile was analyzed. While analyzing the wings, it is assumed that the wings are made of aluminum. The antenna on the flat right side of the airfoil is designated port 1. The antenna on the left side, which is inclined, is designated as port 2 4.4.

In order to see the comparisons of the analyzes more easily, the comparative representations of the analyzes are given on a single graphic. Figure 4.7 and 4.8 below show the airfoil section coated with FSS. For the FSS resonance frequency not to change, attention should be paid to the distance between the two FSS. As can be seen in Figures 4.7 and 4.8, all FSSs are placed in equal dimensions and at equal intervals, paying attention to periodicity.

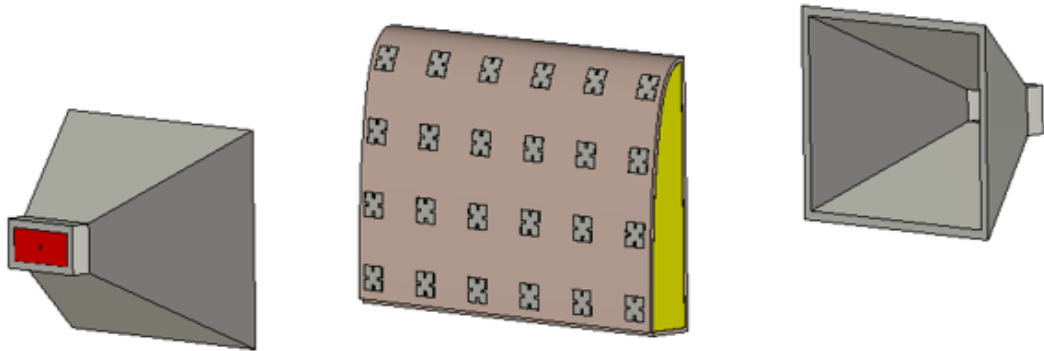


**Figure 4.7** Front view of the FSS coated airfoil

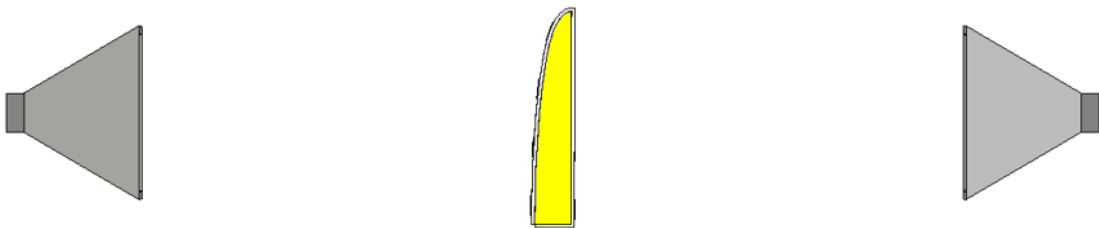


**Figure 4.8** Rear view of the FSS coated airfoil

FSS-coated airfoil is placed in the middle of the antennas for analysis. The flat part of the airfoil is closer to port1, while the curved part is closer to port2. Thus, the setup where the material will be tested has been established. The placement of the airfoil in the test setup is shown in figures 4.9 and 4.10 below.



**Figure 4.9** Cross view of the FSS coated airfoil at material under test setup

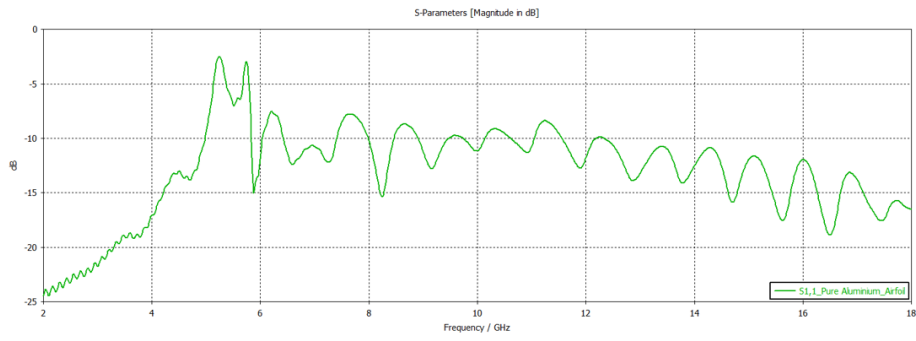


**Figure 4.10** Side view of the FSS coated airfoil at material under test setup

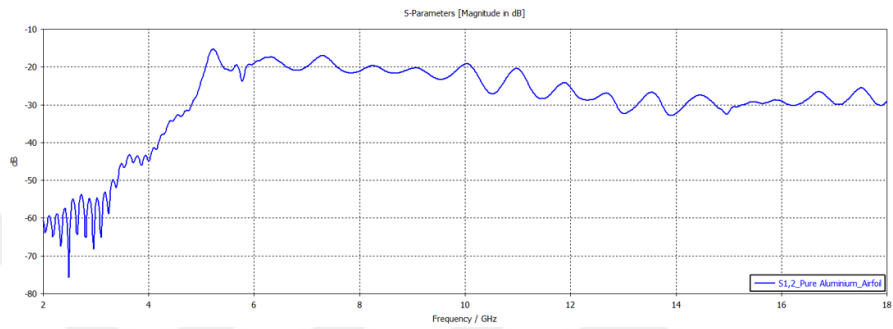
All analyzes in this section were performed with this test setup. Evaluations were mostly made in the 10GHz region and with the parameters  $S_{11}$  and  $S_{21}$  because of absorption. Nevertheless, the graphical results of all parameters are given after the analysis.

While evaluating the analyses, it is expected that the  $S_{11}$  and  $S_{21}$  parameters of the FSS coated materials will have lower values than the non FSS coated materials.

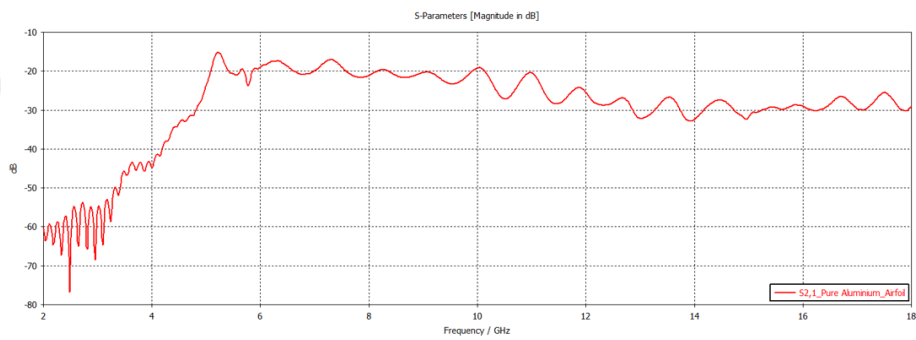
The first analysis results are as follows in Figure 4.11, Figure 4.12, Figure 4.13 and Figure 4.14 below. These results are the analysis results of the airfoil in the form of pure aluminum in the Figure 4.3, with FSS and substrate uncoated. It is the representation of a separate parameter as it is written in each graphic legend. It might be good to look at Figure 3.1 to remember what the S parameters mean.



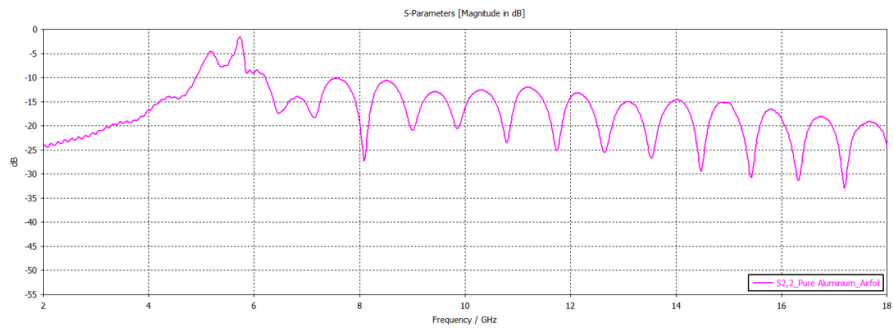
**Figure 4.11** Result of airfoil S11 made of pure aluminum



**Figure 4.12** Result of airfoil S12 made of pure aluminum

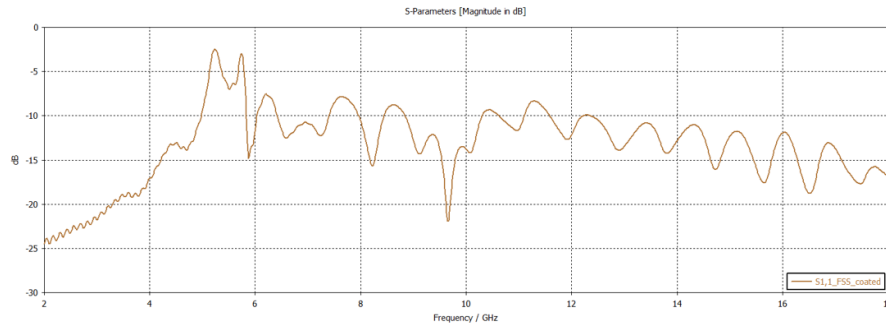


**Figure 4.13** Result of airfoil S21 made of pure aluminum

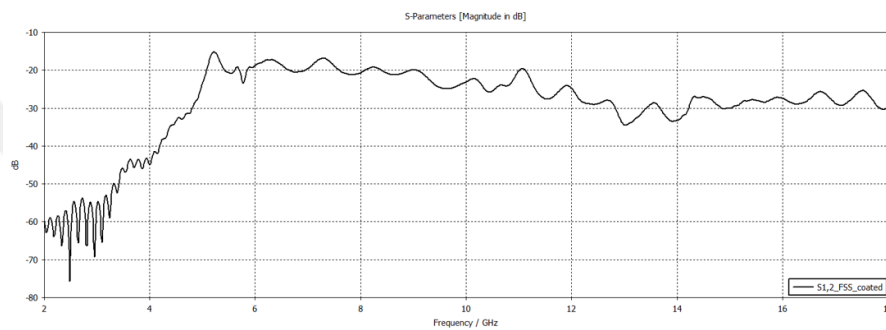


**Figure 4.14** Result of airfoil S22 made of pure aluminum

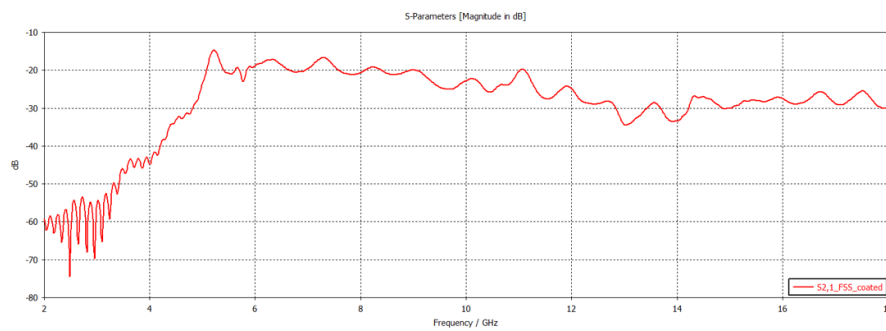
The graphs in Figure 4.15, Figure 4.16, Figure 4.17 and figure 4.18 below are the results of the FSS coated Figure 4.9 analysis.



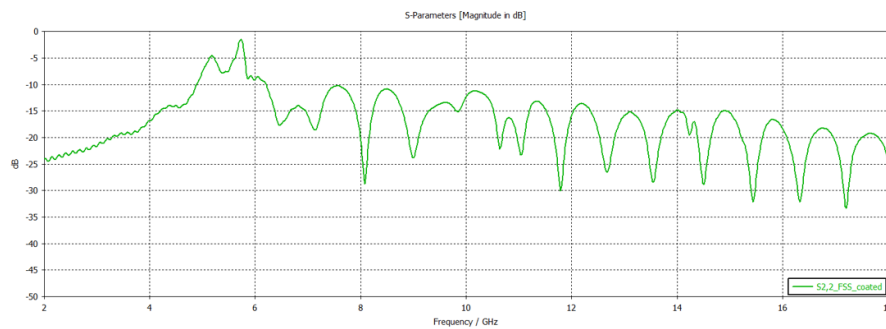
**Figure 4.15** S11 result of FSS coated airfoil



**Figure 4.16** S12 result of FSS coated airfoil

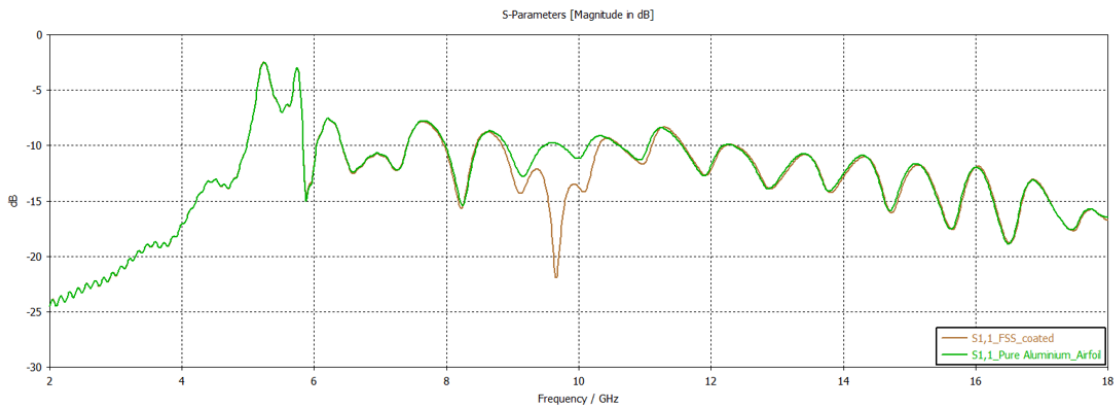


**Figure 4.17** S21 result of FSS coated airfoil

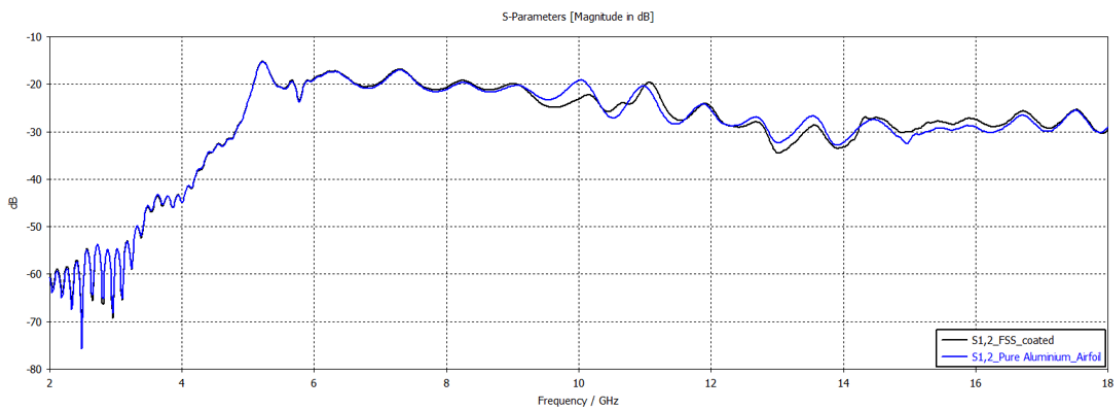


**Figure 4.18** S22 result of FSS coated airfoil

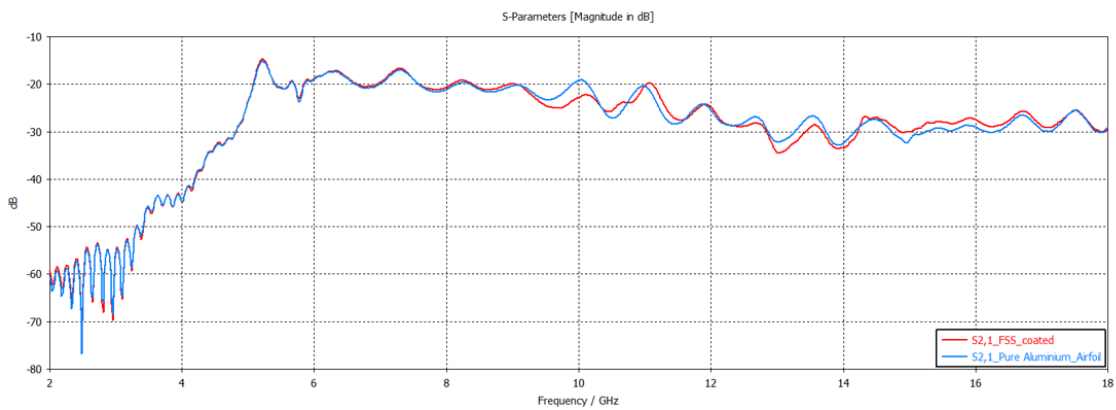
The representation of these results on separate graphs makes it difficult to compare. The graphs in Figure 3, Figure 4, Figure 5 and Figure 6 below show the airfoil analyzes of S parameters made of FSS coated and pure aluminum on the same graphic.



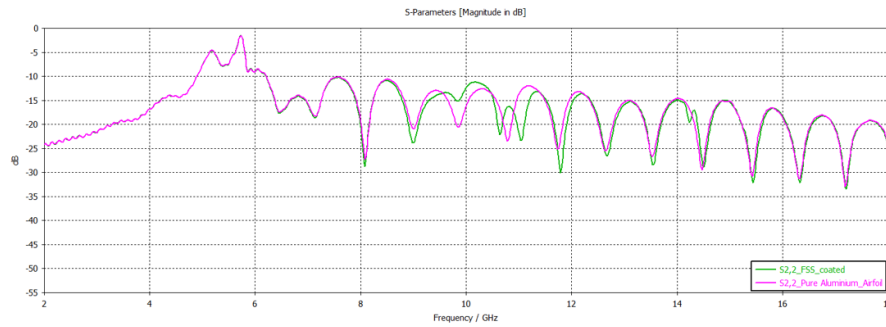
**Figure 4.19** Comparison of S11 parameters of FSS coated airfoil analysis and aluminum airfoil analysis



**Figure 4.20** Comparison of S12 parameters of FSS coated airfoil analysis and aluminum airfoil analysis



**Figure 4.21** Comparison of S21 parameters of FSS coated airfoil analysis and aluminum airfoil analysis



**Figure 4.22** Comparison of S22 parameters of FSS coated airfoil analysis and aluminum airfoil analysis

When the graphic results are examined, good results were obtained, especially around 10 GHz. When we look carefully at the S11 and S21 parameters, the FSS coated airfoil results showed lower values than pure aluminum in both graphs. In Figure 4.19, the FSS coated airfoil decreased from about -12dB to -22dB in the S11 graph. In the same way, In Figure 4.21, the FSS coated airfoil decreased from about -20dB to -25dB in the S21 graph.

In addition, the reason why the result of S11 is better than the result of S22 is that the flat side of the airfoil is from the 1st port. Because the signals from the 2nd port, which is on the curved side, were not well absorbed by the FSS compared to the flat part and showed scattering.

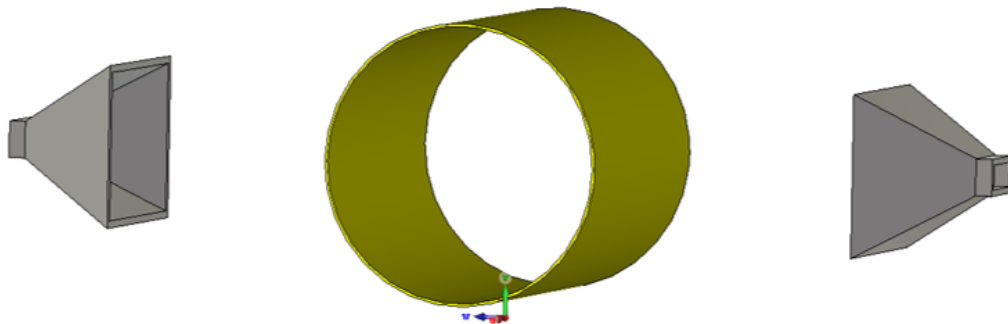
## 4.2 FSS Implementation for Aircraft Body Part in the Form of Cylindrical Surfaces

Geometric structure analysis in real plane dimensions is very costly both in terms of hardware and analysis time. For this reason, in the studies in this thesis, geometric surfaces have been scaled to the dimensions that can be analyzed. In this chapter, the behavior of FSS applied to a cylindrical surface will be examined. As explained in the previous section, airplanes have many different geometric surfaces. In this section, FSS application will be made on surfaces whose geometry resembles a cylinder. The largest cylindrical surfaces on airplanes are actually airframes.

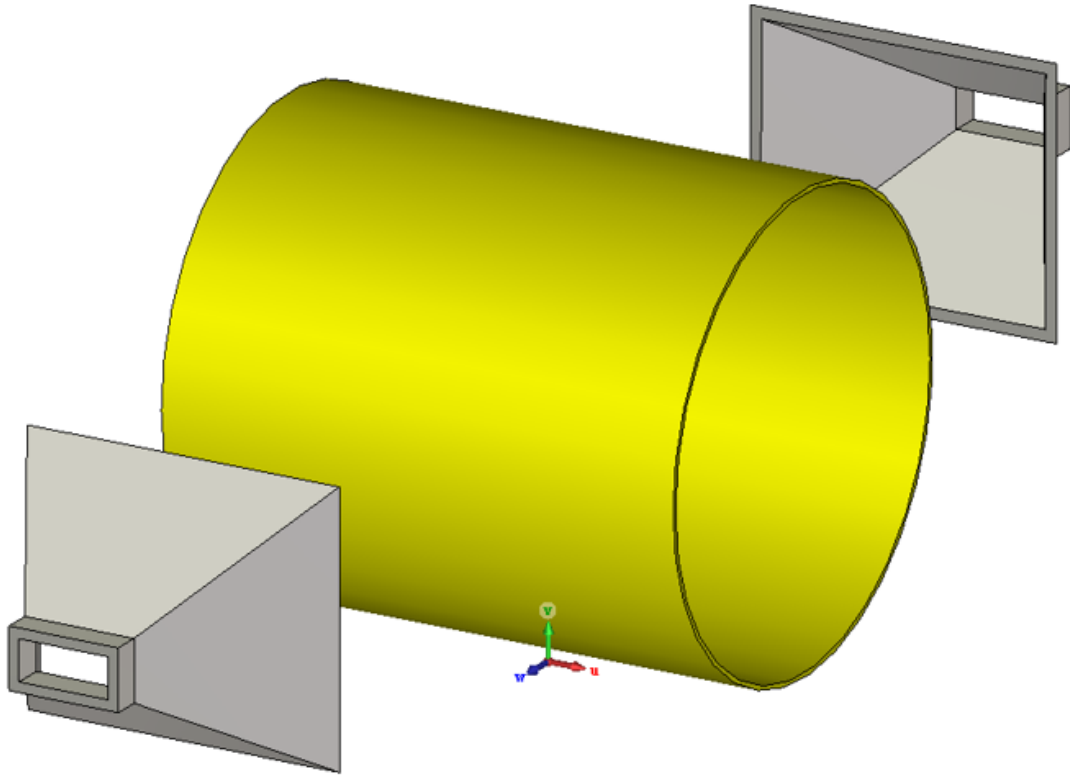
The cylindrical surface analyzed should not always be thought of as an aircraft fuselage. This cylindrical surface can sometimes be a pitot tube and sometimes another pipe. Likewise, the airfoil analysis in the previous section should not be thought of as just a wing modeling. The FSS coating will have the same effect on other surfaces similar to that geometry.

The cylindrical surface is made of aluminum as in the airfoil. Test setup is similar to airfoil. Antenna dimensions and distances have not been changed.

The cylindrical surface to be analyzed in this section is as in Figure 4.23 and Figure 4.24, which are shown from different angles below.



**Figure 4.23** Left cross view of the test setup



**Figure 4.24** Right cross view of the test setup

In these analyzes, the substrate made of FR-4 and PEC FSS coating were applied on the aluminum cylinder.

It is important for the frequency selective surface to be equal to the integer value around the cylinder, for the distance between the FSSs to be equal. Cylinder diameter adjusted to 91.67mm to have 16 array of FSS around it and cylinder length is set to 104mm.

The test setup is set so that the FSS in the middle of the cylinder surface is at right angles to the Antennas. In other words, the ports in the middle of the antennas and the FSSs in the middle of the cylinder are perpendicular to each other.

Figure 4.25 and Figure 4.26 below are representations of the FSS coated cylindrical surface from different angles. In addition, when the dimensions are examined, it can be seen that the FSSs are placed in equal dimensions and at equal intervals, paying attention to the periodicity.

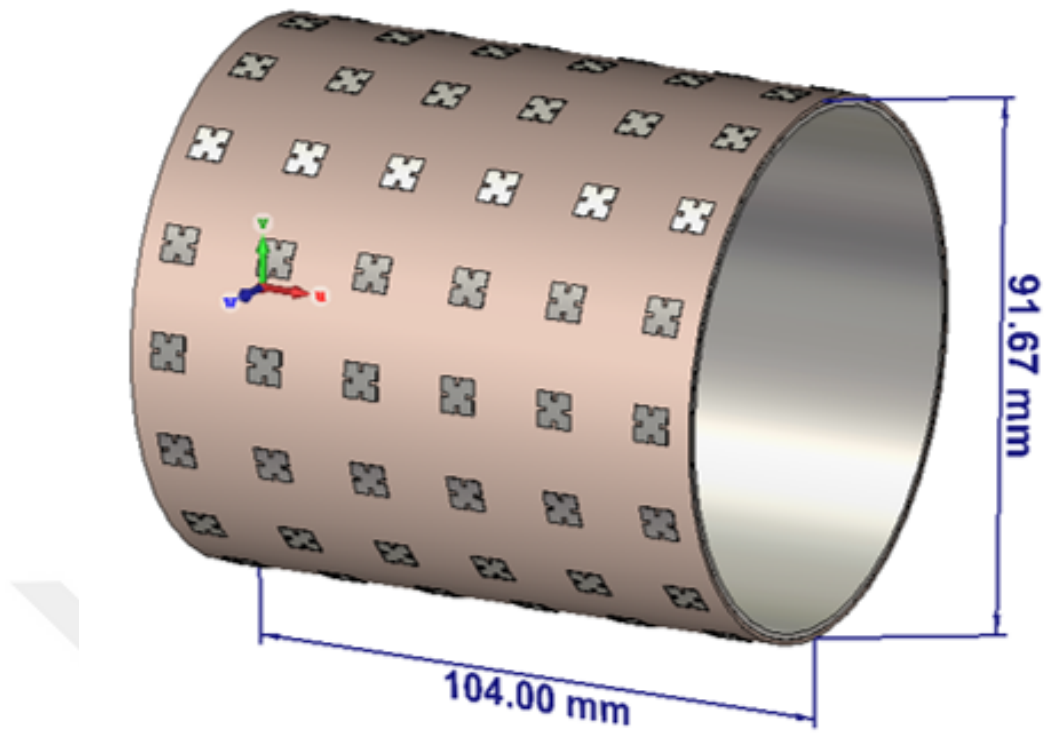


Figure 4.25 Left cross view of the FSS coated cylinder

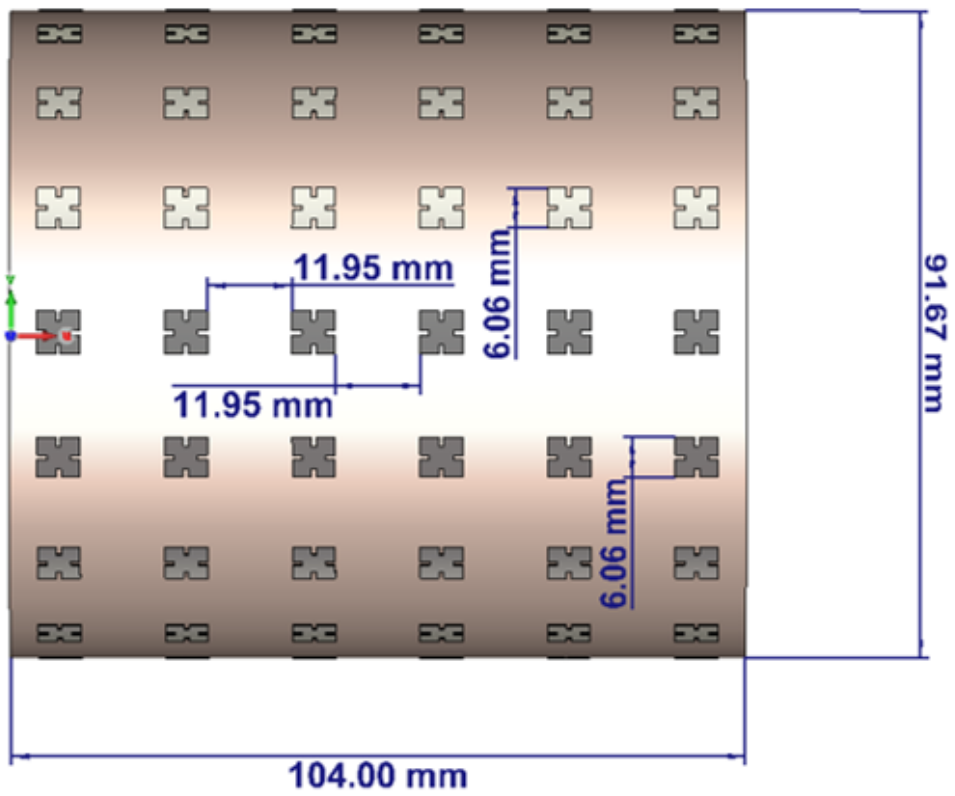
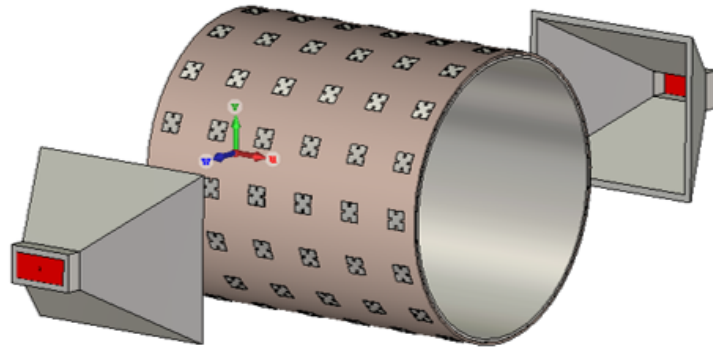
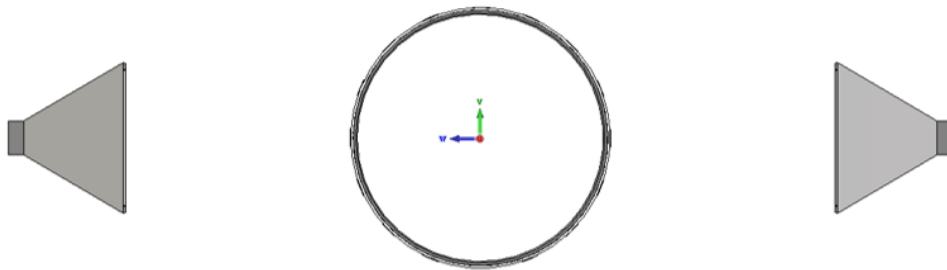


Figure 4.26 Perpendicular view of the FSS coated cylinder

Figure 4.27, Figure 4.28, below are representations of the FSS coated cylindrical surface analysis setup from different angles.

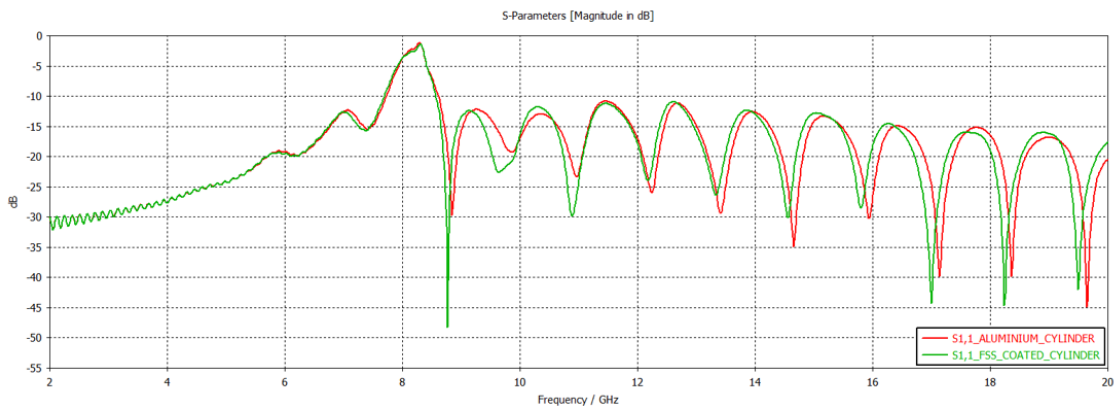


**Figure 4.27** Left cross view of the FSS coated cylinder analysis setup

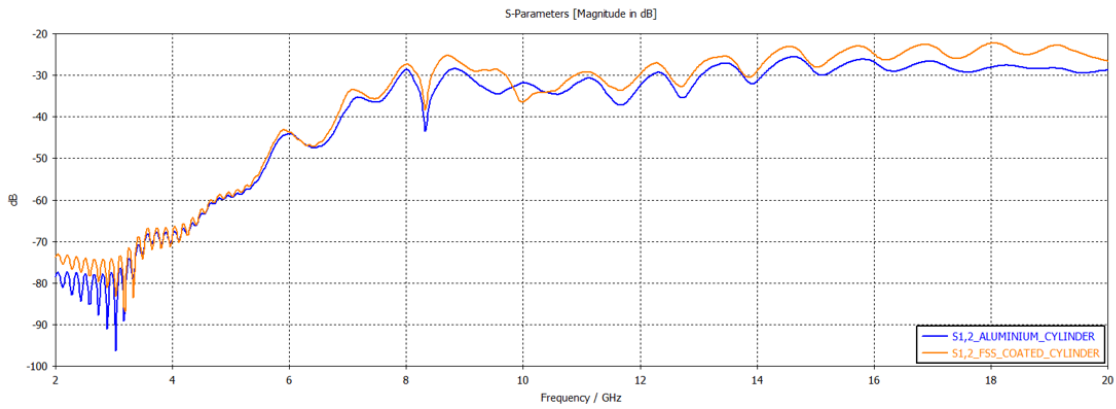


**Figure 4.28** Perpendicular view of the FSS coated cylinder analysis setup

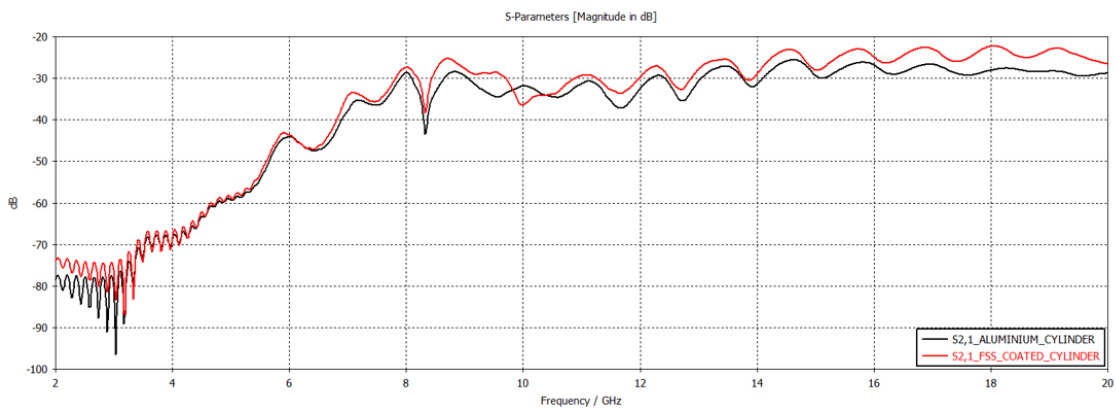
Analysis results of aluminum cylindrical surface and FSS coated cylindrical surface are not shown separately. Comparative results of the two analyzes are shown in Figure 4.29, Figure 4.29, Figure 4.29 and Figure 4.32 below, in the same graph with the S parameters separately.



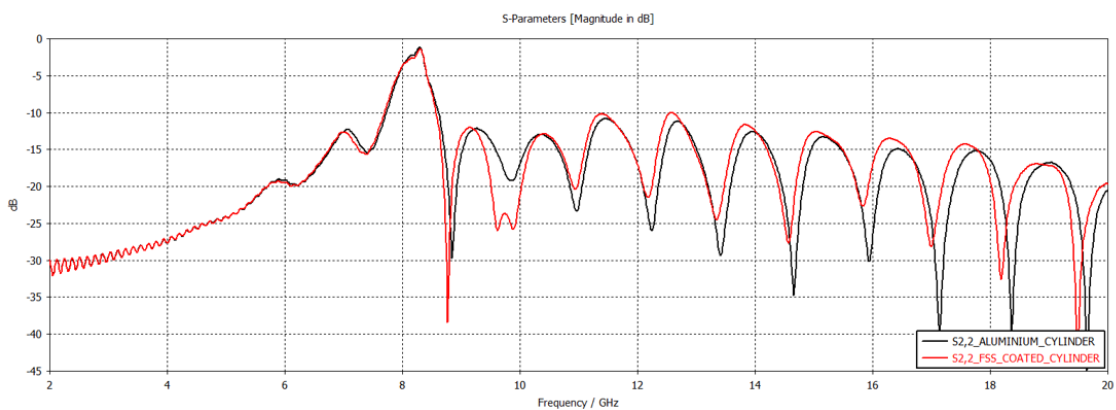
**Figure 4.29** Comparison of S11 parameters of FSS coated cylinder analysis and aluminum cylinder analysis



**Figure 4.30** Comparison of S12 parameters of FSS coated cylinder analysis and aluminum cylinder analysis



**Figure 4.31** Comparison of S21 parameters of FSS coated cylinder analysis and aluminum cylinder analysis



**Figure 4.32** Comparison of S22 parameters of FSS coated cylinder analysis and aluminum cylinder analysis

When the graphic results are examined, good results have been obtained especially at 10 GHz and other frequencies. When the S11 and S21 parameters were examined, the results of the FSS coated cylindrical surface showed lower values than pure aluminum in both graphs.

For example, in Figure 4.29, the FSS coated cylindrical surface decreased from approximately -30dB to -48dB on the S11 graph.

Likewise, in Figure 4.31, the FSS coated cylindrical surface decreased from about -32dB to -38dB on the S21 graph.

Thus, frequency selection has been made effectively, especially in the 10GHz region (8GHz-12GHz).

## **RESULT OF CYLINDRICAL ANALYSIS AND SUMMARY**

The main reason for analyzing the cylinder horizontally is to ensure that it is parallel to the long side of the antenna. The analysis yielded similar results when the cylinder was performed vertically.

The most important factors to consider when analyzing cylindrical surfaces are as follows:

- The substrate to be applied to the cylindrical surface must be equal to the thickness suitable for the FSS design on the entire surface.
- When covering the cylindrical surface with the frequency selective surface, care should be taken to ensure that the distance between all FSSs is the same. To adjust this up;
  - Change in cylinder diameter,
  - Change of substrate thickness and accordingly new FSS design
  - Little tuneability due to new variation of FSS thickness

solutions may be appropriate.

As a result, the FSS design applied to the cylindrical surface, paying attention to the information given above, provided the expected transmission and reflection coefficients in the 10GHz region. The larger the cylindrical surface, the flatter the surface on which FSS is applied, thus the FSS performance will be positively affected.

### 4.3 FSS Implementation for Aircraft Nose Area in The Form of Conical Surfaces

Finally, a cone geometry was chosen for the analysis of the nose and cockpit region. This conical surface, like the previous geometries, has been reduced to a dimensionally analyzable level. It can also be used not only for the analysis of the nose part of the aircraft, but also for another surface similar to a cone.

First of all, the conic chosen for analysis consists of 2 parts with different slopes. The reason for choosing 2 pieces is to observe the FSS effect in different slopes such as nose and cockpit. The cone is made of aluminum as in other analyzes.

In Figure 4.33 and Figure 4.34 below, there are dimensional information and representations of the conical surface examined from different angles.

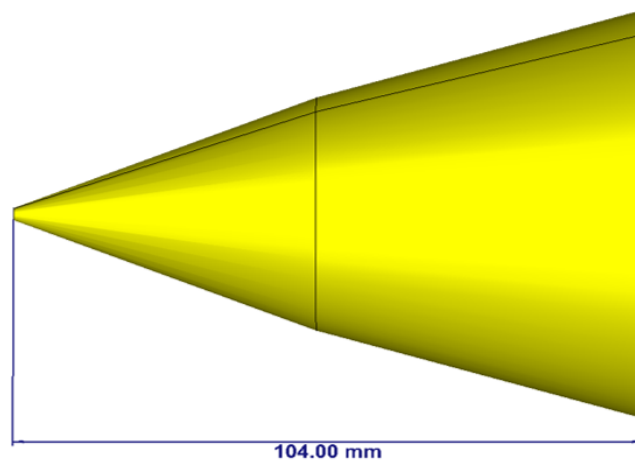


Figure 4.33 Side view of aluminum cone

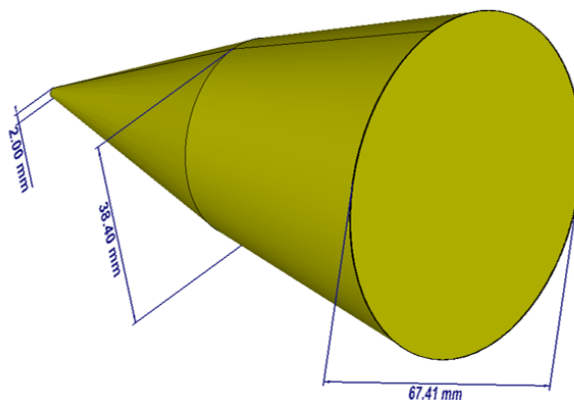
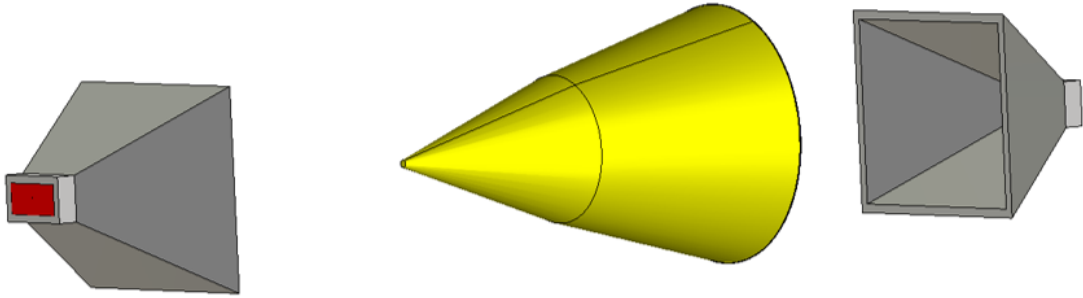


Figure 4.34 Right cross view of aluminum cone

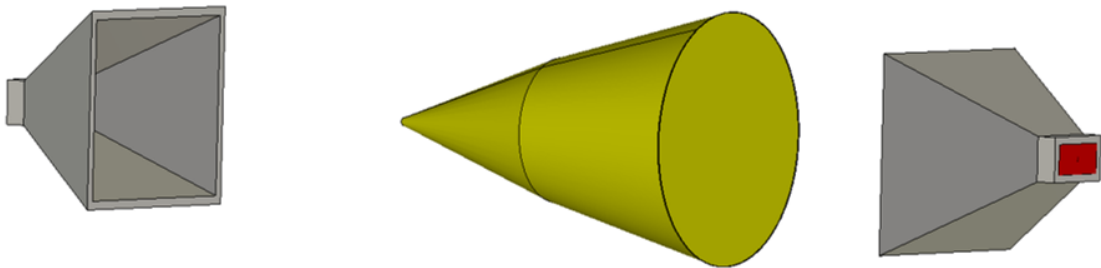
As seen above in Figure 4.34, the diameter of the nose part of the cone increases from 2mm to 38.40mm, and the back part increases from 38.40mm to 67.41mm with a lesser slope.

The analysis setup of the material under test is shown from different angles in Figure 4.35, Figure 4.36 and Figure 4.37 below.

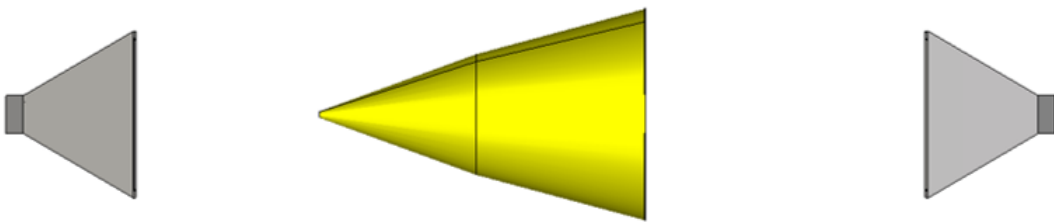
As in all analyzes, the cone is centered both perpendicularly and distance to the antenna.



**Figure 4.35** Left cross view of aluminum cone

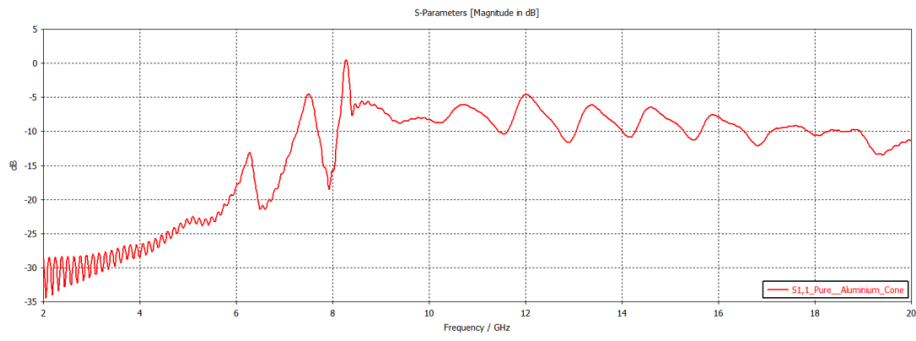


**Figure 4.36** Right cross view of aluminum cone

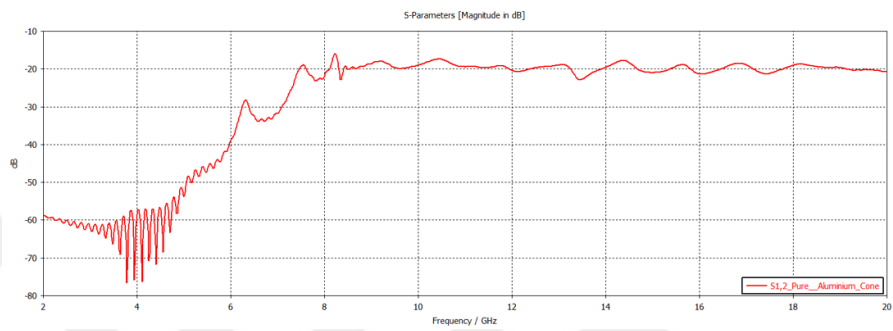


**Figure 4.37** Side view of aluminum cone

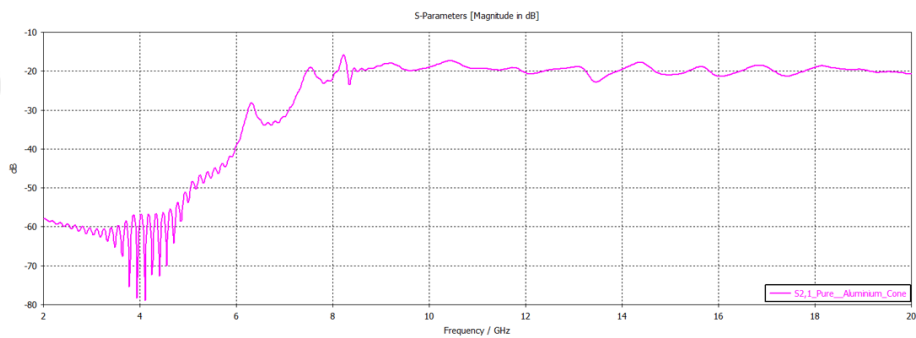
The first analysis results are as follows in Figure 4.38, Figure 4.39, Figure 4.40 and Figure 4.41 below. These results are the analysis results of the cone in the form of pure aluminum like in the Figure 4.33, with FSS and substrate uncoated.



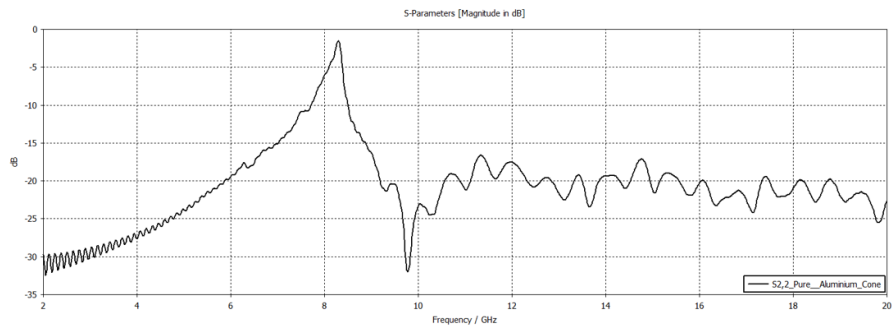
**Figure 4.38** Result of cone S11 made of pure aluminum



**Figure 4.39** Result of cone S12 made of pure aluminum



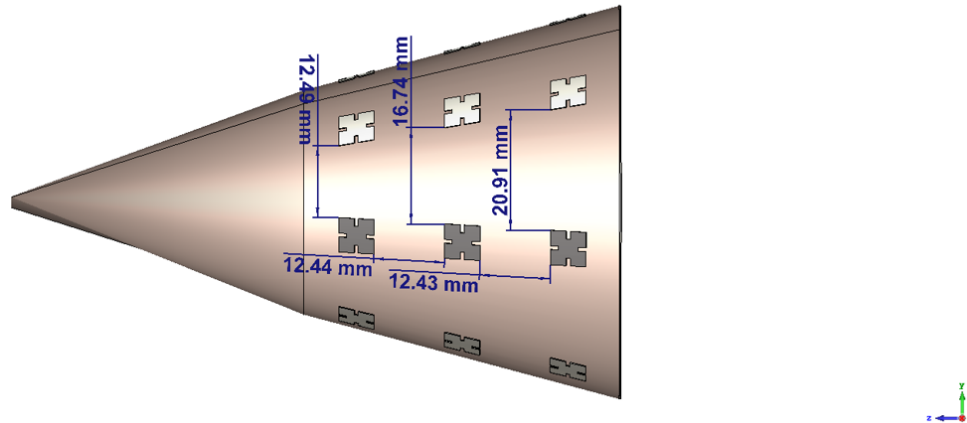
**Figure 4.40** Result of cone S21 made of pure aluminum



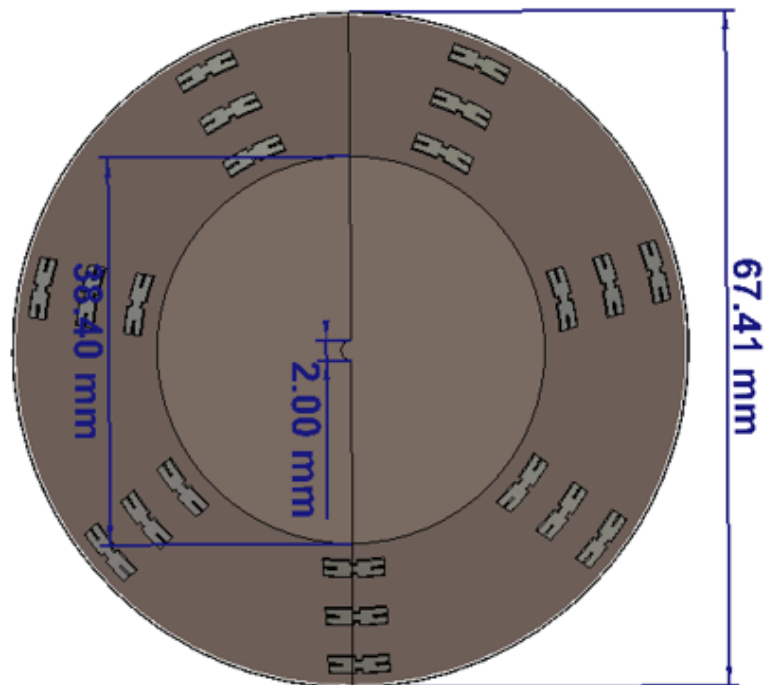
**Figure 4.41** Result of cone S22 made of pure aluminum

Before the FSS coating process, it was coated with FR4 substrate as usual, and then the back with a low slope was coated with FSS. Covering with seven pieces of FSS in a total of one circular loop was the most suitable size for FSSs. A total of three rows were made of this circular loop in an array, thus covering a total of twenty one FSS.

Detailed images of the designed work are shown in Figure 4.42, Figure 4.43 and Figure 4.44 below.

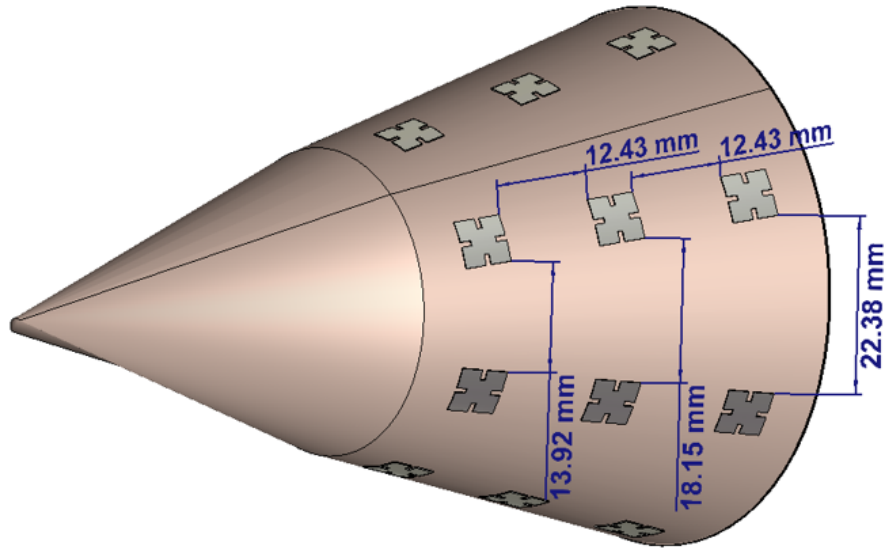


**Figure 4.42** Side view of FSS coated cone with 3 circular loops consisting of 7 FSS



**Figure 4.43** Top view of FSS coated cone with 3 circular loops consisting of 7 FSS

Due to the nature of the cone surface, it is clearly seen in Figure 4.44 that the distance between the FSS on the back is widened.

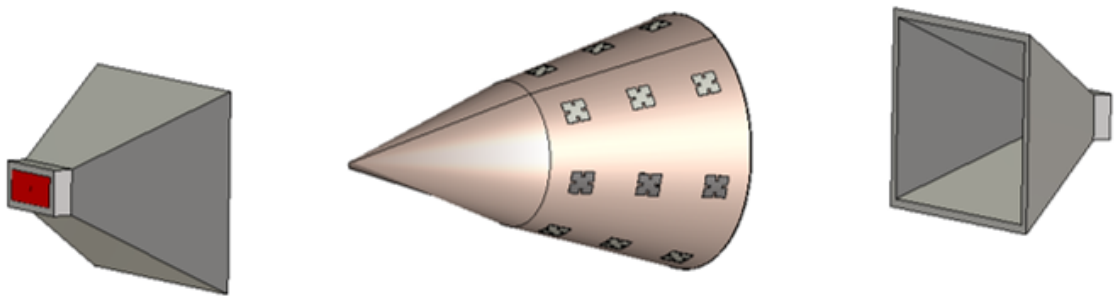


**Figure 4.44** Left cross view of FSS coated cone with 3 circular loops consisting of 7 FSS

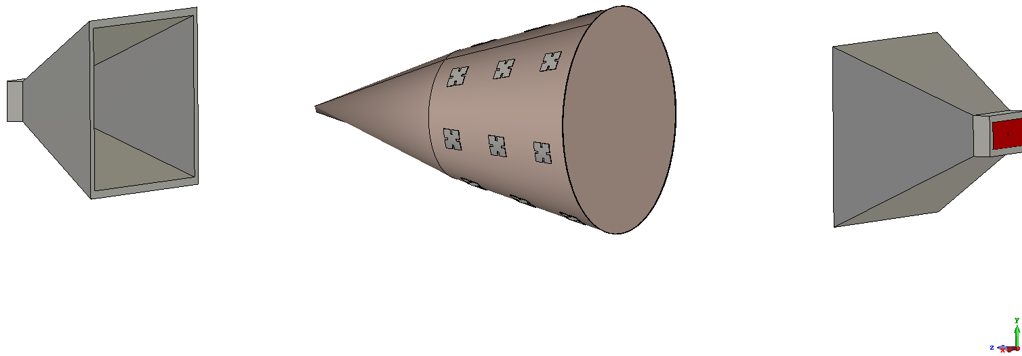
The analysis setup of the material under test is shown from different angles in Figure 4.45, Figure 4.46 and Figure 4.47 below.

As in all analyzes, the cone is centered both perpendicularly and distance to the antenna.

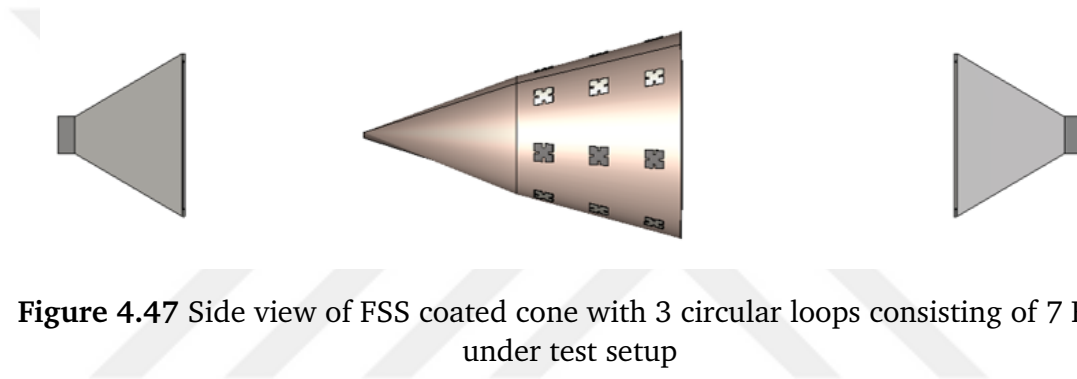
The results with the S Parameters of this analysis are given in the appendix. The following analyzes will be given on the same graph in order to make a more meaningful comparison.



**Figure 4.45** Left cross view of FSS coated cone with 3 circular loops consisting of 7 FSS under test setup



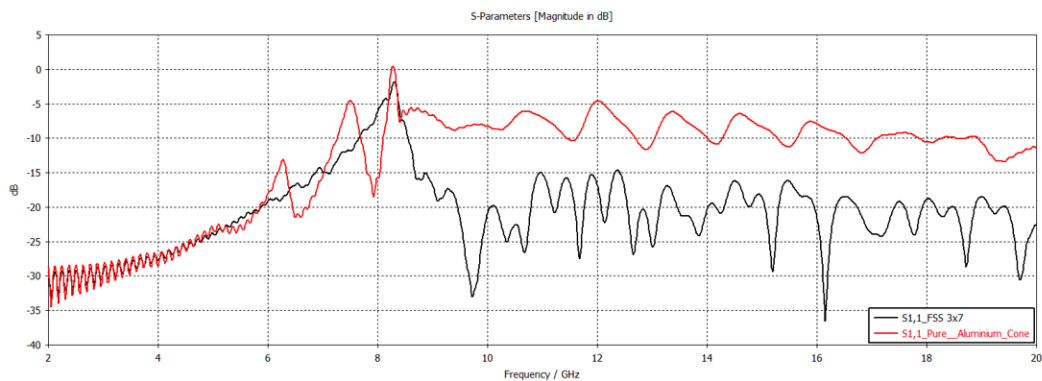
**Figure 4.46** Right cross view of FSS coated cone with 3 circular loops consisting of 7 FSS under test setup



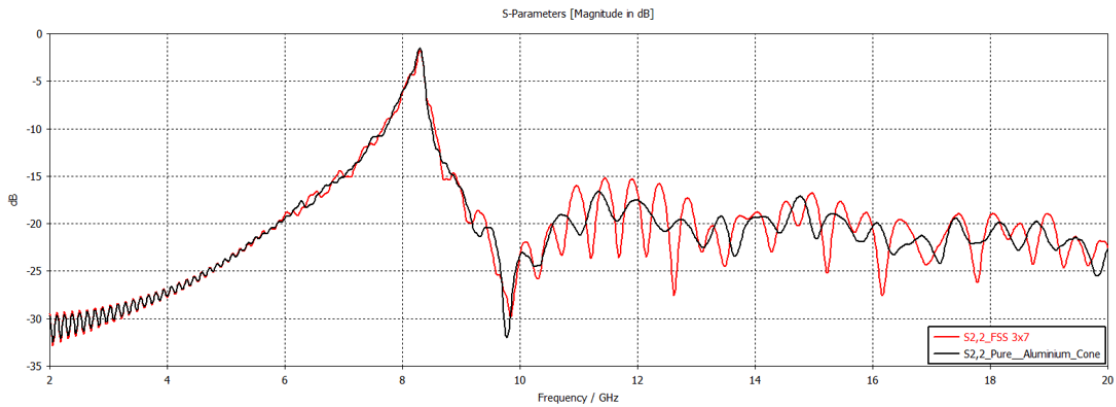
**Figure 4.47** Side view of FSS coated cone with 3 circular loops consisting of 7 FSS under test setup

Analysis results of aluminum cone surface and FSS coated cone surface are not shown separately. Comparative S11 and S22 results of the two analyzes are shown in Figure 4.48 and Figure A.4 below, in the same graph with the S parameters separately.

The result of this analysis and the S parameter results of all subsequent analyzes are attached for traceability.



**Figure 4.48** Comparison of S11 parameters of 3x7 FSS coated cone analysis and aluminum cone analysis



**Figure 4.49** Comparison of S22 parameters of 3x7 FSS coated cone analysis and aluminum cone analysis

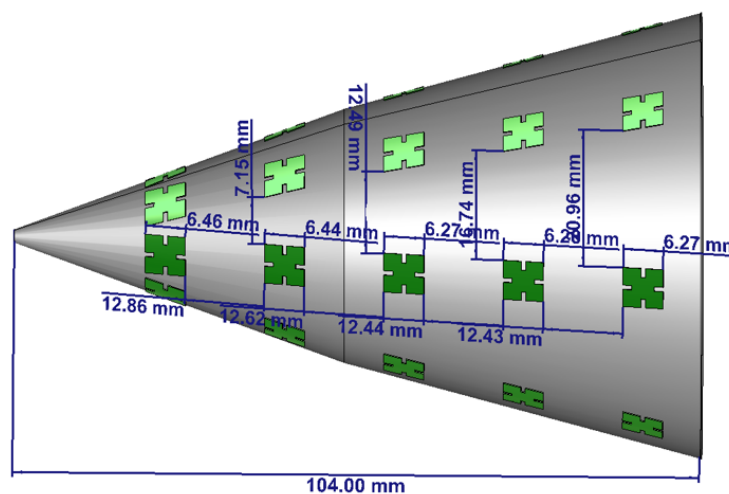
It is understood from the S11 results that it has decreased considerably as reflection. In S22 parameters, it is understood that it selects at different frequencies, but it cannot be said that it gives results as desired.

From this result, it was understood that FSS coating should be done more appropriately to the geometric structure of the cone originating from its natural feature.

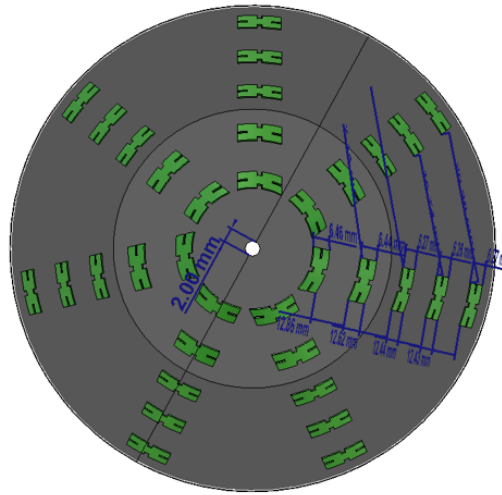
The desired result may not have been achieved due to the uncoated nose part. For this reason, the nose part should also be covered with FSS.

The conical surface covered with FSS in the same way on the nose part is given in figures 4.50 and Figure 4.51 below with detailed images from different angles.

All applied FSSs are the same size. A total of 35 FSS have been implemented.

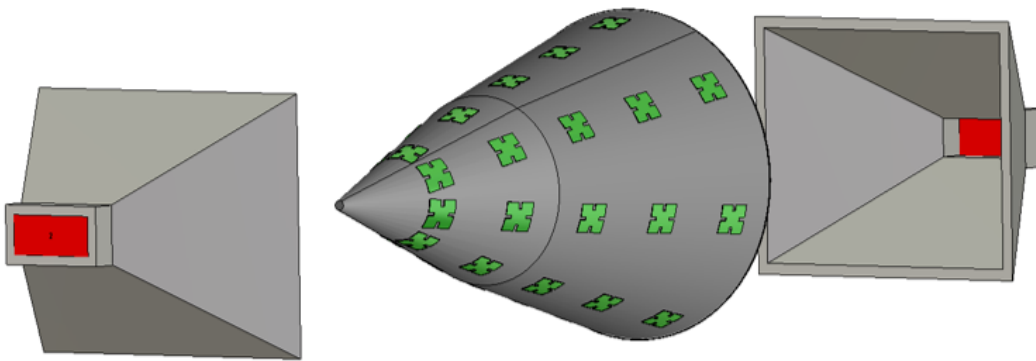


**Figure 4.50** Side view of FSS coated cone with 5 circular loops consisting of 7 FSS

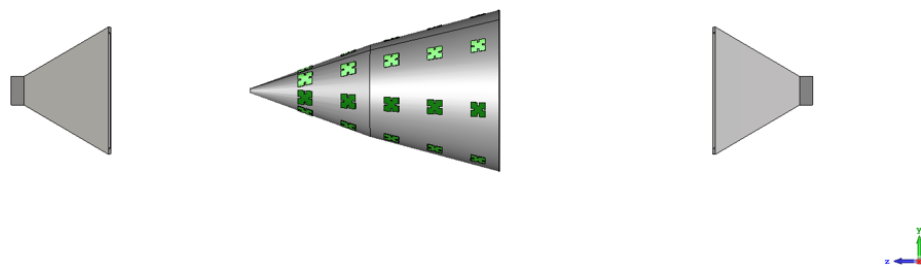


**Figure 4.51** Top view of FSS coated cone with 5 circular loops consisting of 7 FSS

The analysis setup of the material under test is shown from different angles in Figure 4.52 and Figure 4.53 below.

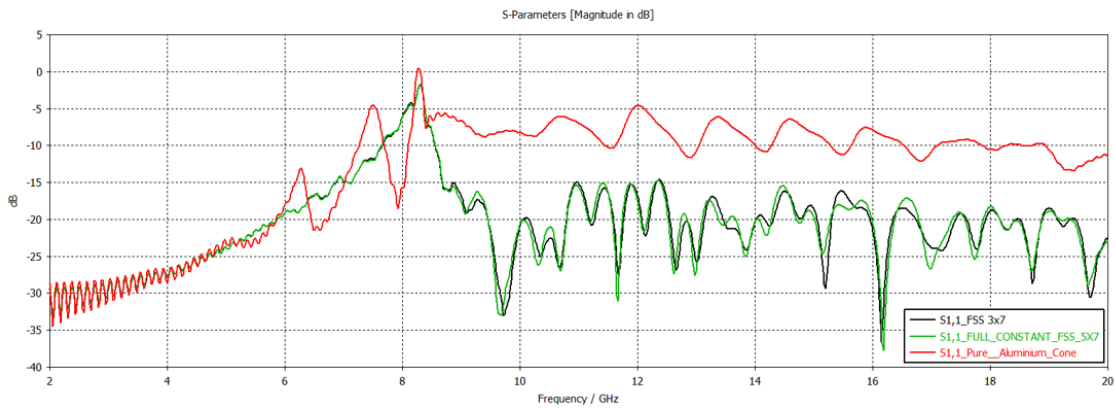


**Figure 4.52** Left cross view of FSS coated cone with 5 circular loops consisting of 7 FSS under test setup

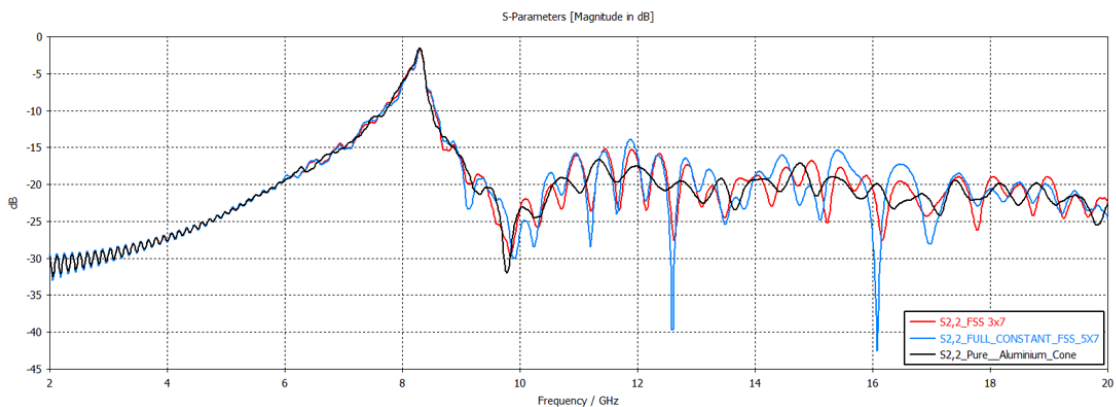


**Figure 4.53** Side view of FSS coated cone with 5 circular loops consisting of 7 FSS under test setup

Analysis results of aluminum cone surface and 5x7 FSS coated cone surface are not shown separately. Comparative S11 and S22 results of the two analyzes are shown in Figure 4.54 and Figure 4.55 below, in the same graph with the S parameters separately.



**Figure 4.54** Comparison of S11 parameters of 5x7 FSS coated cone analysis and aluminum cone analysis



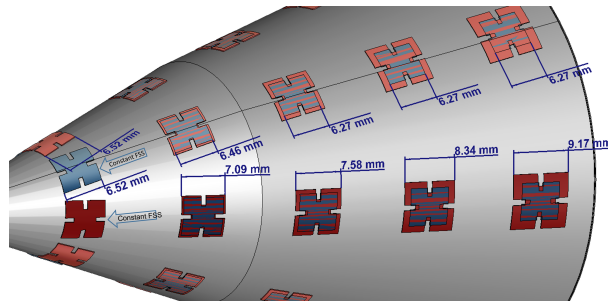
**Figure 4.55** Comparison of S22 parameters of 5x7 FSS coated cone analysis and aluminum cone analysis

After the nose part was covered with FSS, the results improved considerably. It can be concluded that FSS works in the 10GHz region right.

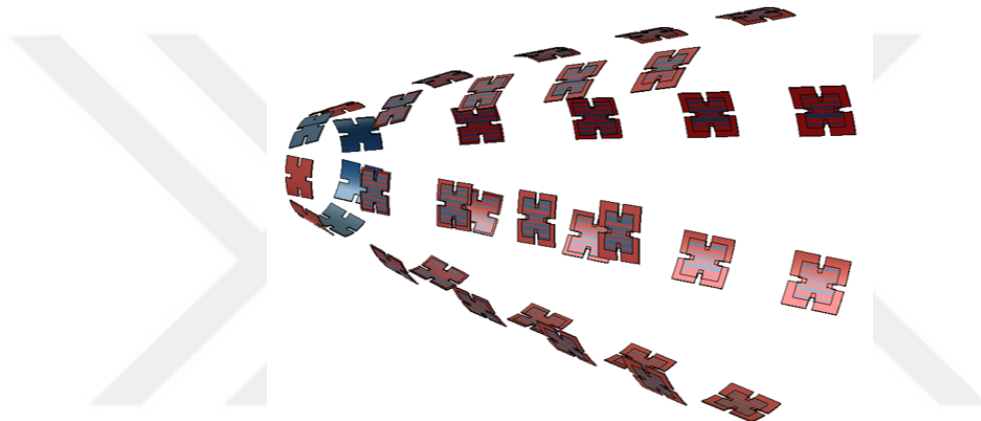
However, due to the change in the diameter of the cone from top to bottom, the gaps between the FSS were widening. In order to understand whether this will pose a problem, the FSS at the front of the nose is fixed and all backward FSSs are applied by magnifying 10% compared to the previous row, as in Figure 4.56, Figure 4.57, Figure 4.58 and Figure 4.59. The results of the S Parameters of this analysis are given in the appendix.



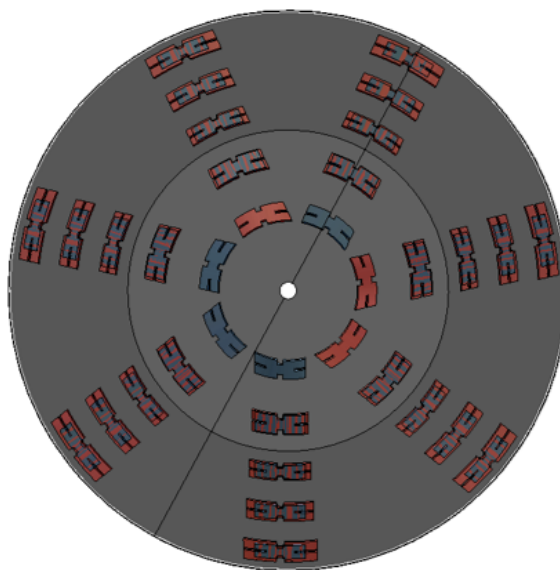
The superimposed FSS design is as in figure 4 and figure 5 below for a better depiction of the size increase.



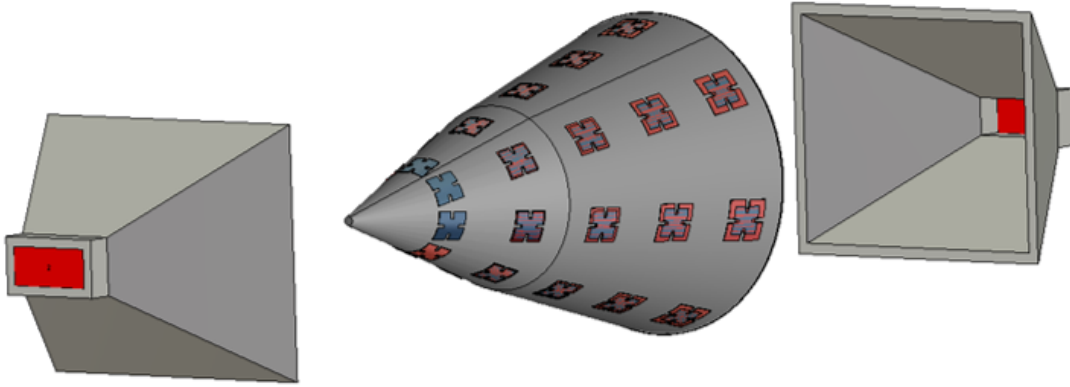
**Figure 4.60** Left cross view of 10% enlarged FSS coated cone and 5x7 constant FSS coated



**Figure 4.61** Right cross view of 10% enlarged FSS coated cone and 5x7 constant FSS coated



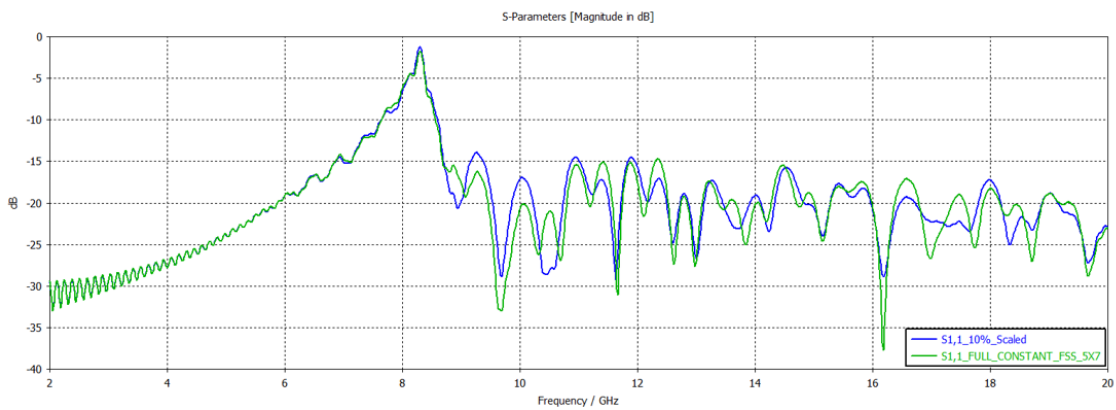
**Figure 4.62** Top view of 10% enlarged FSS coated cone and 5x7 constant FSS coated



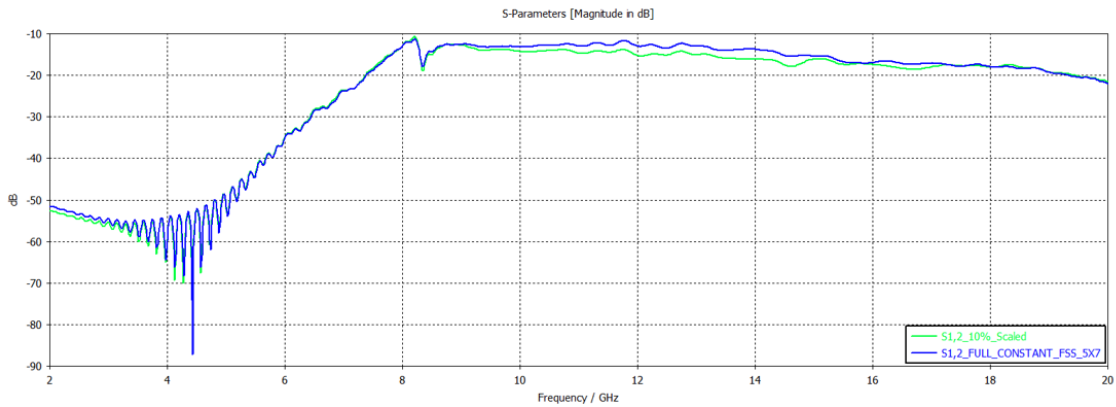
**Figure 4.63** Left cross view 2 of 10% enlarged FSS coated cone and 5x7 constant FSS coated under test

In Figure 4.63 above, the gray FSSs represent constant size FSSs, while the red highlighted FSSs represent continuing FSSs increasing by 10%.

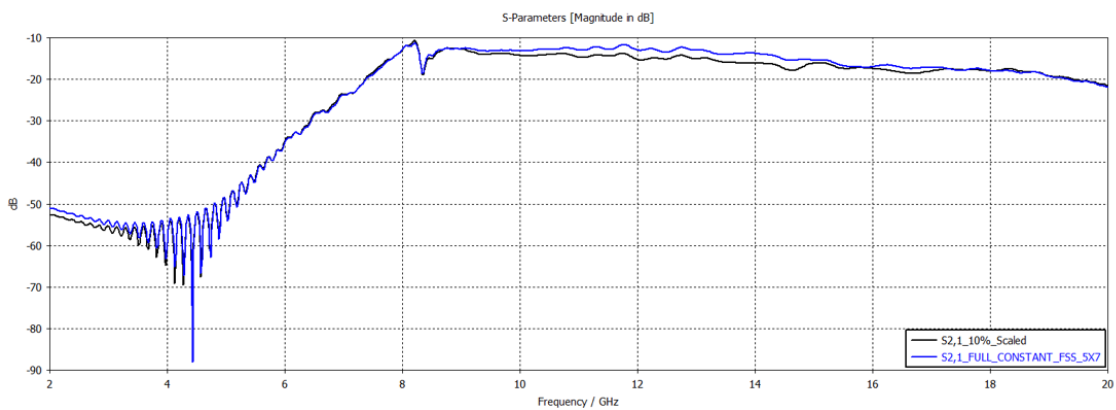
The comparative results of these two analyzes are as in Figure 4.64, Figure 4.65, Figure 4.66 and Figure 4.67 below.



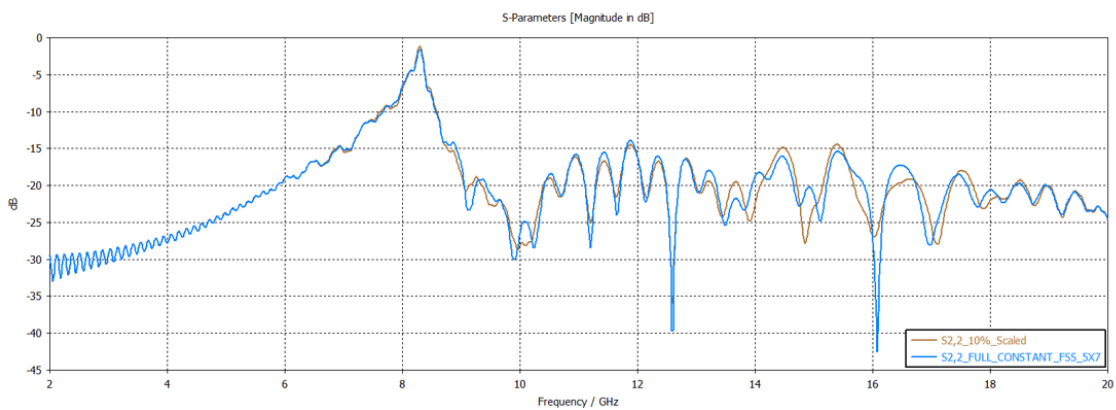
**Figure 4.64** Comparison of S11 parameters of 5x7 constant FSS coated cone analysis and 10% enlarged FSS coated cone analysis



**Figure 4.65** Comparison of S12 parameters of 5x7 constant FSS coated cone analysis and 10% enlarged FSS coated cone analysis



**Figure 4.66** Comparison of S21 parameters of 5x7 constant FSS coated cone analysis and 10% enlarged FSS coated cone analysis



**Figure 4.67** Comparison of S22 parameters of 5x7 constant FSS coated cone analysis and 10% enlarged FSS coated cone analysis

In the 10GHz region, the cone covered with full constant FSS performed better.

Finally, since the back part of the cone is wider, the results of the analysis were examined by adding FSSs there.

The visuals of the design made with added FSSs are as in Figure 4.68, Figure 4.69 and Figure 4.70.

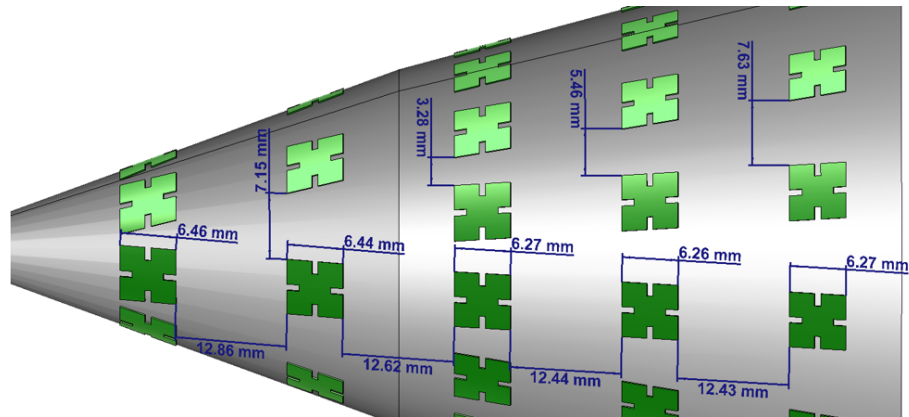


Figure 4.68 Side view of added FSS coated cone

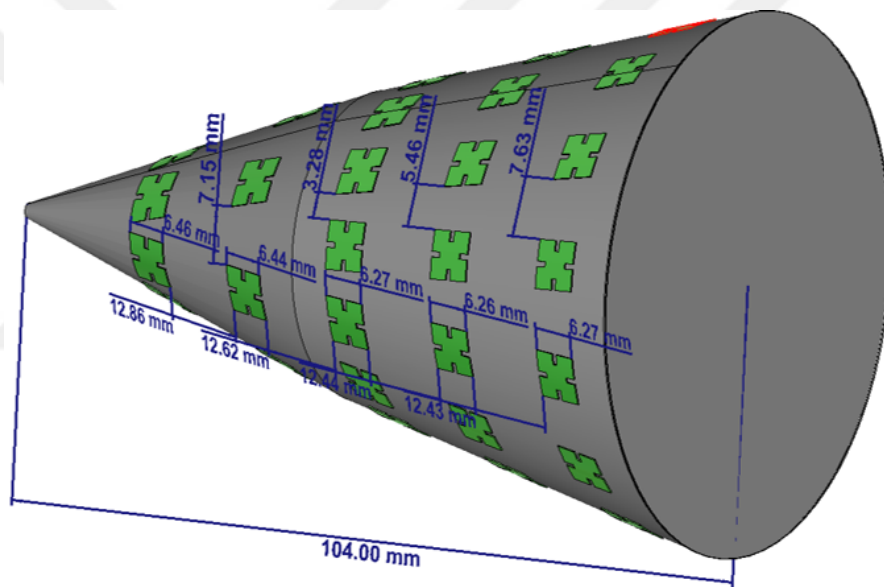
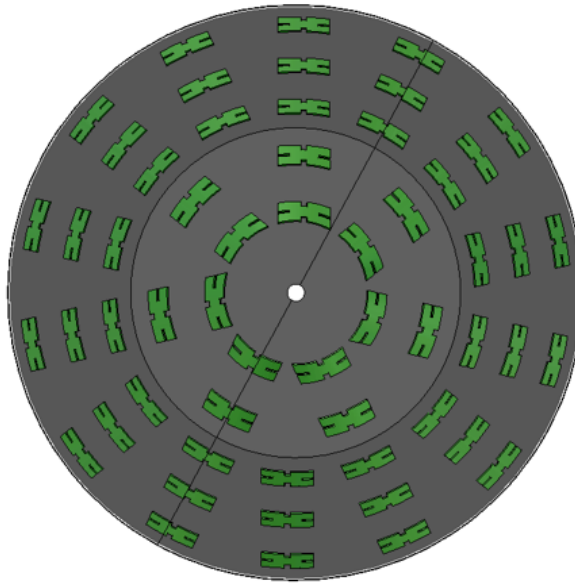
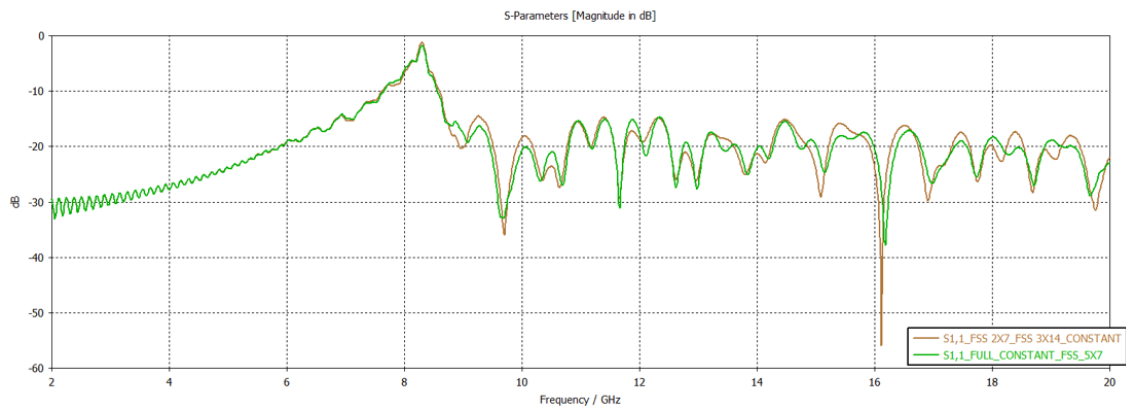


Figure 4.69 Right cross view of added FSS coated cone



**Figure 4.70** Top view of added FSS coated cone

The comparative results of these two analyzes are as in Figure 4.71, Figure 4.72, Figure 4.73 and Figure 4.74 below.



**Figure 4.71** Comparison of S11 parameters of 5x7 constant FSS coated cone analysis and added FSS coated cone analysis

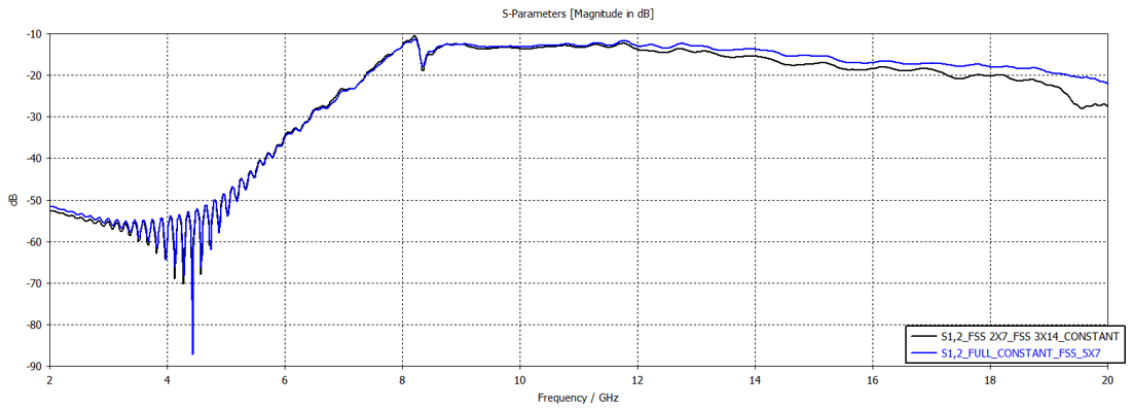


Figure 4.72 Comparison of S12 parameters of 5x7 constant FSS coated cone analysis and added FSS coated cone analysis

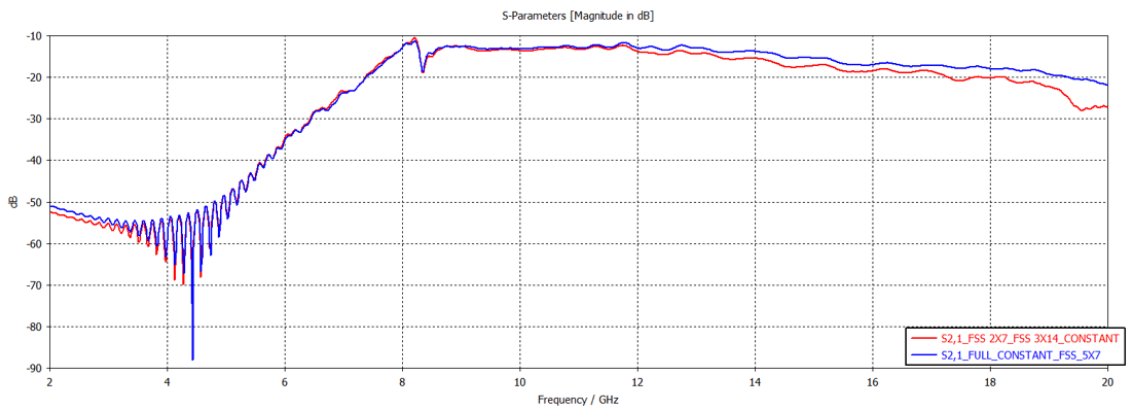


Figure 4.73 Comparison of S21 parameters of 5x7 constant FSS coated cone analysis and added FSS coated cone analysis

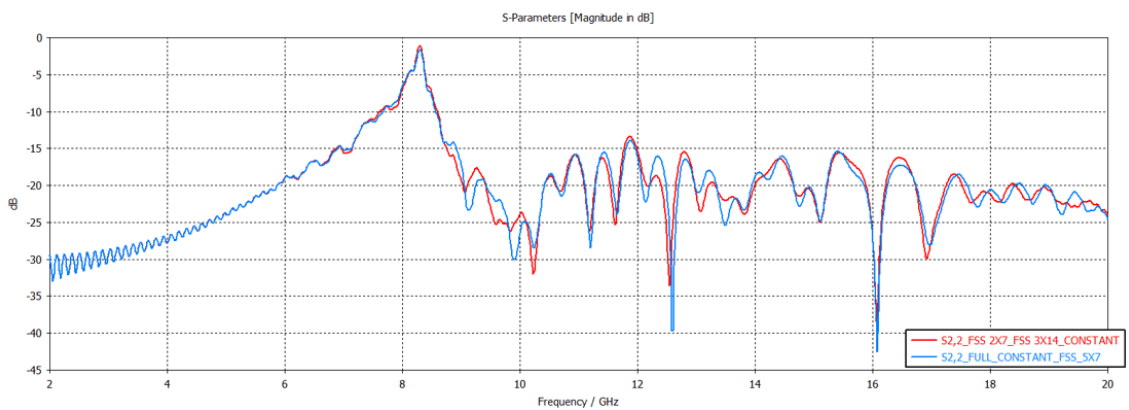


Figure 4.74 Comparison of S22 parameters of 5x7 constant FSS coated cone analysis and added FSS coated cone analysis

As a result of this analysis, they showed close results with constant FSSs thanks to the added FSSs. Constant FSSs showed better results, although with little difference, in the 10 GHz region. In the 16GHz region, the other analysis showed better results.

### COMPARISON OF ALL CONIC ANALYSIS AND SUMMARY

First of all, figure 3, figure 4, figure 5 and figure 6 given below contain the S parameter results of all conical surface analyzes completed so far on the same graph.

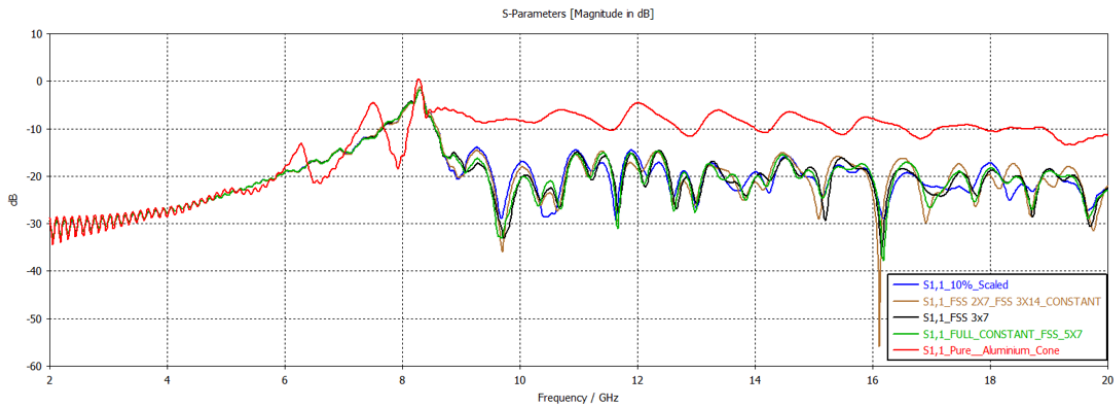


Figure 4.75 Comparison of All S11 Parameter Results

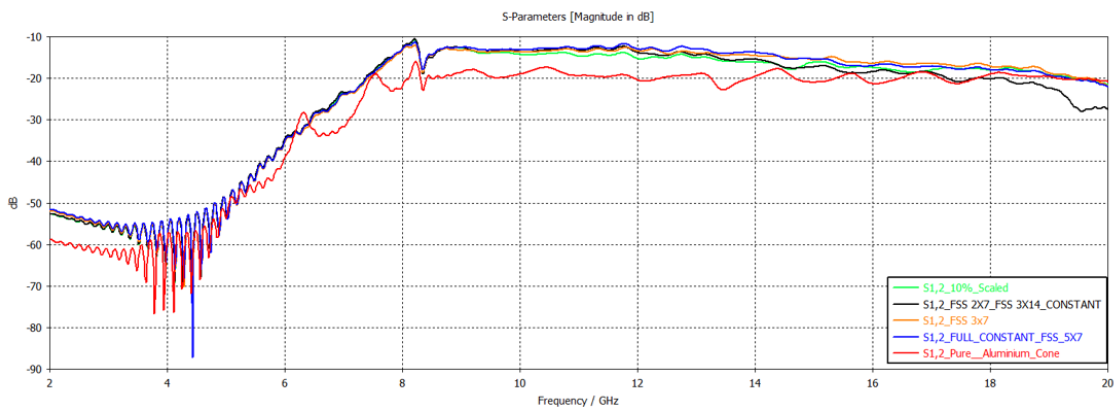


Figure 4.76 Comparison of All S12 Parameter Results

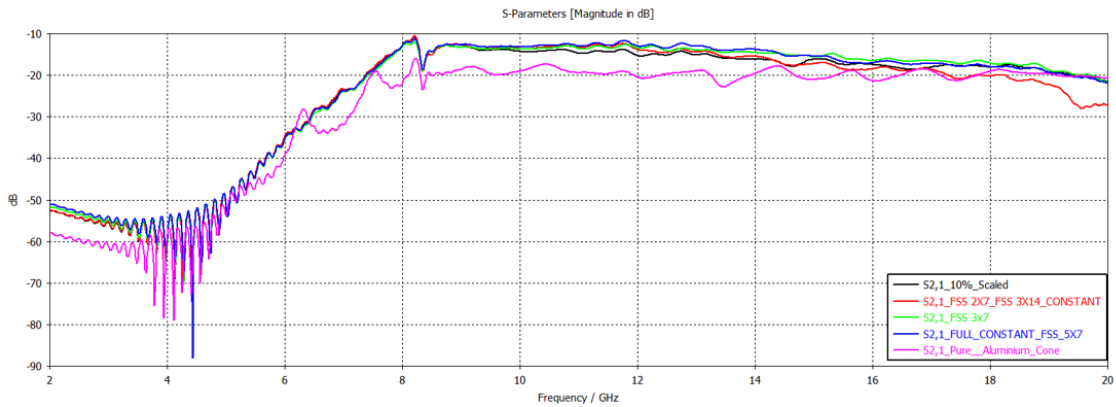


Figure 4.77 Comparison of All S21 Parameter Results

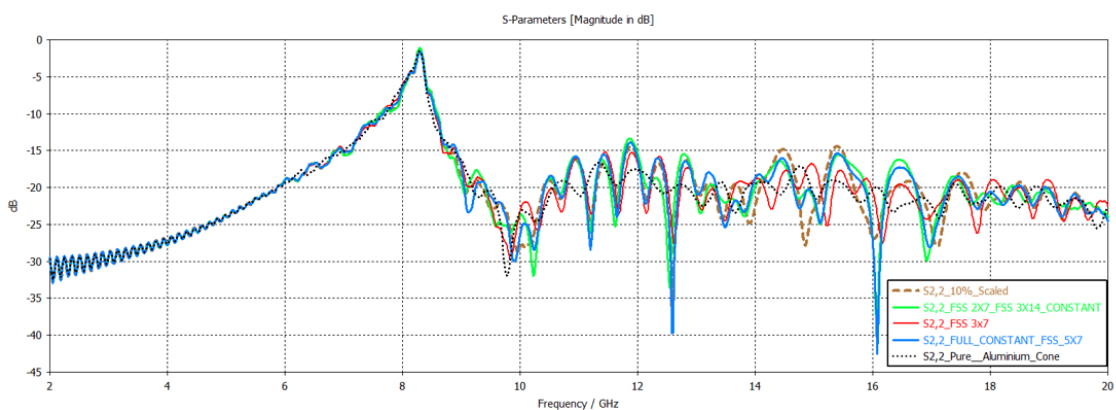


Figure 4.78 Comparison of All S22 Parameter Results

- When the results were examined, the best performance was shown by the analysis covering the entire conical surface with FSS adjusted for 10GHz. So the analysis specified with "FULL\_CONSTANT\_FSS\_5X7" in the legend provided the best results.
- After that the best performing analysis is the one in which only the back surface of the conical surface is covered, with the name "FSS 3X7" in the legend. The main reason why this analysis did not show the best performance is that the FSS does not cover the entire conical surface. From this result, it can be concluded that covering the entire surface of interest with FSS is an important factor for FSS performance.
- The third best result is the one with the name "FSS 2X7\_FSS 3X14\_CONSTANT" in the legend. In this analysis, the original FSS was applied to the anterior part of the nose, while the frequency was doubled to the wide conical surface at the back, and FSSs were added in between. The most important reason for this result to be worse than the other results is that the distance between the FSSs has

deteriorated due to the additional FSS added at the back. Therefore, additional FSSs caused a shift in the resonant frequency. In other words, the requirement in the standard FSS cell design could not be met. Periodicity could not be achieved and FSS was selective at different frequencies.

- Finally, the worst performance was shown by the legend with the name "**10%\_Scaled**". In this design, the FSS at the tip of the nose is the standard FSS design used in other analyses. Each FSS dimension is a 10% enlarging of the standard FSS excluding thickness as it moves towards the back of the conical surface. If the FSS dimension closest to the nose of the cone is accepted as 1X, the other FSS dimensions will be 1.1X, 1.21X, 1.331X and 1.4641X, respectively. This size change can be clearly seen in Figure 4.60, Figure 4.61 and Figure 4.62. The main reason why this analysis could not show the expected performance is that the periodicity, which is one of the most basic elements of the working principle of FSS, could not be achieved. Because every new FSS with 10% magnification created as you move towards the back of the cone works for a different frequency. In fact, each FSS of the new dimension created was tuned to different resonant frequencies.

With the support of these results, while applying to 3D geometry with FSS;

- Should not break the physical structure of the optimized FSS design.
- FSS should be customized according to the requirement of the geometric structure.
- Periodicity should not be impaired by using multiple different FSS designs together.
- Consideration should be given to the thickness of the substrate used for FSS and it should be used in the same way all over the surface without changing it. If a different material is to be used as a substrate, the FSS should be reanalyzed for the new material.
- The distance between two adjacent Frequency-selective surfaces should be constant to ensure periodicity.

# 5

## RESULTS AND DISCUSSION

---

### 5.1 Conclusions

In this study, a new frequency selective surface is designed, which provides absorption in the 10GHz region, which can be called the X band. In order to realize this design, the most frequently used FSSs in recent years have been used. First of all, an FSS with filter characteristics as desired in the design and suitable for terahertz applications was started. Then, the obtained resonance frequency was examined and its physical design was changed accordingly, and it was tuned to the 10GHz band. All analyzes were performed in the CST Microwave Studio program. Conical surface design and airfoil design, which are difficult to design, were implemented in the Catia V5 program, while designs such as the simpler cylindrical surface were implemented in the CST Studio program. Maximum attention has been paid to the periodicity of the FSS applied to all surfaces.

All of the factors affecting the designed FSS unit cell were examined in the simulation environment. The transmission and reflection coefficient graphs of the wave are examined in detail. The optimized and determined FSS design has been applied to all geometric surfaces.

Similar geometric shapes are designed for all surfaces in the sections of the aircraft. The FSS cell is applied to the surface of these three different geometric designs periodically and in a way that does not disturb the FSS structure. These three geometric structures consist of wings, body and nose.

In order to be able to analyze different geometries, interpretations were made on the reflection coefficients and transmission coefficients with two horn antennas that provide suitable radiation characteristics. Since they are not rectangular surfaces, valid cell analysis cannot be performed for periodic analyzes. Although the dimensions of the materials designed as aircraft geometries are small, it has been confirmed by different analyzes that similar results will be obtained when applied to real

dimensions. Because FSSs are not affected by dimension size, they are infinite periodic structures.

The designed FSS is intended to be as independent as possible from the arrival of the electromagnetic wave. The sample produced was supported by three different geometry prototypes and experimental results, computer simulations, and the simulations were made with the CST Studio Suite.

As can be seen in the transmission and reflection coefficients in the measurement results, FSS contributed to the stealth feature of the aircraft in the 10GHz band by providing absorption at the 10 GHz frequency.

## **5.2 Future Perspectives**

This study has some potential for future investigation. These possible future steps includes:

- To ensure the production of FSSs, which are designed depending on the development of 3D printer technology, with 3D printers.
- To ensure that the designed FSS is designed as AFSS so that it can be tuned to other frequencies. It is intended not only to shift the resonant frequency, but also to adjust other values such as the bandwidth.
- To ensure that the most suitable FSS design for surfaces is directly suggested according to the requirements.
- To ensure that to the overall RCS reduction of the aircraft by performing studies specific to smaller surfaces.
- If the filtering characteristic is suitable for the desired application, creating a mathematical model specific to all the parameters affecting the designed FSS and providing the desired resonance frequency by only changing its dimensions.
- Creating a database from frequency responses in different geometries by applying it to different geometries and obtaining results about applicable geometry surfaces.

## REFERENCES

---

- [1] B. A. Munk, *Frequency selective surfaces: theory and design*. John Wiley & Sons, 2005.
- [2] S. Monni, “Frequency selective surfaces integrated with phased array antennas: Analysis and design using multimode equivalent networks,,” 2005.
- [3] S. B. Glybovski, S. A. Tretyakov, P. A. Belov, Y. S. Kivshar, C. R. Simovski, “Metasurfaces: From microwaves to visible,” *Physics reports*, vol. 634, pp. 1–72, 2016.
- [4] J. C. Vardaxoglou, *Frequency selective surfaces: analysis and design*. Research Studies Press, 1997.
- [5] B. Döken, “Geniş bantlı kablosuz iletişime uygun yapısal yüzey malzemesi tasarımı,” Ph.D. dissertation, Yüksek lisans tezi, İstanbul Teknik Üniversitesi, 2011.
- [6] G. Schennum, “Frequency-selective surfaces for multiple-frequency antennas,,” *Microwave Journal*, vol. 16, pp. 55–57, 1973.
- [7] J. Murugan, T. R. Sureshkumar, P. Salil, C. Venkatesh, “Dual frequency selective transparent front doors for microwave oven with different opening areas,” *Progress In Electromagnetics Research Letters*, vol. 52, pp. 11–16, Jan. 2015. DOI: 10.2528/PIERL14121801.
- [8] M. H. Nisanci *et al.*, “Experimental validation of a 3d fss designed by periodic conductive fibers part-2: Band-stop filter characteristic,” 2017.
- [9] P. Saville, “Review of radar absorbing materials,” Defence Research and Development Atlantic Dartmouth (Canada), Tech. Rep., 2005.
- [10] S. Guo, Y.-L. Zhang, Y. He, L. Miao, J.-J. Jiang, “Design of a broadband and switchable absorber using an absorb/reflective fss,” in *2019 Photonics & Electromagnetics Research Symposium-Fall (PIERS-Fall)*, IEEE, 2019, pp. 2144–2148.
- [11] R. Li, F. He, S. Guo, J. Jiang, “Design and analysis of multilayer lossy fss based broadband absorber,” in *2021 IEEE MTT-S International Wireless Symposium (IWS)*, 2021, pp. 1–3. DOI: 10.1109/IWS52775.2021.9499463.
- [12] Y. Han, L. Xu, H. Xu, S. Xie, “Design of wideband frequency selective absorber based on multilayer structures,” in *2020 50th European Microwave Conference (EuMC)*, IEEE, 2021, pp. 1079–1082.
- [13] B. Döken, M. Kartal, Ş. Balta, “A simple frequency selective absorber surface design,” in *2019 9th International Conference on Recent Advances in Space Technologies (RAST)*, IEEE, 2019, pp. 79–82.

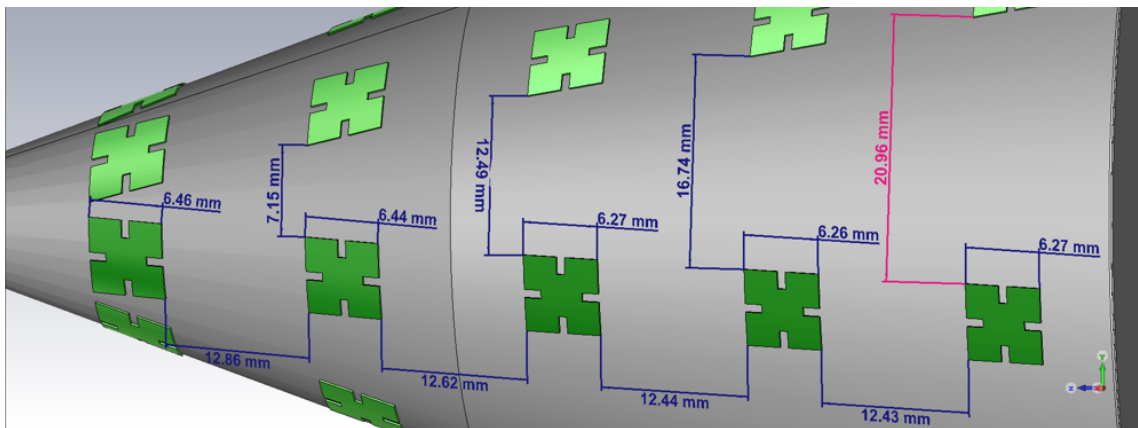
- [14] J. Liang, Q. Cao, H. Yuan, "A tunable frequency selective absorber with reflection function," in *2020 Cross Strait Radio Science & Wireless Technology Conference (CSRSWTC)*, IEEE, 2020, pp. 1–3.
- [15] S.-W. Lee, G. Zarrillo, C.-L. Law, "Simple formulas for transmission through periodic metal grids or plates," *IEEE Transactions on Antennas and Propagation*, vol. 30, no. 5, pp. 904–909, 1982. DOI: 10.1109/TAP.1982.1142923.
- [16] W. Wang, J. Dong, M. Wang, J. Mo, "Frequency selective surface design based on equivalent circuit," in *2020 IEEE MTT-S International Conference on Numerical Electromagnetic and Multiphysics Modeling and Optimization (NEMO)*, 2020, pp. 1–4. DOI: 10.1109/NEMO49486.2020.9343412.
- [17] Y. Han, B. Li, Y. Chang, L. Xu, "Investigation of frequency selective absorber based on antenna-filter-antenna elements," in *2019 IEEE MTT-S International Wireless Symposium (IWS)*, 2019, pp. 1–3. DOI: 10.1109/IEEE-IWS.2019.8803864.
- [18] X. Fan *et al.*, "Design and fabrication of a reconfigurable and flexible frequency selective surface with a buckling dipole via mechanical stretching," *Soft Science*, pp. 1–11, 2021. DOI: 10.20517/ss.2021.18.
- [19] T. Liu S.-S. Kim, "High-capacitive frequency selective surfaces of folded spiral conductor arrays," *Microwave and Optical Technology Letters*, vol. 62, Jan. 2020. DOI: 10.1002/mop.32006.
- [20] J. A. Vásquez-Peralvo, J.-M. Fernández-González, P. Valtr, J. M. Rigelsford, "Inductive frequency selective surface: An application for dichroic sub-reflectors," *IEEE Access*, vol. 8, pp. 22 721–22 732, 2020. DOI: 10.1109/ACCESS.2020.2970271.
- [21] S. Qiu, Q. Guo, Z. Li, "Tunable frequency selective surface based on a sliding 3d-printed inserted dielectric," *IEEE Access*, vol. 9, pp. 19 743–19 748, 2021. DOI: 10.1109/ACCESS.2021.3054434.
- [22] S. M. A. Momeni Hasan Abadi N. Behdad, "Inductively-coupled miniaturized-element frequency selective surfaces with narrowband, high-order bandpass responses," *IEEE Transactions on Antennas and Propagation*, vol. 63, pp. 1–1, Nov. 2015. DOI: 10.1109/TAP.2015.2477850.
- [23] R. S. Anwar, L. Mao, H. Ning, "Frequency selective surfaces: A review," *Applied Sciences*, vol. 8, no. 9, p. 1689, 2018.
- [24] H. Huang, Z. Shen, C. Hua, "Ultra-broadband 3-d absorptive frequency-selective transmission structure using commercial absorber," in *2020 IEEE International Symposium on Antennas and Propagation and North American Radio Science Meeting*, IEEE, 2020, pp. 751–752.
- [25] A. A. Omar, H. Huang, Z. Shen, "Multi-band absorptive frequency-selective reflection structures," in *2019 Joint International Symposium on Electromagnetic Compatibility, Sapporo and Asia-Pacific International Symposium on Electromagnetic Compatibility (EMC Sapporo/APEMC)*, IEEE, 2019, pp. 52–54.
- [26] Y. Zhao, B. Qi, Z. Mei, "Design of a novel absorber with switchable absorption and transmission bands based on pin diode," in *2019 Photonics & Electromagnetics Research Symposium-Fall (PIERS-Fall)*, IEEE, 2019, pp. 2460–2464.

- [27] J. Liang, Q. Cao, H. Yuan, "A tunable frequency selective absorber with reflection function," in *2020 Cross Strait Radio Science & Wireless Technology Conference (CSRSWTC)*, IEEE, 2020, pp. 1–3.
- [28] H. Chen, Q. Cao, Y. Wang, "A wideband switchable absorber/reflector based on active frequency selective surface," *International Journal of RF and Microwave Computer-Aided Engineering*, vol. 31, no. 1, e22474, 2021.
- [29] Z. X. Zhang, Z. H. Jiang, R. F. Ma, Y. Li, W. Hong, "Broadband sequential rotation array of circularly-polarized metasurface antennas at ka-band," in *2019 International Applied Computational Electromagnetics Society Symposium-China (ACES)*, IEEE, vol. 1, 2019, pp. 1–2.
- [30] R. Zhao, B. Gong, F. Xiao, C. He, W. Zhu, "Circuit model analysis of switchable perfect absorption/reflection in an active frequency selective surface," *IEEE Access*, vol. 7, pp. 55 518–55 523, 2019.
- [31] S. Kitagawa, R. Suga, K. Araki, O. Hashimoto, "Active absorption/transmission fss using diodes," in *2015 IEEE International Symposium on Electromagnetic Compatibility (EMC)*, IEEE, 2015, pp. 1538–1541.
- [32] X. Zeng, L. Zhang, G. Wan, B. Hu, B. Huang, J. Shen, "Tunable and broadband radar absorber based on pin diodes controllable fss," in *2016 11th International Symposium on Antennas, Propagation and EM Theory (ISAPE)*, IEEE, 2016, pp. 720–722.
- [33] W. Ming-liang, Z. Sheng-jun, L. Jia-qi, W. Wei-dong, "The research on the effects of an active fss with circle element on the characteristics of radar absorbing materials," 2015.
- [34] Y. He J. Jiang, "An ultra-wideband metamaterial absorber with active frequency selective surface," in *2015 9th International Congress on Advanced Electromagnetic Materials in Microwaves and Optics (METAMATERIALS)*, IEEE, 2015, pp. 100–102.
- [35] G. Qian *et al.*, "Switchable broadband dual-polarized frequency-selective rasorber/absorber," *IEEE Antennas and Wireless Propagation Letters*, vol. 18, no. 12, pp. 2508–2512, 2019.
- [36] A. Kapoor, R. Mishra, P. Kumar, "Frequency selective surfaces as spatial filters: Fundamentals, analysis and applications," *Alexandria Engineering Journal*, 2021.
- [37] J. P. Gianvittorio, J. Romeu, S. Blanch, Y. Rahmat-Samii, "Self-similar prefractal frequency selective surfaces for multiband and dual-polarized applications," *IEEE Transactions on Antennas and Propagation*, vol. 51, no. 11, pp. 3088–3096, 2003.
- [38] H.-O. Peitgen, H. Jürgens, D. Saupe, M. J. Feigenbaum, *Chaos and fractals: new frontiers of science*. Springer, 2004, vol. 106.
- [39] K. Vinoy, J. K. Abraham, V. K. Varadan, "On the relationship between fractal dimension and the performance of multi-resonant dipole antennas using koch curves," *IEEE Transactions on Antennas and Propagation*, vol. 51, no. 9, pp. 2296–2303, 2003.

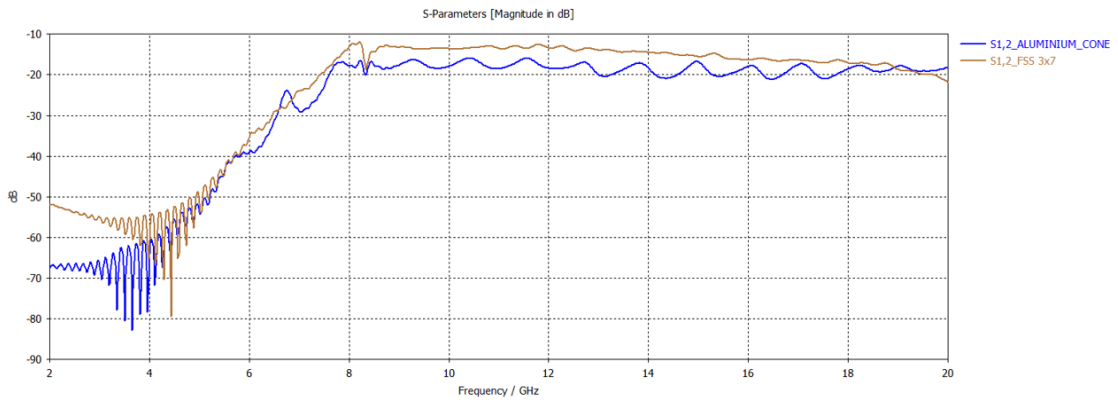
- [40] A. Campos, E. De Oliveira, P. d. F. Silva, "Miniaturization of frequency selective surfaces using fractal koch curves," *Microwave and Optical Technology Letters*, vol. 51, no. 8, pp. 1983–1986, 2009.
- [41] G. H. Sung, K. W. Sowerby, A. G. Williamson, "Angular stable frequency selective wallpapers for mitigating indoor wireless interference," in *International Symposium on Antennas and Propagation*, 2008.
- [42] K. Katoch, N. Jaglan, S. D. Gupta, "A review on frequency selective surfaces and its applications," in *2019 International Conference on Signal Processing and Communication (ICSC)*, IEEE, 2019, pp. 75–81.
- [43] H. Zhang, J. Lu, G. Sun, H. Xiao, "Influence of substrate process tolerances on transmission characteristics of frequency-selective surface," *Chinese Optics Letters*, vol. 6, no. 1, pp. 54–56, 2008.
- [44] Y. Xu M. He, "Design of multilayer frequency-selective surfaces by equivalent circuit method and basic building blocks," *International Journal of Antennas and Propagation*, vol. 2019, 2019.
- [45] P. Martin-Iglesias, F. Teberio, M. A. Laso, "Analysis of the multipactor effect with linear frequency modulated signals," in *2018 IEEE MTT-S International Conference on Numerical Electromagnetic and Multiphysics Modeling and Optimization (NEMO)*, IEEE, 2018, pp. 1–4.
- [46] R. Orta, P. Savi, R. Tascone, "The effect of finite conductivity on frequency selective surface behavior," *Electromagnetics*, vol. 10, no. 3, pp. 213–227, 1990.
- [47] D. Kanchana, R. Sankararajan, B. Sreeja, E. Manikandan, "Polarization independent bandstop frequency selective surface for x-band application," *Circuit World*, 2019.
- [48] E. Unal, A. Gokcen, Y. Kutlu, "Effective electromagnetic shielding," *IEEE Microwave magazine*, vol. 7, no. 4, pp. 48–54, 2006.
- [49] M. Nauman, R. Saleem, A. K. Rashid, M. F. Shafique, "A miniaturized flexible frequency selective surface for x-band applications," *IEEE Transactions on Electromagnetic Compatibility*, vol. 58, no. 2, pp. 419–428, 2016.
- [50] M. Bilal, R. Saleem, F. A. Khan, A. Quddus, M. F. Shafique, "Frequency selective surface for x-band shielding applications," in *2016 16th Mediterranean Microwave Symposium (MMS)*, IEEE, 2016, pp. 1–3.
- [51] X. Sheng, J. Ge, K. Han, X.-C. Zhu, "Transmissive/reflective frequency selective surface for satellite applications," *IEEE Antennas and Wireless Propagation Letters*, vol. 17, no. 7, pp. 1136–1140, 2018.
- [52] M. R. Chaharmir J. Shaker, "Design of a multilayer x-/ka-band frequency-selective surface-backed reflectarray for satellite applications," *IEEE Transactions on Antennas and Propagation*, vol. 63, no. 4, pp. 1255–1262, 2015.
- [53] T. Rahim J. Xu, "X-band Band-pass Frequency Selective Surface for Radome Applications," *TELKOMNIKA Indonesian Journal of Electrical Engineering*, vol. 16, no. 2, p. 281, 2015, ISSN: 2302-4046. DOI: 10.11591/tijee.v16i2.1613.

- [54] A. A. Omar Z. Shen, "Thin 3-d bandpass frequency-selective structure based on folded substrate for conformal radome applications," *IEEE Transactions on Antennas and Propagation*, vol. 67, no. 1, pp. 282–290, 2019. DOI: 10.1109/TAP.2018.2876706.
- [55] T. Rahim, F. A. Khan, X. Jiadong, "Design of x-band frequency selective surface (fss) with band pass characteristics based on miniaturized unit cell," in *2016 13th International Bhurban Conference on Applied Sciences and Technology (IB-CAST)*, 2016, pp. 592–594. DOI: 10.1109/IBCAST.2016.7429937.
- [56] M. Ramzan *et al.*, "Terahertz bandpass frequency selective surfaces on glass substrates using a wet micromachining process," *Journal of Infrared, Millimeter, and Terahertz Waves*, vol. 38, no. 8, pp. 945–957, 2017.
- [57] B. J. Chen, C. H. Chan, *et al.*, "High-selectivity bandpass frequency-selective surface in terahertz band," *IEEE Transactions on Terahertz Science and Technology*, vol. 6, no. 2, pp. 284–291, 2016.
- [58] S. Sutradhar, N. Sayadat, A. Rahman, S. Munira, A. F. Haque, S. Sakib, "Iir based digital filter design and performance analysis," Aug. 2017, pp. 1–6. DOI: 10.1109/TEL-NET.2017.8343596.
- [59] X. Li H. Gao, "Min-max approximation of transfer functions with application to filter design," *IEEE Transactions on Signal Processing*, vol. 63, no. 1, pp. 31–40, 2015. DOI: 10.1109/TSP.2014.2364787.
- [60] A. Papoulis, "On the approximation problem in filter design," in *PROCEEDINGS OF THE INSTITUTE OF RADIO ENGINEERS*, vol. 45, 1957, pp. 402–402.
- [61] W. Laghari, M. Baloch, M. Mengal, S. Shah, "Performance analysis of analog butterworth low pass filter as compared to chebyshev type-i filter, chebyshev type-ii filter and elliptical filter," *Circuits and Systems*, vol. 05, pp. 209–216, Jan. 2014. DOI: 10.4236/cs.2014.59023.
- [62] H. Aroudakj, V. Hansen, H.-P. Gemund, E. Kreysa, "Analysis of low-pass filters consisting of multiple stacked fss's of different periodicities with applications in the submillimeter radioastronomy," *IEEE Transactions on Antennas and Propagation*, vol. 43, no. 12, pp. 1486–1491, 1995. DOI: 10.1109/8.475943.
- [63] A. Ebrahimi *et al.*, "Second-order terahertz bandpass frequency selective surface with miniaturized elements," *IEEE Transactions on Terahertz Science and Technology*, vol. 5, no. 5, pp. 761–769, 2015.
- [64] M. Salehi N. Behdad, "A second-order dual x-/ka-band frequency selective surface," *IEEE Microwave and Wireless Components Letters*, vol. 18, no. 12, pp. 785–787, 2008.
- [65] M. Lu, W. Li, E. R. Brown, "Second-order bandpass terahertz filter achieved by multilayer complementary metamaterial structures," *Optics letters*, vol. 36, no. 7, pp. 1071–1073, 2011.

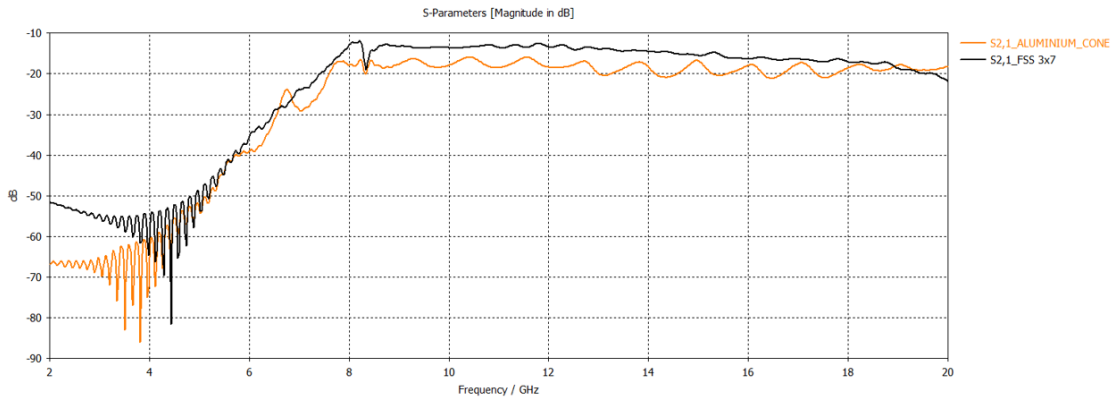
- [66] H. Mohammadi Nemat-Abad, E. Zareian-Jahromi, R. Basiri, "Design and equivalent circuit model extraction of a third-order band-pass frequency selective surface filter for terahertz applications," *Engineering Science and Technology, an International Journal*, vol. 22, no. 3, pp. 862–868, 2019, ISSN: 2215-0986. DOI: <https://doi.org/10.1016/j.jestch.2019.01.008>. [Online]. Available: <https://www.sciencedirect.com/science/article/pii/S2215098618319499>.
- [67] D. M. Pozar, *Microwave engineering*. John Wiley & sons, 2011.
- [68] T. Weiland, "A discretization model for the solution of maxwell's equations for six-component fields," *Archiv Elektronik und Uebertragungstechnik*, vol. 31, pp. 116–120, 1977.
- [69] K. Yee, "Numerical solution of initial boundary value problems involving maxwell's equations in isotropic media," *IEEE Transactions on antennas and propagation*, vol. 14, no. 3, pp. 302–307, 1966.
- [70] T. Weiland, M. Timm, I. Munteanu, "A practical guide to 3-d simulation," *IEEE Microwave Magazine*, vol. 9, no. 6, pp. 62–75, 2008.
- [71] S. Gudmundsson, *General aviation aircraft design: Applied Methods and Procedures*. Butterworth-Heinemann, 2013.
- [72] *Airfoil*, <https://www.sciencedirect.com/science/article/pii/S2215098618319>, [Online; accessed 21-December-2021], 2021.



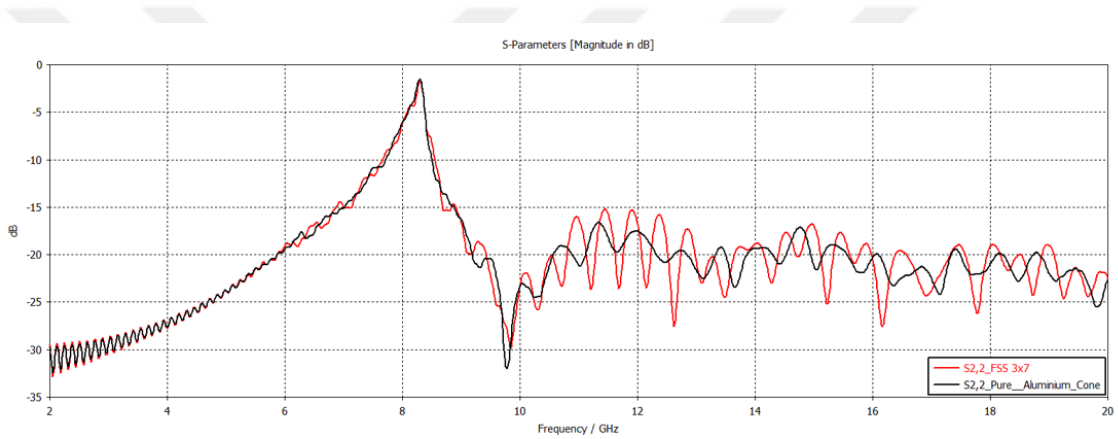
**Figure A.1** Right cross detailed view of FSS coated cone with 5 circular loops consisting of 7 FSS



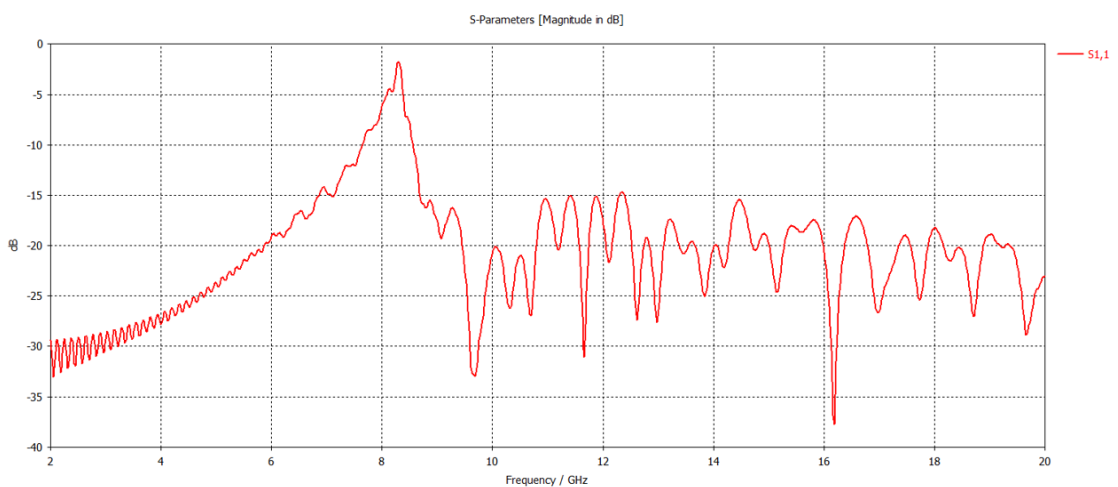
**Figure A.2** Comparison of S12 parameters of 3x7 FSS coated cone analysis and aluminum cone analysis



**Figure A.3** Comparison of S21 parameters of 3x7 FSS coated cone analysis and aluminum cone analysis



**Figure A.4** Comparison of S22 parameters of 3x7 FSS coated cone analysis and aluminum cone analysis



**Figure A.5** Result of S11 parameters of 5x7 FSS coated cone analysis

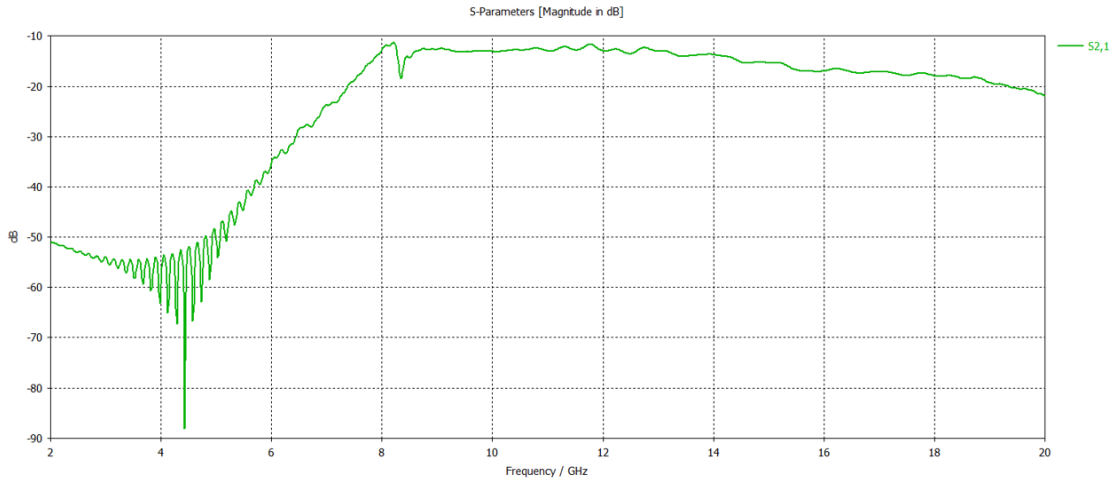


Figure A.6 Result of S21 parameters of 5x7 FSS coated cone analysis

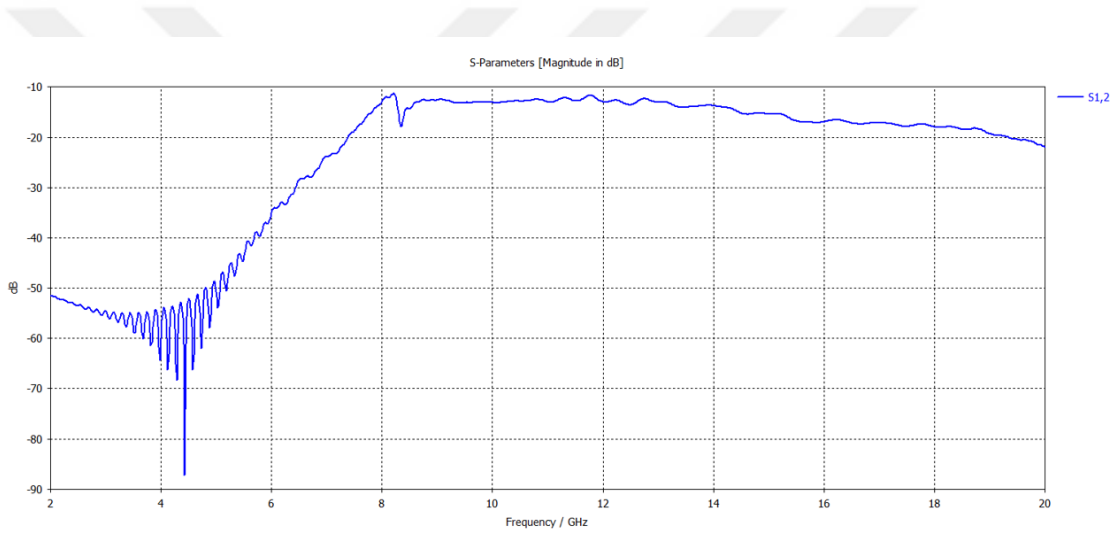


Figure A.7 Result of S12 parameters of 5x7 FSS coated cone analysis

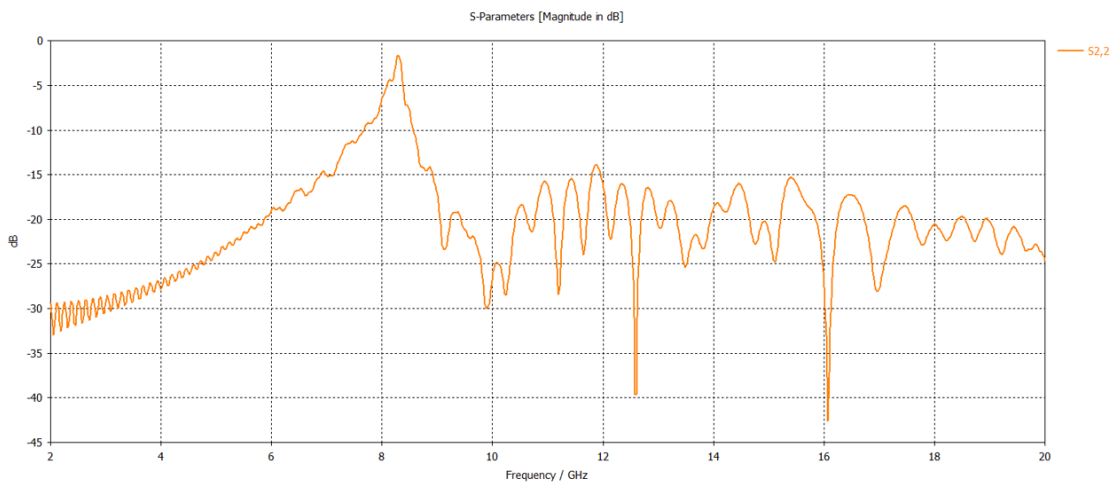
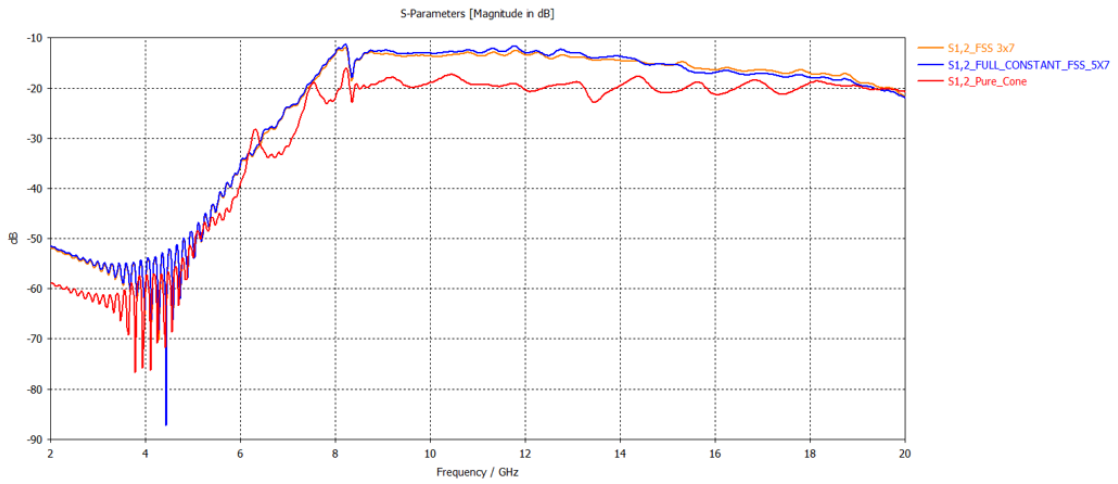
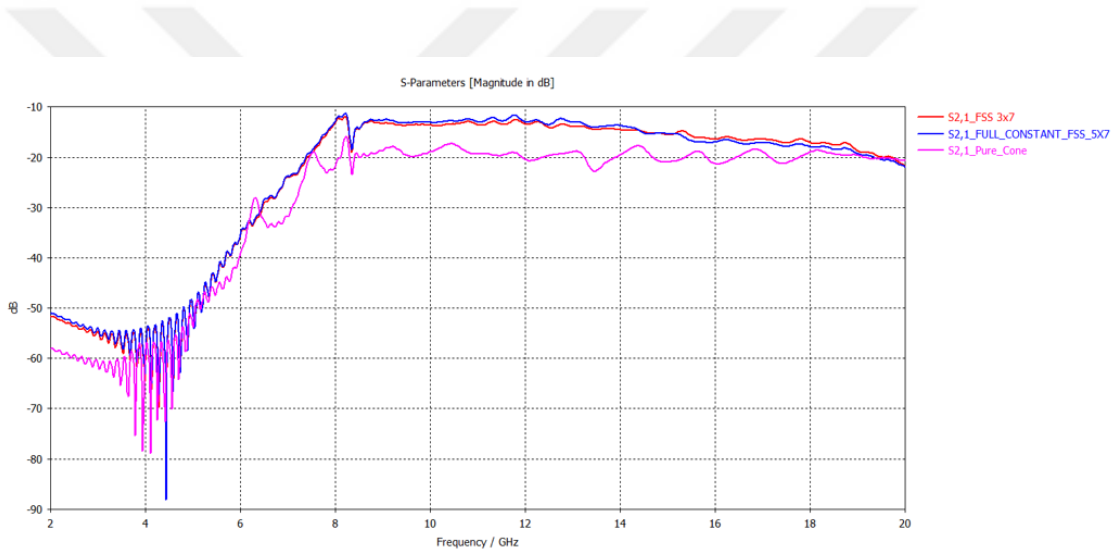


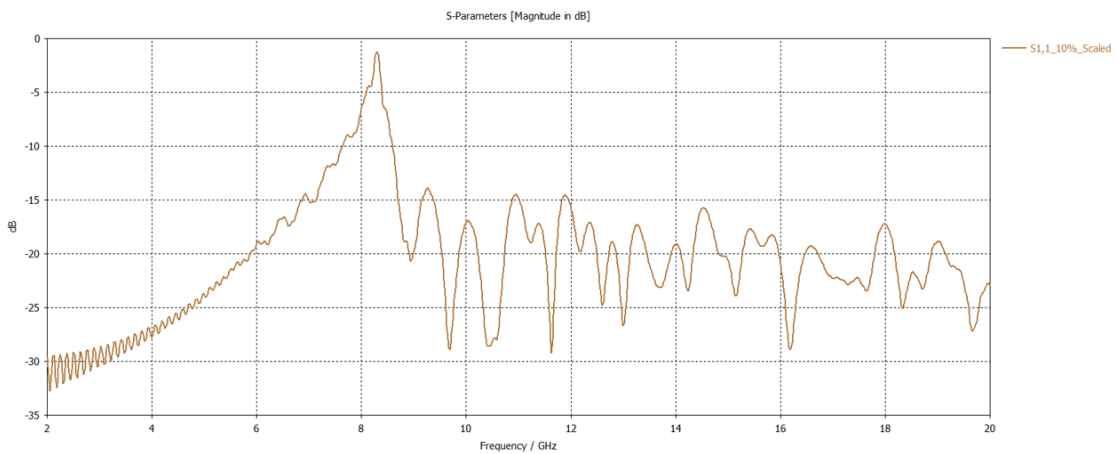
Figure A.8 Result of S22 parameters of 5x7 FSS coated cone analysis



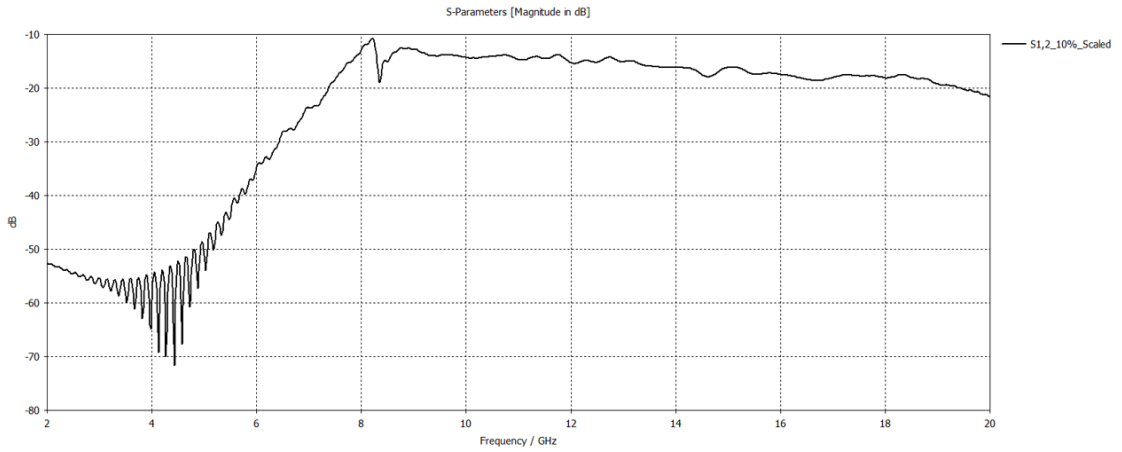
**Figure A.9** Comparison of S12 parameters of 5x7 FSS coated cone analysis and aluminum cone analysis



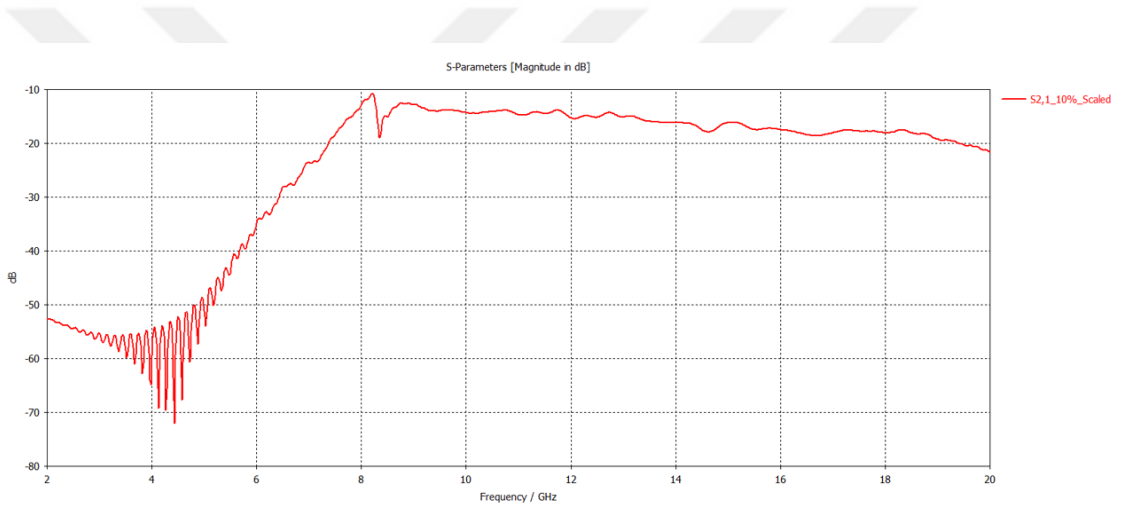
**Figure A.10** Comparison of S21 parameters of 5x7 FSS coated cone analysis and aluminum cone analysis



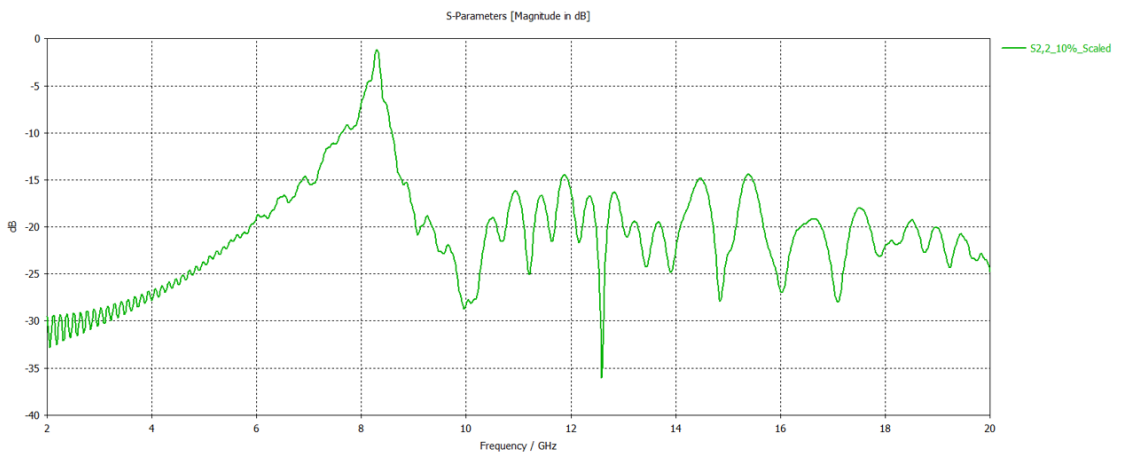
**Figure A.11** Result of S11 parameters of 10% enlarged FSS coated cone analysis



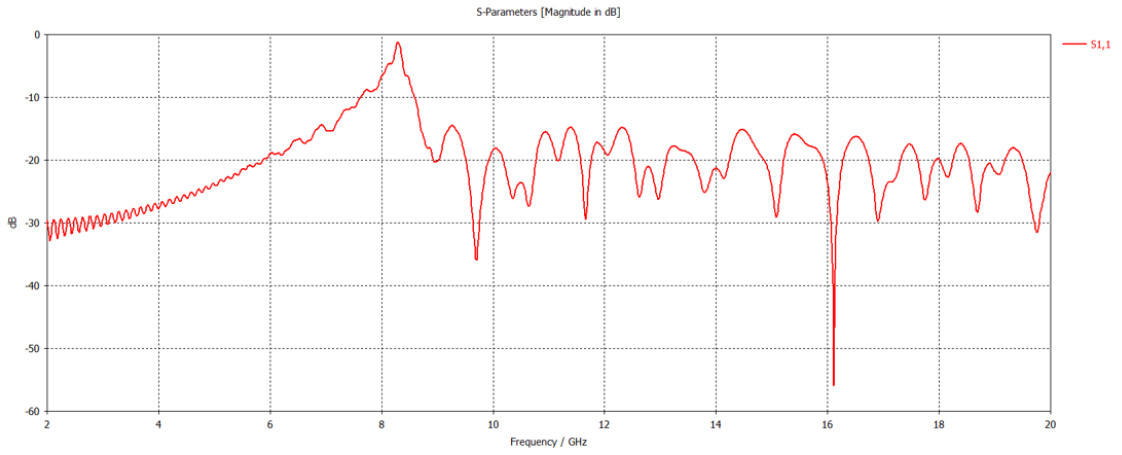
**Figure A.12** Result of S12 parameters of 10% enlarged FSS coated cone analysis



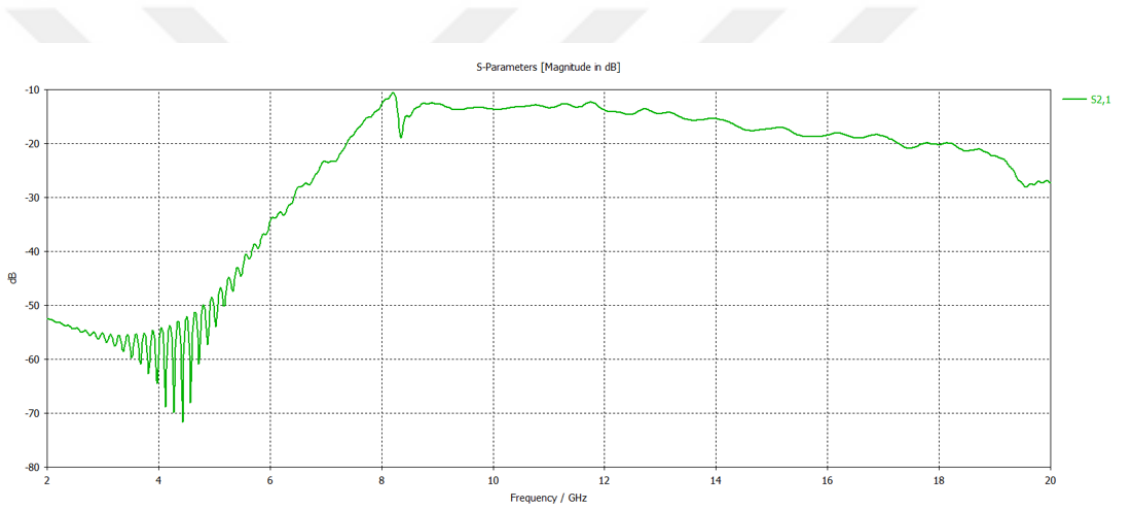
**Figure A.13** Result of S21 parameters of 10% enlarged FSS coated cone analysis



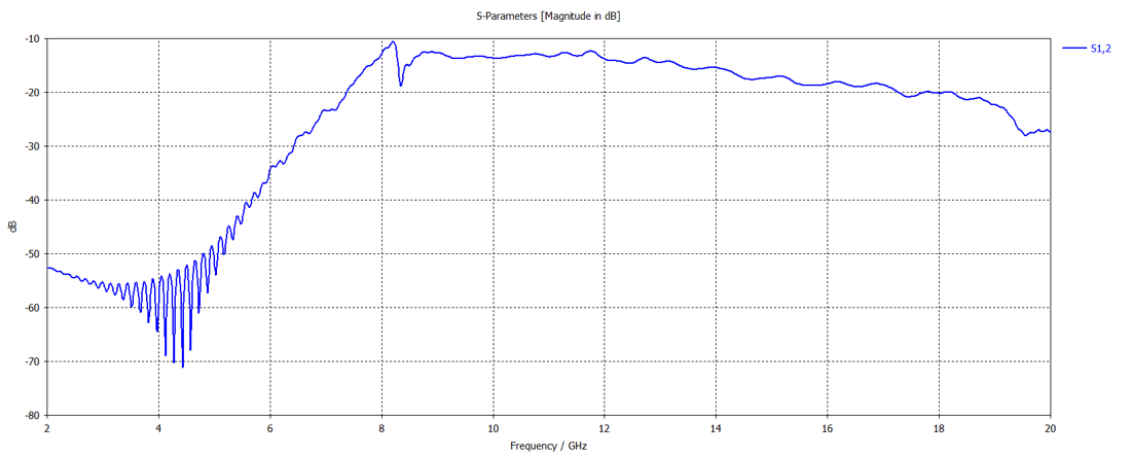
**Figure A.14** Result of S22 parameters of 10% enlarged FSS coated cone analysis



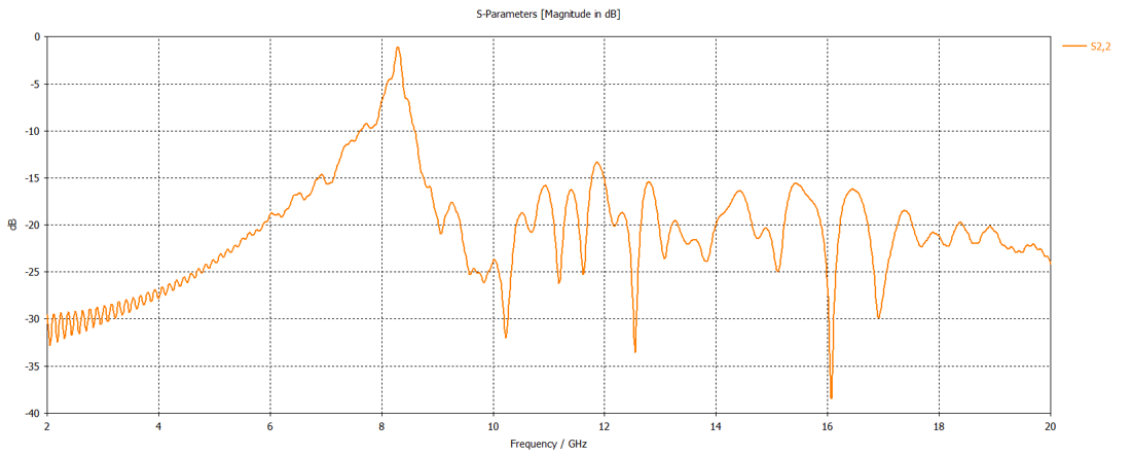
**Figure A.15** Result of S11 parameters of added FSS coated cone analysis



**Figure A.16** Result of S21 parameters of added FSS coated cone analysis



**Figure A.17** Result of S12 parameters of added FSS coated cone analysis



**Figure A.18** Result of S<sub>22</sub> parameters of added FSS coated cone analysis



## PUBLICATIONS FROM THESIS

---

### Conference Papers

1. Global Conference on Engineering Research (GLOBCER'21)  
June 02-05, 2021, Balıkesir, Turkey  
Investigation of Absorption Performance of Frequency Selective Surfaces in Simulation Programs

